UNIVERSITÀ DEGLI STUDI
DI GENOVA

DITEN - Department of Electrical, Electronics and Telecommunication Engineering and Naval Architecture
SCNL- Satellite Communications and heterogeneous Networking Laboratory

Ph.D. in Science and Technology for Electronic and Telecommunication Engineering – Cycle XXXVI (2020-2023)

Integration of Satellites into 5G Eco-systems

PhD Thesis

PhD Candidate:

Nour Badini

Tutor:

Prof. Mario Marchese

Prof. Fabio Patrone

Coordinator of the PhD Course: Prof. Carlo Regazzoni

Declaration

I hereby declare that except where specific reference is made to the work of others,the contents of this dissertation are original and have not been submitted in whole for consideration for any other degree or qualification in this, or any other universities. This dissertation is my own work and contains nothing which is the outcome of work done in collaboration with others, except as specified in the text and Acknowledgements. This dissertation contains fewer than 65,000 words including bibliography, footnotes, tables and equations and has fewer than 150 figures.

Nour Badini

November 2023

Acknowledgements

The successful completion of my Ph.D. journey is a result of the collective efforts of numerous individuals who have stood by my side, providing support, encouragement, and love. Each of you has left an unforgettable mark on this journey, and I owe you a heartfelt acknowledgment.

First, I would like to convey my deep appreciation to my exceptional thesis supervisor, Professor Mario Marchese for his support and guidance. Additionally, I extend my sincere thanks to Professor Carlo Regazzoni (Coordinator of the JDICE PhD Program), and Professor Lucio Marcenaro for their followup and valuable feedbacks.

I deeply thank my mentor, Professor Fabio Patrone, for his consistent encouragement and extensive support throughout my Ph.D. program. His mentorship has been invaluable, and I have gained significant knowledge from his expertise.

I would also like to thank my colleagues at the SCNL lab, and all my friends, especially my dear friend Lama, for the support and happy moments.

Furthermore, I am deeply appreciative of Professors Claudio Sacchi and Giovanni Giambene for their thorough review and insightful feedback of this thesis that have been instrumental in bringing this thesis to completion.

My sincerest gratitude goes to my amazing family, who have been a constant presence in my life, offering guidance, endless encouragement, and boundless wisdom. Your love and faith in me have been a source of inspiration, and this accomplishment would not have been possible without you. I owe this achievement to their support and dedication.

Last but not least, my heartfelt appreciation to my partner, Ali, for being by my side, providing support, constant encouragement, and boundless love throughout this journey.

This acknowledgment is more than a mere formality; it is a heartfelt expression of gratitude to all those who have been part of this incredible journey. Each of you has contributed to this milestone, and I hope that the lessons learned, friendships forged, and the support given will forever be cherished.

Nour Badini

Abstract

The Fifth-Generation of Mobile Communications (5G) is intended to satisfy the growing needs of users which can be summarised in the ability to access good quality services anywhere and at any time. Those needs can be supported by the integration of satellites in 5G systems due to the unique characteristics of satellites in terms of higher coverage, reliability, and availability. In particular, Low Earth Orbit (LEO) satellite constellations offer an appealing approach for supporting and complementing Fifth-Generation of Mobile Communications (5G) New Radio (NR) communications as they have the advantages of low propagation delay and low energy consumption which makes them the best candidates for direct access 5G Non-Terrestrial Networks (NTN). However, the major problem of LEO satellites is their higher speed relative to the terrestrial mobile terminals, which causes mobile users to hand over between satellites which has a negative impact on users' Quality of Service (QoS) if occured in high frequency. Moreover, 5G communication technologies are designed to support a wide spectrum of applications, including Artificial Intelligence, Virtual Reality, and the Internet of Things (IoT). Thus, differentiating User Equipments (UEs) with different and varying Traffic-Profiles (TP) has become necessary due to each application's unique performance requirements. Complicating matters further, LEO satellites operate with limited onboard resources, including energy and channel resources. Thus a satellite handover management strategy is needed to tackle all the above challenges.

To tackle these challenges, we propose innovative LEO Satellite Handover management strategies. These strategies mark a groundbreaking advancement by accounting for application diversity per user and addressing the limited energy resources of LEO satellites. Notably, these strategies successfully minimize the number of HOs, achieving a zero blocking rate while effectively balancing the load among satellites.
On the other hand, to minimize blind exploitation of new systems, new technologies should be verified and enhanced before being implemented to reduce the required cost and time. In this context, we implemented an open-source System Level Simulator (SLS) built on the foundation of the Network Simulator 3 (NS-3). This tool enables the simulation of 5G Satellite-Terrestrial Integrated Networks (STIN) and surpasses existing solutions by supporting Non-Terrestrial Networks (NTN) handover decisions, dynamic BandWidth Part (BWP) selection, and Component Carrier (CC) configurations tailored to different traffic profiles.

Contents

iii

Acknowledgements **v**

Abstract **vii**

List of Figures **xiii**

List of Tables **xvii**

1 Introduction **1**

1.1 Motivation and Objectives 1

1.2 Contributions 5

1.3 List of Publications 6

1.4 Organization of the Thesis Document 6

2 Literature Review **9**

2.1 Introduction 9

2.2 Communications Evolution 10

2.3 Satellite Communications 15

2.4 Satellite Network Simulators 19

2.5 Satellite Handover Strategies 21

2.6 Conclusion 24

3 NS-3-based 5G Satellite-Terrestrial Integrated Network Simulator 27
3.1 Introduction 27
3.2 5G SATELLITE-TERRESTRIAL NETWORK SIMULATOR 28
3.2.1 Simulator Main Components 29
3.2.2 Reference Scenario 32
3.2.3 Module Integration 35
3.3 Performance Evaluation 38
3.3.1 Satellite Handover 40
3.4 Conclusion 42

4 Handover Management in 5G Networks 45
4.1 Introduction 45
4.2 Handovers in 5G Terrestrial Network Scenarios 46
4.3 Handover in 5G Leo Satellite Network Scenarios 48
4.4 Conclusion 52

5 LEO Satellite Handover Management for Single Traffic Profile Scenarios 53
5.1 Introduction 53
5.2 Reference scenario and Network Assumptions 54
5.2.1 Problem Formulation 57
5.3 5G Satellite Handover based on Reinforcement Learning 58
5.4 Q-Learning Algoritm 60
5.5 Simulation Results 66
5.6 Conclusion 70

6 LEO Satellite Handover for Multiple Traffic Profile Scenarios 73
6.1 Introduction 73
6.2 Problem Formulation 75
6.3 Methodology 76

6.3.1 Satellite Handover Based on Deep-RL 76
6.4 Performance evaluation 83
6.4.1 Scenario setup 83
6.4.2 Multi-Agent Deep Q-Learning Satellite Handover for a Single Traffic Profile 85
6.4.3 Multi-Agent Deep Q-Learning Satellite Handover for Different and Varying Traffic Profiles 88
6.5 Conclusion 95

7 Energy Aware LEO Satellite Handover Management Based on Deep-Reinforcement Learning 99
7.1 Introduction 99
7.2 Energy onboard of a LEO Satellite 100
7.3 Methodology 104
7.4 Performance evaluation 106
7.5 Conclusion 112

8 Conclusion and Future Work 113

Bibliography 117

List of Figures

Figure 1.1 Satellite use cases in 5G Networks 3

Figure 3.1 5G NTN reference scenario, Composed of : 1- 5G user equipments which are communication devices implemented as terrestrial or aerial nodes able to get access to the internet through a LEO satellite 5G radio access network. 2- Leo satellite nodes that constitute the 5G radio access network, which is able to generate 5G cell that offers direct access to the 5G user equipments. 3- 5G core network which manages all the functionalities related to the establishment and maintenance of the 5G network. It consists of multiple nodes strictly connected to each other including a point of presence towards the internet through a packet gateway. 32

Figure 3.2 Bandwidth Part and Component Carrier Configuration Example. . 34

Figure 3.3 Example of resource allocation within the proposed simulator. In the depicted network portion and time instant, two User Equipment (UE)s $U_{0,0}$ and $U_{1,1}$, belonging to TF_0 and TF_1, respectively, are attached to satellite S_0, while UE $U_{2,0}$, belonging to the TF_0, is the only one attached to the second satellite S_1. 36

Figure 3.4 Packet ADT by changing the number of UEs and by considering networks with terrestrial or satellite gNBs 39

Figure 4.1 Handover scenario in a terrestrial base station case, where the user is in continuous motion while the terrestrial base station is always fixed on the ground 47

Figure 4.2 Handover scenario in a low earth orbit satellite base station case. Where the LEO satellite is in continuous motion while the user is in a fixed position 49

Figure 5.1 Satellite Handover Scenario; The considered scenario consists of K UEs and N LEO satellites. The UEs are ground nodes that can connect to the network directly via LEO satellites that operate as network base stations. Each UE is often covered by more than one satellite at any given time. 55

Figure 5.2 Geometric representation of the elevation angle θ between a satellite and a ground user 56

Figure 5.3 Component of the Q-learning framework- In Q-learning, the Q-table serves as the agent's brain, where the state and the action of the agent are the inputs of the Q-Table, and the Q-value of those inputs is the output of the Q-Table. Higher the Q-value, better the action, higher the received reward. 61

Figure 5.4 Multi-Agent: Average Cumulative Reward as a function of Number of Episodes (NEP) 67

Figure 5.5 Multi-Agent: Average Number of Handovers as a function of NEP 68

Figure 5.6 Multi-Agent: Average Blocking Rate as a function of NEP 69

Figure 6.1 5G ERA Enabling New Applications 74

Figure 6.2 Compositions of the proposed Deep Q-Learning strategy: Environment and Deep Neural Network (DNN) structure. The Environment is composed of a number of LEO satellites and users. The Deep neural network (Agent's brain) is composed of an input layer of dimensions equal to the state size, three fully connected hidden dense layers to learn the features of the state information, two drop-out layers, a flatten layer, and an output layer of dimension equal to the action space size 77

Figure 6.3 Q-Learning vs Deep-Q-Learning: Difference in the agent's brain. In Q-learning, the Q-table serves as the agent's brain, where the state and the action of the agent are the inputs of the Q-Table, and the Q-value of those inputs is the output of the Q-Table, while in Deep-Q-Learning a deep neural network acts as the brain, where the state is the input of the deep neural network and the approximation of all the Q-values of each corresponding possible action for this specific state are the output of the neural network. 78

Figure 6.4 Single TP: Average Number of Handovers as a function of the episodes for the five considered approaches: Minimum Distance, Minimum Load, MCLA(Load Aware), MARL(Load Balance), and MADQL . . 86

Figure 6.5 Single TP: Average Blocking Rate as a Function of the Number of episodes for the five considered approaches: Minimum Distance, Minimum Load, MCLA(Load Aware), MARL(Load Balance), and MADQL 87

Figure 6.6 Multiple TPs - MADQL: Average Cumulative Rewards as a function of the number of episodes 88

Figure 6.7 Multiple TPs - MARL: Average Cumulative Rewards as a function of the number of episodes 89

Figure 6.8 Multiple TPs - MADQL vs Minimum Load and Minimum Distance: Average Number of Handovers as a function of the number of episodes . 90

Figure 6.9 Multiple TPs - MADQL vs Minimum Load: Average Blocking rate as a function of the number of episodes 92
Figure 6.10 Multiple TPs - MADQL vs Minimum Load and Minimum Distance: Average Number of Handovers as a function of the number of episodes with 80% of the users requiring a high number of resources ($TP1$ or $TP2$) and 20% a low number of resources ($TP3$ or $TP4$) 93
Figure 6.11 Multiple TPs - MADQL vs Minimum Load: Average Blocking rate as a function of the number of episodes with 80% of the users requiring a high number of resources ($TP1$ or $TP2$) and 20% a low number of resources ($TP3$ or $TP4$) 94
Figure 6.12 Multiple TPs - MADQL vs Minimum Load and Minimum Distance: Average Number of Handovers as a function of the number of episodes with 20% of the users requiring a high number of resources ($TP1$ or $TP2$) and 80% a low number of resources ($TP3$ or $TP4$) 95
Figure 6.13 Multiple TPs - MADQL vs Minimum Load: Average Blocking rate as a function of the number of episodes with 20% of the users requiring a high number of resources ($TP1$ or $TP2$) and 80% a low number of resources ($TP3$ or $TP4$) 96

Figure 7.1 Charging and Discharging statuses of a LEO satellite 102
Figure 7.2 Average Cumulative Rewards as a function of the number of episodes 109
Figure 7.3 Average Number of Handovers as a function of the number of episodes 110
Figure 7.4 Average Blocking Rate [%] due to insufficient Channel Resources 111
Figure 7.5 Average Blocking Rate [%] due to insufficient Energy Resources . 111

List of Tables

Table 3.1 Simulated scenario design parameters 39
Table 3.2 Handover Traces UE0 41

Table 5.1 Simulated scenario parameters 66

Table 6.1 Simulated scenarios parameters 84
Table 6.2 Methods Comparison: comparison of the Minimum Distance, Minimum Load, MCLA, MARL, and MADQL methods for a single traffic profile (left-hand side) and for multiple traffic profiles (right-hand side) 91

Table 7.1 Simulated scenario parameters 108

Glossary

3GPP 3^{rd} Generation Partnership Project. 16, 20, 30, 75

4G Fourth-Generation of Mobile Communications. 14, 15, 20, 30

5G Fifth-Generation of Mobile Communications. vii, 1, 9, 10, 14, 15, 17–21, 24, 25, 27–30, 32–38, 40, 42, 55, 62, 70, 71

ADT Average Delivery Time. 38

AI Artificial Intelligence. 23

BWP Bandwidth Part. 21, 28, 33–37

CC Component Carrier. 21, 28, 33–37

CN Core Network. 33, 35

DNN Deep Neural Network. xv, 77–79, 81, 82, 86, 106, 107

DQL Deep Q-Learning. 77–81, 104, 106

DQN Deep Q Network. 107

eMBB Enhanced Mobile Broadband. 40

EMS Electromagnetic Spectrum. 11

EPC Evolved Packet Core. 30

ESA European Space Agency. 28

FDD Frequency Division Duplexing. 30

gNB Next Generation Base Station. 20, 21, 28, 32, 33, 35–38, 40–43

HO Handover. 2–7, 21–24, 46–48, 53, 54, 57, 60, 63, 67–71, 73–75, 79, 80, 83–87, 90–93, 95–97, 100, 103–105, 108, 109, 112–115

IoT Internet of Things. 23, 73

LAA Licensed Assisted Access. 29

LASH Load Aware Satellite Handover. 68–70

LBEASH Load Balancing Energy Aware Satellite Handover. 24, 100, 106, 109, 112

LBSH Load Balancing Satellite Handover. 54, 64, 67–71, 77

LDPC Low-density parity-check. 31

LEO Low Earth Orbit. vii, xiv, xv, 2–4, 18, 21, 24, 25, 28, 29, 31, 35, 38, 40–42, 45, 46, 48, 53–55, 57, 63, 73, 75, 77, 78, 83, 100, 106, 108, 113

LTE Long Term Evolution. 29, 30

LTE-A LTE-Advanced. 29

LTE-U LTE-Unlicensed. 29

MADQL Multi-Agent Deep Q-Learning. 5, 74, 81, 86–88, 90–95

MARL Multi-Agent Reinforcement Learning. 22, 23, 58, 74, 84–87, 89

MCLA Multi Criteria Load Aware. 83, 85, 87, 89

MCS Modulation Coding Scheme. 31

mMTC Massive Machine-Type Communication. 40

MTS Mobile Telephone System. 11

NEP Number of Episodes. xiv, 61, 67–69

NoE Number of Episodes. 84, 89, 107, 109

NR New Radio. vii, 20, 29–31, 38

NS-3 Network Simulator 3. 20, 27–32, 62, 83, 114

NSA Non-Standalone. 14, 15, 30

NTN Non-Terrestrial Networks. vii, 20, 21, 28, 35, 38, 40

OFDMA Orthogonal Frequency-Division Multiple Access. 31

QoE Quality of Experience. 22

QoS Quality of Service. 2, 24, 47, 87, 100

RAN Radio Access Network. 30, 33, 55

RL Reinforcement Learning. 22, 23, 58, 60, 61, 63, 64, 83, 92

RR Resource Requirements. 23, 24, 89

RSS Received Signal Strength. 22

RVT Remaining Visibility Time. 21, 24, 41, 42, 62, 63, 65, 68, 80, 84, 100, 104

SA Standalone. 14, 15

SINR Signal-to-Interference-Plus-Noise Ratio. 19

SLS System Level Simulator. 19, 20, 27, 28

STIN Satellite-Terrestrial Integrated Network. 5, 6, 21, 28, 32, 35, 67, 70, 71, 83, 85, 106, 112, 114

TDD Time Division Duplexing. 30

TDMA Time-Division Multiple Access. 31

TLE Two-Line Element. 31

TP Traffic-Profiles. 3, 23, 35, 73–77, 81, 84, 85, 90, 91, 95–97, 106, 108, 112

TTI Transmission Time Interval. 31

UE User Equipment. xiii, xiv, 2–4, 22–24, 32, 33, 35–42, 46–48, 54, 55, 57, 58, 64, 67, 68, 70, 73, 75, 77–81, 83, 84, 87, 89, 91, 95, 100, 102–104, 106–109, 112, 114

VR Virtual Reality. 23

Chapter 1

Introduction

1.1 Motivation and Objectives

Today's world is driven by a growing need for communication between people and objects. In recent years, the demand for heterogeneous, reliable, secure, low-latency, broadband, and high-speed services has exploded in wireless communications. This phenomenon motivated the definition of new standards and technologies, known as 5G [1]. Currently, 5G is the hot topic of the world's leading telecommunication companies. It is the first generation that devotes itself to connecting both humans and machines at any time and from any location by using wireless technologies in a variety of applications. The promising benefit of 5G is creating a suitable ecosystem for technical and business innovation involving vertical markets such as automotive, energy, food and agriculture, city management, government, healthcare, manufacturing, public transportation, and public safety, among many others. In comparison to the current wireless technologies, 5G is intended to deliver significantly increased network capacity ($\times$ 1000), enable huge device connection density with lower latency and cost, give ubiquitous coverage, and achieve significant energy savings.

Thus, the telecommunications industry is evolving towards expanding services and extensively exploiting the anywhere-anytime communication paradigm which has led to unprecedented requirements [2]. Terrestrial technologies, however, cannot solely fully meet these high requirements, since they are not worldwide present and can be damaged by wars or natural disasters. To deal with these challenges and ensure global connections, many researchers have focused on the integration of satellites with terrestrial networks.

Satellite communications can help next-generation communication technologies extend their reach to where terrestrial networks are incapable of providing Internet access, such as in remote areas or on high-speed vehicles (e.g., airplanes and high-speed trains) [3]. This makes them the most efficient way to reliably link the world's neglected, hard-to-reach, and poorly served places. The integration of satellite communications with terrestrial networks has attracted the interest of many researchers [4–9], especially LEO satellites, whose altitudes range between 200 and 2000 km, due to their low propagation delay, suppressed signaling attenuation, low power to transmit, and low operational costs for satellite deployment and maintenance compared to other satellites with different altitudes [10]. Figure 1.1 shows the main use cases where satellites can offer benefits in communications.

LEO satellites, on the other hand, orbit Earth quickly, with a consequent limited window of visibility between each satellite and a ground UE. This needs regular Handover (HO)s to provide stable communications as satellites frequently shift coverage areas [11]. This aspect prompted the development and deployment of ultra-dense constellations, such as the Starlink project, to cover large portions of the world simultaneously. They generally guarantee that each ground UE will be covered by more than one LEO satellite at any given time, posing the difficulty of picking the best satellite to ensure the best Quality of Service (QoS) per UE. Moreover, LEO satellites have limited onboard resources, while, at the same time, billions of devices that support an unprecedented variety of

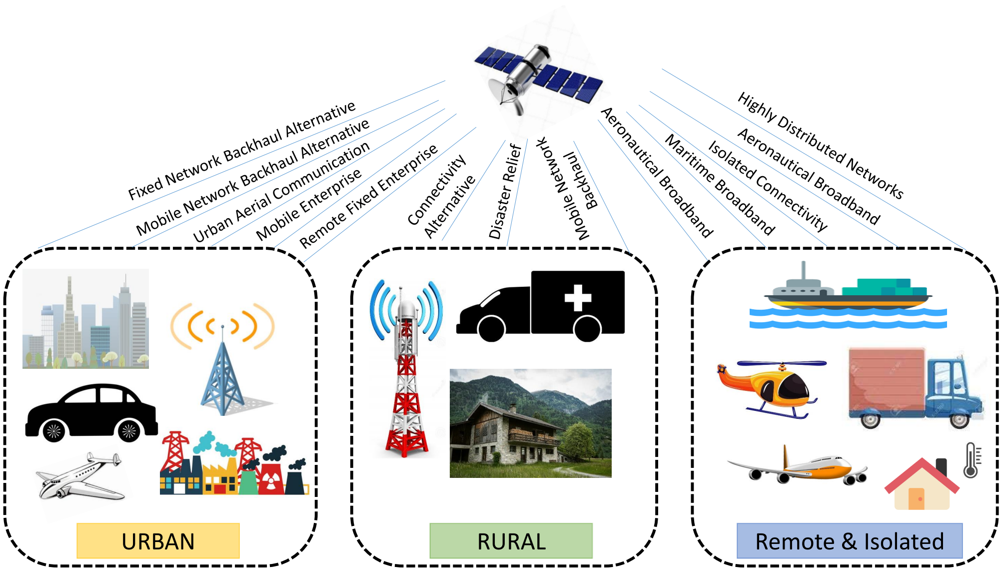

Figure 1.1: Satellite use cases in 5G Networks

emerging applications must be served globally [12]. Those various applications led to distinguishing different UE's Traffic-Profiles (TP)s, i.e., applications with different resource and performance requirements. To solve this issue and meet the increasing demand, it is critical to consider the limited satellite's available energy and bandwidth resources in the HO criteria, in order to fully exploit the available resources and prevent network congestion.

Hence, managing HO in LEO satellite networks presents a significant challenge in enabling worldwide mobile communication. It is crucial to develop efficient and precise techniques for facilitating seamless LEO satellite HOs as the satellite constellations move across the sky. Researchers are primarily focused on ensuring a dependable service for users to prevent communication disruptions resulting from HOs, where frequent HOs can lead to a significant signaling overhead, resource consumption, and UE dissatisfaction due to interruptions [13–15].

Mainly due to the lack of already deployed satellite systems implementing 5G technologies, especially the 5G New Radio (NR) Radio Access Technology (RAT), The best option is to proceed with a simulation approach. However, due to the lack of proper simulation tools suitable for our needs, we decided to develop an ad-hoc network simulator considering what was available at the state-of-the-art and developing code parts to properly integrate already available components.

The primary objectives of this thesis encompass the development and exploration of innovative solutions in the realm of satellite-terrestrial integrated networks (STIN). These objectives are driven by the need for efficient, robust, and adaptive satellite communication systems within the context of evolving terrestrial networks and diverse user requirements. The specific objectives that guided this research are:

1. Development of an open-Source Satellite-Terrestrial Integrated Network (STIN) Simulator, to address the limitations of existing simulation tools, and incorporates features such as modeling 5G New Radio cellular networks and satellite communication networks. That allows researchers to implement and test their proposed strategies in a simulation environment that is close to the real-world scenario before being incorporated into live systems, which reduces the time and cost required to test these systems.

2. Development of a LEO satellite HO management strategy that can reduce the number of HOs and minimize the blocking rate by balancing the load among satellites taking into account different and varying resource requirements per UE. These objectives are particularly critical in scenarios involving LEO satellite networks, where frequent HOs can lead to a significant signaling overhead, resource consumption, and UE dissatisfaction due to interruptions.

3. Synthesize the knowledge of satellite energy availability and consumption to devise a strategic approach that enhances the performance of satellite networks, by intelligently utilizing energy information in the HO strategy.

4. Analyzing the performance measures of proposed HO management models in a Satellite-Terrestrial Integrated Network (STIN) scenario created within the NS-3-based STIN simulator to test it in closer to the real-world testbed.

1.2 Contributions

This thesis makes significant contributions to the field of satellite-terrestrial integrated networks, addressing critical challenges and advancing the state of the art. The key contributions of this research are:

1. Development of an Open-Source STIN Simulator: The creation of an open-source STIN simulator built on NS-3, capable of modeling 5G New Radio cellular networks and supporting NTN communications. This simulator offers a valuable resource for researchers and practitioners in the field.

2. Development of a novel decentralized HO strategy based on reinforcement Q-learning, offering substantial reductions in the number of HOs and blocking rates, contributing to network efficiency and user experience.

3. Development of a novel Multi-Agent Deep Q-Learning (MADQL)-based HO optimization approach that takes into account the variation and diversity of performance requirements of different UE classes. It allows more efficient management of the limited available satellite resources and achieves a low blocking rate per user.

4. Development of a load balancing energy aware satellite HO strategy, taking into account satellite energy constraints when making HO decisions, leads to eliminating unnecessary handovers and a zero blocking rate.

5. Implementation of all the proposed methods to access HO decisions in a STIN scenario created within the NS-3-based STIN simulator that tests them and proves their efficiency in a closer to the real-world testbed.

1.3 List of Publications

This dissertation is based in part on the following publications:

- Badini, N., Marchese, M. and Patrone, F., 2022, June. NS-3-based 5G Satellite-Terrestrial Integrated Network Simulator. In 2022 IEEE 21st Mediterranean Electrotechnical Conference (MELECON) (pp. 154-159). IEEE.
- Badini, N., Jaber, M. Marchese, M. and Patrone, F., 2023, Reinforcement Learning-Based Load Balancing Satellite Handover Using NS-3. In 2023 IEEE International Conference on Communications (ICC). IEEE.
- Badini, N., Jaber, M. Marchese, M. and Patrone, F., 2023, Energy-Aware Satellite Handover based on Deep Reinforcement Learning. In 2023 IEEE Global Communications Conference (GLOBECOM). IEEE.
- Badini, N., Jaber, M. Marchese, M. and Patrone, F., 2023, User Centric Satellite Handover for Multiple Traffic Profiles Using Deep Q-Learning. Under major revision to IEEE Transactions on Aerospace and Electronic Systems (TAES). IEEE.

1.4 Organization of the Thesis Document

The rest of the thesis is organized as follows:
Chapter 2 begins with a historical perspective, tracing the evolution of communication networks and satellite communications separately. It offers a comprehensive overview of their respective developments. The chapter then delves into the contemporary

landscape of satellite integration into 5G networks, with a particular focus on satellite network simulators and strategies for seamless satellite HOs.

Chapter 3 introduces the satellite-terrestrial integrated network simulator that has been implemented for this study. In this chapter, A detailed breakdown of the simulator's primary components is provided, and the complexities of how they are integrated are explained.

Chapter 4 provides an overview of handover management in 5G differentiating between terrestrial and satellite base station scenarios.

Chapter 5 focuses on the development, implementation, and evaluation of a load-balancing satellite HO method. This chapter furnishes concrete evidence of its success in achieving load balancing and minimizing the probability of blocking in scenarios involving single traffic profiles.

Chapter 6 is dedicated to detailing the methodology used to implement a user-centric satellite HO strategy. This strategy is specifically tailored to optimize HO decisions, particularly in multi-traffic profile scenarios, ensuring a superior quality of service.

Chapter 7 delves into the technical intricacies of a groundbreaking load-balancing, energy-aware satellite HO approach. The overarching objective of this chapter is to synthesize knowledge about satellite energy availability and consumption to devise a strategic approach that enhances satellite network performance. By intelligently utilizing energy information in our HO strategy, The aim is to minimize the number of HOs and reduce blocking rates, ultimately providing a smoother and more reliable user experience.

Chapter 8 concludes this thesis, summarizes major contributions, and presents possible research directions for further investigation.

Chapter 2

Literature Review

2.1 Introduction

The integration of satellites into the structure of 5G networks has emerged as a critical area of study and innovation in the fast-evolving environment of modern telecommunications. The integration of terrestrial and satellite networks has a huge potential for bringing in a new era of communication capabilities as demand for seamless connectivity, ultra-high data speeds, and ubiquitous coverage continues to rise. This chapter investigates the multidimensional route toward "Integration of Satellites into 5G Systems". This investigation unfolds across a series of interconnected sections, each offering a distinct viewpoint on the main issue. It begins with section 2.2 that summarizes the progressive evolution of communication technology. It sets the foundation for understanding the drive for the integration of satellite communication within this paradigm by providing a historical background that highlights the dynamic factors leading to the development of the fifth generation - 5G. Then, section 2.3 focuses its attention on the historical evolution of satellite communications and their integration with the 5G architecture. As satellites grow from isolated systems, they provide a unique contribution to complementing terrestrial networks by extending coverage to remote places, providing important services, and increasing network resilience. This combination demonstrates the benefits and challenges of the integration of satellites into 5G. The next section 2.4 explores the available satellite network simulators, which are vital tools for understanding the complexities of integrated satellite-5G networks. These simulators enable academics and engineers to model and analyze diverse situations, test innovative algorithms, and forecast network behavior prior to real-world deployment. This section investigates improvements in simulation approaches, offering insight into simulation-driven research that drives the smooth incorporation of satellites into the 5G ecosystem. Section 2.5 analyzes the difficulties associated with satellite handovers and examines the unique solutions used to provide continuous interrupted communication experiences. Finally section 2.6 provides a comprehensive conclusion of this chapter.

2.2 Communications Evolution

Telecommunications systems are increasingly playing a vital role all over the world. In fact, the rapid development of communication and information technologies in a constantly changing world has paved the way for the rapid growth of communication applications that use digital technologies with new application systems and the ability to send and receive data over the network. The evolution of mobile wireless communication systems has advanced through different stages in the last few decades. In the mid-1860s, James Clerk Maxwell's equations predicted the presence of electromagnetic waves, which were later proved experimentally. It took around 20 years to confirm these predictions, and another 20 years for practical applications to emerge [16]. Guglielmo Marconi established practical mobile radio communication in 1899 by delivering historic radio telegraph signals from a ship to the Twin Lights in New Jersey. These broadcasts used high-energy radio noise pulses created by a spark generator and detected by a "coherer" device that sensed radio signals by altering the coherence of metallic particles within it [17]. Marconi enhanced his system within a year by adding filtering to allow numerous simultaneous transmissions in the same region. He accomplished transatlantic radio transmission in three years. Radio telegraphy was widely used on ocean-going boats and had an important part in reporting incidents such as the Titanic's sinking in 1912. Although analog voice transmission began in 1905, it was first driven by military requirements. In 1919, an experimental ship-to-shore radiotelephone service began, and commercial radio-telephony for ship passengers began in 1929. Radios were compact and durable enough at this time to be installed in vehicles, resulting in the first "land mobile" radio system developed by the Detroit police in 1928. The trend continued, with municipal and state police departments establishing radio stations and outfitting police cars by 1934, starting the age of mobile radio [18].

The Mobile Telephone System (MTS) was the first civil mobile system, launching in 25 locations throughout the United States in 1946 [19]. The MTS used push-to-talk technology to communicate. A central station supplied communication services to all of the city's mobile users (MUs). This centralized service, along with the bandwidth constraints imposed on all wireless systems to manage the Electromagnetic Spectrum (EMS), severely limits the MTS's capabilities. The concept of cellular phone networks, established at Bell Labs in the 1940s [20], addressed network congestion issues and facilitated the widespread adoption of mobile telephony. The core idea was to enhance network capacity by partitioning the coverage area into smaller cells. Within each cell, a base station (BS) links to the public phone network to provide services. The concept allows for the assignment of separate RF channels to nearby cells in order to prevent interference between them, as well as the reuse of RF channels in cells that are far enough apart to create insignificant interference. The cellular network architecture is the foundation of commercial mobile telephony, and these communication networks are thus referred to as mobile cellular networks. Each generation of mobile cellular networks has been created over a ten-year period, with the need to increase coverage, attain better transmission rates, and offer new mobile services driving the shift to the next generation [21].

At the end of the 1970s, the First Generation (1G) of mobile cellular networks hit the commercial market. Japan was the first to build a 1G network then deployed in the Nordic nations (Norway, Sweden, Denmark, and Finland) in 1981. By the mid-1980s, 1G networks were available in the United Kingdom, the United States, Canada, and Mexico. This initial version was created with analog technology for voice services. It had a low spectral efficiency, and because there were no international agreements governing the usage and control of such networks, a broad range of incompatible standards were in use. As a result, the service was limited to national – and even regional – coverage [17]. Despite their incompatibility, all 1G networks used Frequency Division Multiple Access (FDMA) technology and used circuit switching to connect calls. Sections of the 800 MHz spectrum were set aside for 1G in Japan and the United States. Meanwhile, Sweden and the United Kingdom have reserved the 900 MHz spectrum, while Germany and France have picked the 450 and 200 MHz frequencies, respectively [22]. However, 1G has several shortcomings as unencrypted communications pose a serious problem since they allow anybody with a radio scanner to join a connection. Additionally, it had flaws including bad audio quality, insufficient coverage, no support for roaming between operators, and incompatibility with equipment that used several frequency bands.

The second generation of mobile communications 2G was introduced to address the drawbacks of first-generation analog technology. 2G cellular networks began operating in the early 1990s and was distinguished by the transition to digital technology. The employment of time-division multiple access (TDMA) and code division multiple access (CDMA) techniques, as well as the advent of channel coding techniques, enhanced spectral efficiency. Support for data transfer for short message service (SMS) was a significant invention. The commercial success of 2G networks was due to the creation of international standards, particularly the Global System for Mobile Communications (GSM) and the Interim Standard 95 (IS-95) [23]. Both standards use a circuit switched design to broadcast in the 810 and 960 MHz frequencies. With GSM's high-speed circuit-switched data augmentation, the potential data transmission speed of 2G was 115.2 kbps. The digital foundation of the 2G service enabled the emergence of tiny hand-held phones with more efficient battery consumption. However, because the communications were based on circuit switching, which is ideal for voice traffic but not for data traffic, 2G networks transferred data inefficiently.

In the early 2000s, the switch to third generation (3G) cellular networks began. One of the most significant 3G advancements was the ability to handle both circuit and packet switched connections; the latter are essential for Internet Protocol (IP) services. This generation enabled the introduction of new mobile services, such as Internet access and video calls. 3G RAN is based on CDMA technology, with the primary 3G standards being wideband CDMA (WCDMA) and CDMA 2000 [24]. Both standards are worldwide in scope, with theoretical downlink (DL) transmission rates of up to 14.4 Mbps [22]. 3G networks paved the way for smart phones, which included a more tactile and visually pleasing interface, as well as a processing engine that enabled a variety of mobile apps.

The fourth generation (4G) deployment began in early 2010, with a peak transmission rate of up to 300 Mbps on the downlink (DL) and 75 Mbps on the uplink (UL); however, with subsequent enhancements, these networks attain rates of up to 1 Gbps on the DL [25]. The orthogonal frequency division multiple access (OFDMA), single carrier FDMA (SC-FDMA), scalable OFDMA (SOFDMA), and multiple-input multiple-output (MIMO) transmission methods are used in 4G RAN. Long Term Evolution (LTE) and its enhanced variant, LTE enhanced (LTE-A), are the primary 4G protocols [26]. The communications sector has grown significantly as a result of the investment of several commercial companies and the special attention of governments. The growth of mobile devices and different services, on the other hand, has revealed issues in fourth-generation mobile communication systems, such as excessive power consumption and inadequate frequency spectrum. Those difficulties indicate that 4G systems are not able to fulfill future needs, which accelerated the transition to the next generation of 5G mobile communication systems.

Fifth generation of mobile communication 5G is more than a simple evolution of 4G, it brings a new revolution to data transmission, as it aims to achieve universal wireless connection, allowing for seamless communication across a wide range of applications and locations. This technology has the potential to enable innovation in a variety of industries that extend well beyond smartphones, including automotive, energy, healthcare, and others. In contrast to present wireless technologies, 5G is expected to provide greatly higher network capacity, greater device connectivity with lower latency and costs, broad coverage, and improved energy efficiency. The main attributes of 5G are ultra-reliable low latency communication (uRLLC), enhanced mobile broadband (eMBB), and massive machine-type communication (mMTC).

There are two deployment modes for the fifth generation of mobile networks. While planning the deployment, mobile network operators must select between Standalone (SA) 5G core and Non-Standalone (NSA) 5G. SA and NSA, on the other hand, utilise a 5G New Radio interface and have capabilities and characteristics defined by 3GPP [27]. The service provider can use the existing 4G LTE core infrastructures to manage the control plane and signal traffic in the 5G non-standalone solution. Using the dual connection, 5G RAN might be built on top of the current Fourth-Generation of Mobile Communications (4G) infrastructure. It is reliant on 4G and 5G base stations. NSA dominates early 5G deployment and is the primary choice for many MNOs, particularly those unprepared for the first large investment and unable to handle the price of migrating to 5G networks. However, there are a few limitations to NSA 5G [28].

Although it lowers initial deployment costs, it lags behind SA 5G in some locations. Because it employs two distinct cellular technologies, the NSA necessitates significant power consumption. Furthermore, it lacks low latency, which is a critical 5G capability. 5G SA is comprised of a completely new core architecture that is distinct from existing 4G and legacy networks and is not dependent on 4G networks in any way. 5G SA is a completely new virtualized network that is intended to be more efficient than NSA and capable of delivering critical 5G services. Unlike the NSA network, the SA network can perform critical 5G services including improving latency and centrally regulating network management operations [29]. On the other side, 5G SA is highly expensive to deploy, and it might take a long time for specialists to master and grasp the infrastructure. Regardless, the bulk of carriers are considering migrating to SA in order to gain the benefits of genuine 5G.

The telecommunications industry's advancement towards comprehensive services and the ubiquitous anywhere-anytime communication model has generated exceptional demands. Terrestrial technologies, however, cannot solely fully meet these high requirements, given their limited global presence and sensitivity to wars and natural disasters. To deal with these challenges and ensure global connections, many researchers have focused on the integration of satellites with terrestrial networks.

2.3 Satellite Communications

Satellite communications have been and continue to be an important part of people's daily lives for many years, such as receiving TV and radio, providing essential communications to remote land areas and on the sea or in the air, allowing us to see and predict our climate/environment, and allowing us to position and navigate actively. The Russian Sputnik-I (93 days) was the first satellite with an onboard radio transmitter launched on October 4, 1957. Project SCORE (Signal Communications Orbit Relay

Equipment), the first American satellite to relay communications, was launched on December 18, 1958. In 1960, NASA launched the Echo satellite. The Courier 1B was introduced on October 4, 1960, by the American company Philco. Telstar1, the first operating telecommunications satellite, was launched on July 10, 1962. The first relay of television pictures took place between the stations of Andover (EU) and Pleumeur-Bodou (France). Satellite communications have advanced at a breakneck pace since then. For example, the first communications satellite (IDSCS, Initial Defense Satellite Communication System) was launched in 1962, the first GEO communications satellite (Syncom II) was launched one year later, and the first military communications satellite (IDSCS, Initial Defense Satellite Communication System) was launched in 1965 [30]. The integration of satellites in the communication system has gained a lot of interest from academics and industries, as noticeable by the 3^{rd} Generation Partnership Project (3GPP) standardization activities in relation to the so-called Non-Terrestrial Networks (NTN). 3GPP has carried out studies to define the possible role of NTNs and the technical specifics of their integration in Release 15 [31] along with possible solutions from the networking viewpoint in Release 16 [32].

Satellite systems have suffered from a number of challenges over the last few decades, including technological complexities, increased prices, significant delay, and signal deterioration at high frequencies (Ka band). As a result, satellite communication has primarily served specific markets, such as professional use where terrestrial options were limited, radio localization (GPS, GNSS) using satellites as "radio-beacons", the Direct-To-Home TV (DTH) market for digital TV broadcasting (standard DVB-S) where satellites functioned as relay nodes, and, more recently, data backhauling in remote regions. In these applications, the utilization of satellite communication systems is typically motivated by their inherent strengths. These strengths include extensive coverage, rapid deployment, and built-in multicasting and broadcasting capabilities. These advantages are leveraged to compete effectively against conventional terrestrial networks [33]. Recent advances in satellite technology, such as the launch of High Throughput Satellites (HTS) in Geostationary Earth Orbit (GEO) with much greater throughput rates than their predecessors, are altering the satellite landscape with 100+ HTS systems expected to be in orbit by 2020-2025. These satellites will enable Tbps connectivity in the Ku and Ka bands at a lower cost [34]. Furthermore, novel concepts incorporating non-GEO constellations comprised of several low-cost micro-satellites are positioned to significantly lower bit transmission costs while improving Quality of Service (QoS) measures such as latency [35]. The changing environment is affecting market capacity dynamics, pushing down cost per bit and increasing the attraction of satellite broadband communications. Given this scenario, the distinct characteristics of satellite communication, such as extensive geographical coverage, inherent broadcasting/multicasting capabilities, and dependable connectivity, combined with significant amounts of new satellite satellite capacities, open up a variety of options for integrating satellite components into terrestrial communication networks. For instance, as discussed in [31], non-terrestrial access networks are anticipated to be integral to 5G service deployment by extending coverage to areas challenging for terrestrial networks, ensuring service reliability in the face of attacks and disasters, enabling widespread 5G network deployment, connecting airborne and moving platforms to 5G services, facilitating efficient multicast/broadcast services, and offering flexibility in traffic management between terrestrial and non-terrestrial networks. Moreover, satellite backhaul is one of the most attractive possibilities expected to gain popularity in 5G [36]. It can be useful in providing backhaul connectivity to base stations placed in difficult-to-reach places or installed on board a transportation/moving vehicle with no other viable options. Furthermore, satellite backhaul links can be deployed and operated in line with terrestrial backhaul links, resulting in increased network availability and resiliency (e.g. backup capacity for total/partial terrestrial link failures in critical cell sites), improved support for temporary cell deployments such as coverage of special events or emergency situations [37], and, ultimately, more efficient traffic delivery to base stations. A pool of satellite capacity, for example, can be used in conjunction with terrestrial capacity for traffic offloading and load balancing (e.g. diverting traffic from congested areas so that terrestrial capacity is supplemented during peak times), as well as for multicast/broadcast traffic delivery to multiple cell sites (e.g. content edge caches, live TV stream distribution) in a more resource efficient manner [37]. The integration of satellites into the communication system challenges, opportunities, key features, architecture, and standardization has been discussed in numerous articles [4–9].

Several studies have been done to propose solutions for those challenges. For example, Bao et al. proposed a novel satellite network architecture based on the idea of decoupling the data and control planes to gain high efficiency, fine-grained control, and flexibility [38]. In [1], a heterogeneous architecture in which a LEO mega-constellations satellite system provides backhaul connectivity to terrestrial 5G relay nodes is proposed. [39] presents a 5G edge node idea that was created and tested over-the-air utilizing geostationary satellites. Agapiou et al. developed a revolutionary satellite-terrestrial architecture that integrated NFV into satellite communication and made use of SDN-based resource management [40]. Wang and Yu presented a satellite network architecture based on SDN and virtualization, with a ground center controller and layer controllers in each satellite layer [41]. SoftSpace, a software-defined architecture for next-generation satellite networks, is proposed in [42]. SoftSpace makes use of the principles of network function virtualization (NFV), network virtualization (NV), and software-defined radio (SDR) to ease the introduction of new applications, services, and satellite communication technologies. The authors in [43] proposed enabling network architecture for dense LEO satellite access networks through various physical-layer techniques, such as effective interference management, diversity techniques, and cognitive radio schemes. In [44], a top-down network architecture for the integration of nanosatellites in 5G systems in the millimeter wave domain is described. The system performance is evaluated in terms of Signal-to-Interference-Plus-Noise Ratio (SINR) in the presence of fading, shadowing, and interference, and both random access and routing aspects are discussed. However, attaining total integration of a combined satellite-terrestrial backhauling scenario needs new tactics for the satellite component's flexible, efficient, and cost-effective functioning. This requires converting existing satellite ground segment systems, such as gateways and terminals, from closed to more open designs based on Software Defined Networking (SDN) and Network Function Virtualization (NFV) technologies [45, 46]. This move is expected to not only bring benefits from 5G network softwarization improvements to the satellite area, but also to considerably improve the smooth integration and operation of integrated satellite and terrestrial networks. Significantly, terrestrial 5G systems are increasingly utilizing SDN technology to offer unified, vendor-neutral networking control and management. As a result, satellite networks must have control and administration interfaces that are inter-operable with the standard SDN designs and 5G technologies. This alignment attempts to establish a full End-to-End (E2E) networking model in which the whole satellite-terrestrial network's behaviour may be configured in a coherent and interoperable way [47].

2.4 Satellite Network Simulators

To minimize the blind exploitation of new systems, new technologies should be verified and enhanced before being incorporated into live systems. Creating a System Level Simulator (SLS) is an excellent way to evaluate new ideas. It can allow effectively studying the system performance and evaluating different implementation options, minimizing the cost and time required to test these systems. Several research activities were aimed at developing 5G communication and network simulators equipped with different functionalities. For example, "5G KSimulator" [48] was developed at the

Korean Institute of Science and Technology. It is capable of running in a cloud computing environment. However, at the time of writing, the source code was not available, limiting further assessments. 5G extension for Simu5G Omnet++ simulator was created at the University of Pisa [49]. It is an evolution of the SimuLTE 4G network simulator that incorporates 5G NR access. The idea behind Simu5G is to let researchers simulate and benchmark their solutions on an easy-to-use framework. It borrows the concept of modularity from OMNeT++ (a C++ simulation library and framework, used primarily for building network simulators), thus it is easy to extend but requires a commercial license for industrial usage. Politecnico di Bari proposed what is called "5Gairsimulator" [50]. 5G-air-simulator is an open-source and event-driven tool that models the key elements of the 5G air interface from a system-level perspective. It allows a flexible configuration, arrangement, and extension of its capabilities to model both new scenarios and new technical components. However, it focuses only on the air interface technology. A Matlab-based 5G system simulator was developed by the Vienna University of Technology [51]. This simulator requires various licenses, as it was licensed under an academic license, which makes it not suitable for commercial use. With the Satellite Communications Toolbox, MATLAB [52] provides a powerful tool for planning, modeling, and validating satellite communication networks. It is, however, a paid program, thus open-source alternatives such as OMNeT++ [53] and ns-3 [54] are preferable. For network topology definition, OMNeT++ features a proprietary NED language and a graphical interface, whereas ns-3 provides precise packet representation and interoperability with other analysis tools like Wireshark. Recently, the authors in [55] proposed a SLS by using the Network Simulator 3 (NS-3) network simulator for 5G NTN evaluations that has a very important role in the 3GPP standardization process, as it can be exploited to study the integrated system performance and to evaluate different implementation options and parameterizations. However, they assumed a transparent satellite payload, where the Next Generation Base Station (gNB) is on the ground and the satellite acts only as an analog radio frequency repeater. Whereas in this project, the satellite was assumed to serve as the 5G NTN gNB, in order to fully exploit the integration of satellites into 5G systems that allow simulating 5G STIN which overcomes the state-of-the-art solutions by supporting NTN handover decisions, dynamic Bandwidth Part (BWP) selection, and Component Carrier (CC) configurations based on different defined traffic profiles as will be discussed in Chp.3.

2.5 Satellite Handover Strategies

Since the position of the base stations in terrestrial networks is fixed, users typically perform HO due to users' movements and based on the measured received signal strength, reference signal received power, or reference signal received quality [56]. However, LEO satellites move at a very high speed and rapidly change their footprints on the Earth's surface, which makes the satellites' movements the main reason for HO and the above measurements not fully applicable. Thus, other parameters should also be considered, such as remaining service time, number of available resources, and received signal strength. For instance, in [57] and [58] the number of available channels per satellite was regarded as the fundamental HO criterion. To achieve minimal drop blocking and enforced termination chances, the authors in [57] separated the multimedia traffic into two groups and handled the satellite HO requests according to the queue condition of each traffic type. On the other hand, in order to prevent resource reservations, the authors in [58] suggested a dynamic Doppler-based HO prioritizing approach that utilizes Doppler shift monitoring to estimate the number of HO demands along with the actual occurrence time. The HO criterion adopted in the aforementioned papers can establish a balanced load in the system, but cannot ensure high communication quality since it may lead to a severe number of HO events with consequent unstable and often interrupted communications. The highest Remaining

Visibility Time (RVT) is considered as the main criterion for satellite selection in [59] and [60]. This criterion significantly reduces the number of HO occurrences, and thus reduces interruptions, at the cost of a high blocking rate per UE. The authors in [61] introduced an antenna gain-based HO strategy that takes advantage of the predictability of satellite movement and the antenna gain of satellite beams to reduce service failures and unwanted HO events. An inter-satellite HO approach based on potential game theory is presented in [62] for the purpose of lowering the average number of HO occurrences and balancing the constellation network load. A handover control strategy based on the Received Signal Strength (RSS) is suggested in [63]. However, multiple UEs could connect to the satellite that has the best RSS, which can cause access congestion on that satellite and result in extreme load imbalance among the satellites. Authors in [64] performed a mobility performance study of the Release-16 conditional HO which reduces the radio link and HO failures but numerously increases unnecessary HOs rate.

The mentioned literature papers only analyze a single handover criterion for a given optimization aim, making it difficult to propose a complete and satisfactory solution. Therefore, many studies have emphasized the use of Reinforcement Learning (RL) multi-criteria decision-making processes to reach an overall satellite selection solution. For example, the authors in [65] presented a Load-aware Multi-Agent Reinforcement Learning (MARL) HO approach that intends to limit the number of HOs while taking into consideration the load of the satellite. They considered two HO criteria, which are the minimum elevation angle and the currently available satellite channels and have been able to achieve a lower blocking rate compared to load-unaware systems. The authors in [66] adopted a RL strategy that takes into account the service time, communication channel resources, and the relay overhead for the HO events execution in order to maximize the UE's Quality of Experience (QoE). The authors in [67] proposed a RL satellite HO scheme that aims to reduce the number of satellite handovers while minimizing the handover-failure rate by taking into consideration the carrier-to-noise ratio and interference-to-noise ratio criteria.

Most recent studies either evaluate one HO criterion for a given optimization objective or propose a method that considers numerous criteria from the perspective of a single UE only. Nonetheless, in the absence of a central controller, UEs may only obtain limited information about the satellite system in relation to themselves. Additionally, due to the limited satellite channel budget, competition for available channels between UEs served by the same satellite may potentially lead to a severely unbalanced satellite load. This mandates the adoption of a decentralized (user-centric) satellite HO method that considers the UE's real-time resource competition. For example, the authors in [65] used multi-agent RL, and the authors in [68] and [69] used multi-agent deep-RL to tackle the decentralization challenge by treating each user as an agent with a partial perspective of the system and the ability to take actions independently. However, these approaches do not encourage load balancing among satellites, as they do not provide preference for connecting to the satellite with more available channels, increasing the likelihood of future UE blockage. Therefore, a load-balancing HO technique was implemented with a distributed MARL that was successful in minimizing the number of HOs and lowering the blockage rate by balancing the load among the satellites, as will be discussed in Chp. 5

Moreover, next-generation communication technologies are intended to support the unprecedented diversity of various emerging applications, such as Artificial Intelligence (AI), Virtual Reality (VR), three-dimensional media, and the Internet of Things (IoT), which have led to distinguishing UEs with different and varying TP, i.e., different performance requirements and generated traffic statistics, from the network resource viewpoint. This requires the implementation of a satellite HO strategy that respects the varied Resource Requirements (RR) per TP to efficiently use the limited available resources and avoid network congestion. However, to the best of our knowledge, there is no study that takes into consideration the diversity of UEs applications where each user has different and varying RR. This makes the available studies limited to one type of application. Supporting the diversity of various emerging applications is the main innovation aspect introduced in the user-centric Multi-Agent Deep Q-Network (MADQN) satellite HO strategy that has been implemented and discussed in Chp. 6. On the other hand, LEO satellites have limited onboard resources, thus to meet the increasing demand of connectivity for those various types of applications, it is critical to consider the limited satellite's available energy and bandwidth resources in the HO criteria, in order to fully exploit the available resources and prevent network congestion. To address the aforementioned challenges, a Load Balancing Energy Aware Satellite Handover (LBEASH) strategy will be proposed, that takes into account various factors, such as elevation angle, RVT, amount of available bandwidth, and energy resources per satellite, and accordingly assists each UE in selecting the best satellite candidate from its covering satellite set to ensure the required QoS throughout the entire communication duration, avoiding unnecessary HOs and achieving zero blocking rate per UE as will be discussed in Chp. 7

2.6 Conclusion

This chapter delves into the current hot topic of integrating satellites into the 5G infrastructure. It has investigated the dynamic evolution of communication systems over generations, leading to the present convergence of satellite and terrestrial networks within the 5G environment. The chapter addressed how satellite technologies have progressed from their historical isolation to play a revolutionary role in supplementing terrestrial networks. This convergence paradigm takes advantage of satellites' unique characteristics to expand coverage to remote places, support important services, and improve network resilience in the face of increasing demands.

The potential integration between satellite and terrestrial networks has been emphasized as an essential factor in achieving the 5G revolution's high goals. While this integration provides outstanding benefits, it also introduces new obstacles that need innovative solutions. The importance of satellite network simulators in understanding integrated systems and smooth handover techniques to assure continuous connectivity was covered in the chapter. Several studies have focused on those two aspects and suggested different solutions to insure the optimal integration of satellites into the 5G systems. Different satellite simulators that have been developed in the state of the art were presented and discussed in this chapter. In addition to the literature review that focuses on the use of LEO satellites in this integration due to their capacity to attain reduced propagation latency, minimal transmission loss, and low transmit power demands. However, LEO satellites orbit the Earth at high speed, resulting in a narrow window of visibility between each satellite and a ground user. This needs regular Handovers to provide stable communications as satellites frequently shift coverage areas. Multiple researchers used different machine learning techniques for implementing effective handover techniques that take into account multiple expectations avoiding single manual thresholds.

This in-depth investigation lays the basics for understanding the benefits and challenges of combining satellite and terrestrial networks in the 5G future.

Chapter 3

NS-3-based 5G Satellite-Terrestrial Integrated Network Simulator

3.1 Introduction

In order to realize the full potential of 5G networks, the integration of satellite and terrestrial communication systems arises as an important issue. This chapter introduces a significant improvement in this field, introducing the "NS-3-based 5G Satellite-Terrestrial Integrated Network Simulator." This simulator is an effective tool for learning the complexities of integrated communication systems, allowing performance evaluation, and paving the road for innovative advancements. It is an excellent way to evaluate new ideas since it can enable effectively studying the system performance and evaluating different implementation options, minimizing the cost and time required to test these systems. Even though several SLS have been created, they were intended to simulate networks with only one type of access technology which limits their uses considering the demand for the interworking among various access technologies, which will include a combination of different terrestrial and satellite networks. In this chapter, an open-source SLS [70] is proposed, which is based on the software NS-3 and was under development within the European Space Agency (ESA) project "Data-driven Network Controller and Orchestrator for Real-time Network Management – ANChOR" [71]. The developed Simulator prototype is a C++-based software that allows the simulation of 5G satellite-terrestrial networks. In principle, it has been developed and is used within the project to simulate networks where LEO satellites operate as 5G access nodes, i.e., gNBs, even if it can be easily used to simulate networks where satellites have a different role, such as backhaul. The developed 5G STIN overcomes the state-of-the-art solutions by supporting NTN handover decisions, dynamic BWP selection, and CC configurations based on different defined traffic profiles.

The rest of the chapter is organized as follows. Section 3.2 describes in detail our developed 5G-NTN SLS, highlighting the integration effort among the different main simulator components. These components serve as the foundation for a complete model that simulates the dynamics of real-world 5G satellite-terrestrial networks. Section 3.3 evaluates the simulator's ability to reproduce real-world circumstances and is tested through some preliminary performance results obtained considering a defined simulated scenario with satellite gNB making a comparison with a second simulated scenario with terrestrial gNB. Finally, Section 3.4 provides the conclusions of the present work.

3.2 5G SATELLITE-TERRESTRIAL NETWORK SIMULATOR

Within this section, The developed 5G NTN simulator will be introduced. The Simulator's foundation was formed by exploiting existing resources instead of creating an entirely new solution. This strategy attempted to shorten development time by finding well-established software platforms that could be used as a starting point before being modified and seamlessly integrated with external modules. Following an extensive investigation of the existing tools, the simulator was built on top of NS-3 that simulates packet data networks with user-defined traffic models [72]. This decision was influenced by the fact that NS-3 included a wide range of features, libraries, and modules that could be properly modified to meet the goals of our simulator. In addition, the 5G-LENA module [73] was employed to model 5G NR cellular networks [74] and the SGP4 mathematical model was used to estimate the speed and position of LEO satellites [75]. The simulator's main components that are already available or have been developed, namely the NS-3 software official release, NS-3 5G LENA module, and NS-3 satellite mobility module will be described in detail in the following sections.

3.2.1 Simulator Main Components

Network Simulator 3 (NS-3)

NS-3 is a discrete-event network simulator that has been developed to provide an open and extensible network simulation platform for networking research and education. The NS-3 project is committed to building a solid, well-documented, easy-to-use, and debug simulation core, which caters to the needs of the entire simulation workflow, from simulation configuration to trace collection and analysis. Compared to other open source simulators, NS-3 offers multi-RAT (Radio Access Technology) and multi-band simulation capabilities, along with Wi-Fi, Long Term Evolution (LTE) (LTE-Advanced (LTE-A), Licensed Assisted Access (LAA), LTE-Unlicensed (LTE-U)), and NR which are already openly available. It provides models of how packet data networks work and a simulation engine for users to conduct simulation experiments [72]. It was created as a set of C++ libraries that may be merged and connected with other external software libraries. It is generally used on Linux or macOS platforms, while Windows frameworks that can compile Linux code are supported. Users of the NS-3 C++ libraries can write code to configure the network they want to simulate within the main() program by using ad-hoc C++ codewords related to network elements such as nodes, links, interfaces, network protocols such as Ethernet or Wi-Fi, and network algorithms such as routing and scheduling algorithms. Python may also be used to write user applications, however, a development environment is required to compile and build the libraries first, followed by the user program. NS-3 is the simulator's main component, which is used to establish the network simulation environment, and set it with fundamental network components such as nodes, links, and data traffic applications, in addition to analyzing the behavior of the simulated network. Although NS-3 has many features that encouraged us to use it as the basis of our simulator, the latest NS-3-3.36 official release (used to develop the simulator) does not include the capability to simulate either satellite communication networks or 5G networks. Thus, the need arose to develop and seamlessly integrate additional modules for both satellite communication networks and 5G networks into the official NS-3 release in order to enable the simulation of these crucial aspects.

5G-LENA Module

5G-LENA Module [73] was developed within the Mobile Networks group of a public research institute, Centre Tecnològic de Telecommunications de Catalunya (CTTC) starting from the homonym module which implements 4G-LTE networks [76]. The 5G-LENA module was used to allow the tool to simulate 5G networks. It implements a 3GPP release 15-compliant NR module and is intended for inclusion in the official NS-3 release. 5G-LENA was originally developed as a tool to simulate communications in millimeter-wave bands through a collaboration between New York University and the University of Padova. It is a pluggable module of the software NS-3 open to the interested community to foster early adoption and contributions by industrial and academic partners that can be used to mimic 5G NR cellular networks. It supports many features, including NSA architecture that supports both 5G Radio Access Network (RAN) and 4G Evolved Packet Core (EPC) at the same time, Time Division Duplexing (TDD) and Frequency Division Duplexing (FDD) modes with configurable TDD patterns, flexible and automatic configuration of the NR frame structure through multiple numerologies [74]. It also implements Time-Division Multiple Access (TDMA) and Orthogonal Frequency-Division Multiple Access (OFDMA)-based access with variable transmission time intervals and single beam capability, Enhanced MAC layer, including flexible MAC schedulers that simultaneously consider time- and frequency-domain resources both for TDMA and OFDMA-based access schemes with variable Transmission Time Interval (TTI), NR PHY layer abstraction, considering Low-density parity-check (LDPC) codes, Modulation Coding Scheme (MCS) up to 256-QAM, LDPC base graph selection and NR block segmentation [77, 78]. This module is still under development, especially considering that the NR specifications are still evolving, and the version used to develop the simulator prototype is v2.2.

Satellite Mobility Module

Numerous mobility models in NS-3 are designed to imitate moving nodes, including moving people or cars, that can move randomly or more predictably by maintaining a consistent speed and direction. Even with the SNS3 [79], which is more focused on the lower layer aspects of Geostationary Earth Orbit (GEO) satellite communications, no mobility model can accurately simulate how LEO satellites change their position as they travel along their orbital paths. Thus, to allow implementing nodes in the NS-3 simulation environment that moves as LEO satellites, an ad-hoc NS-3 module was developed based on the NORAD Simplified General Perturbations 4 (SGP4) mathematical model [75], this model is commonly used to predict the position and velocity of LEO satellites at any given time from satellite orbital parameters, such as altitude, inclination angle, and initial position, formatted as input in the form of Two-Line Element (TLE) sets [80]. This module takes as input each satellite's TLE set and gives as output its Earth-Centered Inertial (ECI) coordinates, a three-dimensional Cartesian system with the origin at the Earth's center mass and axes fixed concerning the stars. This module is used to allow NS-3 nodes defined as satellite gNBs and terrestrial UEs to change their position during the simulation following the SGP4 mathematical model and the related position updates required by the considered ECI coordinate system.

3.2.2 Reference Scenario

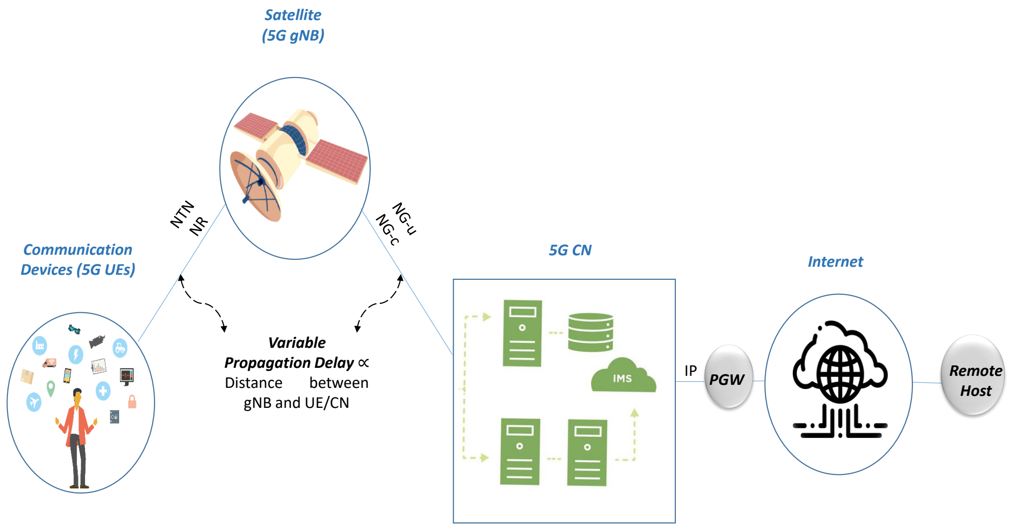

Figure 3.1: 5G NTN reference scenario, Composed of : 1- 5G user equipments which are communication devices implemented as terrestrial or aerial nodes able to get access to the internet through a LEO satellite 5G radio access network. 2- Leo satellite nodes that constitute the 5G radio access network, which is able to generate 5G cell that offers direct access to the 5G user equipments. 3- 5G core network which manages all the functionalities related to the establishment and maintenance of the 5G network. It consists of multiple nodes strictly connected to each other including a point of presence towards the internet through a packet gateway.

Using the previously described modules, the simulator allows the implementation of the 5G STIN depicted in Figure 3.1, and to arbitrarily set the number of nodes in the network, define the traffic flow configuration to simulate different kinds of applications, set the base station and satellite positions in a 3-D space and update them accordingly, and properly allocate the 5G access resources depending on the current network configuration and user performance requirements.

Its main components are:

- *5G UEs*: terrestrial or aerial nodes which act as devices able to get access to the internet to send or receive data through a 5G RAN. UEs can include a wide range of devices, from smartphones, tablets, and laptops to IoT devices and even drones.
- *5G gNBs*: satellite nodes that constitute the 5G RAN. Each satellite is able to generate a 5G cell which acts as a coverage area for 5G UEs and offers direct access to them.
- *5G Core Network (CN)*: an entity that manages all the functionalities related to the establishment and maintenance of a 5G network. It can consist of one or multiple physical or virtual nodes strictly connected to each other. It also includes a Point of Presence (POP) towards the internet through a Packet Gateway (PGW) to allow data exchange from the 5G network to the outside and vice versa.

Moreover, in the context of 5G networks, flexibility is essential to address the diverse requirements of users. These networks are expected to support a wide array of services, including voice, data, images, videos, and various applications, each with unique demands in terms of data rates and traffic profiles. These traffic profiles encompass key attributes such as bandwidth requirements and delay tolerance. For instance, the traffic characteristics of telephony and voice-over IP applications differ significantly from those of video streaming and background data transfers. Such distinctions in source traffic profiles are crucial for classifying the corresponding application types.
To address the diverse service requirements in 5G networks, it is important to first define the BWP and the CC concepts, which aim to optimize resource allocation, and efficiently manage the available spectrum, and they can be defined as follows:

- *Bandwidth Part (BWP): In 5G networks, a BWP is a fundamental concept introduced to facilitate the management and allocation of different portions of the available spectrum for specific purposes. The available spectrum can be subdivided into smaller* *segments known as Bandwidth Parts (BWPs). Each BWP can be allocated to serve specific types of devices or applications, thereby optimizing the use of available resources. This approach leads to more efficient spectrum utilization and improved network resource management, especially in scenarios characterized by varying demands and distinct service requirements.*

- *Component Carrier (CC): The concept of a CC is another cornerstone of 5G networks. It refers to an individual block of the available spectrum used for transmitting and receiving data. Each CC may possess a specific bandwidth and frequency range. Each CC can have one or multiple BWP segments as shown in Figure 3.2. 5G networks allow the aggregation of multiple CCs, resulting in higher data rates, increased capacity, and enhanced overall network performance. This aggregation of CCs empowers the network to adapt to changing user demands and optimize resource utilization.*

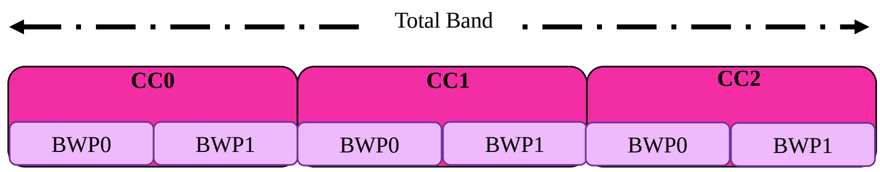

Figure 3.2: Bandwidth Part and Component Carrier Configuration Example.

The core principle underpinning the proposed configuration is to group multiple UEs with similar performance requirements into classes, referred to as TPs. Each TP is then allocated a distinct portion of the available spectrum, appropriately configured in terms of BWP and CC configurations.

3.2.3 Module Integration

The integration process of these modules was not straightforward. A few modifications were required to allow the tool to properly simulate 5G STIN with satellites as 5G access nodes.

One major difference between 5G terrestrial networks and 5G satellite networks, with satellites as access nodes, is the presence and consequent impact of a higher propagation delay between gNBs and UEs due to the higher distances among these nodes. Besides, in the case of terrestrial networks, gNB position is fixed on the ground, while, in the case of NTNs with LEO satellites as gNB, it continuously and rapidly changes due to the satellite movement. To allow our tool to simulate this, a new variable propagation delay was added on the links between UEs and gNBs which affects all communications between these nodes in both directions and is periodically updated right after each position, and consequently distance, update (which takes place once per second). A similar delay has been defined and affects the satellite links between satellites and satellite base stations, defined as the physical access points to the portion of the ground network where the 5G CN and the Internet access is located.

Due to the continuous motion with high speed of the LEO satellites, an UE will be in visibility with, and so attached to, a satellite gNB only for a limited time window (typically just a few minutes) [81]. This aspect led to focusing on the handover process which has to follow different dynamics than the one in terrestrial networks. A handover mechanism that does not depend on the UE mobility but on the gNB movements is required to allow each UE to be always attached to a valid gNB (if any). In order to fulfill the aforementioned need, an inter-satellite handover process has been introduced. Information about distance, elevation angle, and remaining visibility time between each UE-satellite pair are periodically updated and can be considered to decide handover events. A set of valid gNB candidates for each UE is created and kept updated fixing proper thresholds on the mentioned parameters, such as minimum elevation angle or distance. Different strategies can be implemented, starting from the simplest one, i.e. minimum distance, that can be considered similar to the one used in terrestrial networks which is based on the maximum received SNR, to more complex aim to, for example, minimize the number of handovers events per UE.

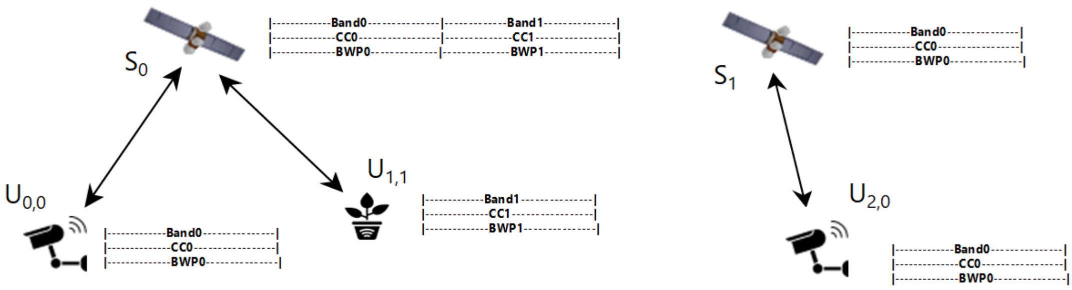

Figure 3.3: Example of resource allocation within the proposed simulator. In the depicted network portion and time instant, two UEs $U_{0,0}$ and $U_{1,1}$, belonging to TF_0 and TF_1, respectively, are attached to satellite S_0, while UE $U_{2,0}$, belonging to the TF_0, is the only one attached to the second satellite S_1.

Furthermore, 5G networks need extreme flexibility in order to provide subscribers with a variety of services such as voice, data, images, videos, and various applications with largely different requirements in terms of data rates and traffic profiles. In the proposed tool, dynamic BWP and CC (Frequency block) configuration criteria were implemented. The proposed configuration creates a number of BWPs proportional to the available traffic profiles with different numerologies, where for instance, one CC was allocated for each BWP. Another aspect was considered related to the dynamic spectrum resource allocation. Different applications may have different requirements in terms of needed resources, such as bandwidth, and QoS parameters like latency.

Some applications need low latency whereas others accept high latency but need high bandwidth or security support. 5G networks need extreme flexibility in order to support various applications and services with largely different requirements. A dynamic BWP and CC configuration is implemented. A BWPis a concept introduced in 5G networks to manage and allocate different portions of the available spectrum for specific purposes. In a 5G network, the available spectrum can be divided into smaller segments called Bandwidth Parts. Each Bandwidth Part can be allocated to serve specific types of devices or applications, optimizing the use of available resources. This approach allows for more efficient spectrum utilization and better management of network resources, especially in scenarios with varying demands and different service requirements. Moreover, CC is a fundamental concept in 5G networks that refers to an individual block of the available spectrum that is used for transmitting and receiving data. Each Component Carrier can have a specific bandwidth and frequency range. In 5G, multiple CCs can be aggregated together to provide higher data rates, increased capacity, and improved overall network performance. This aggregation of CCs allows the network to adapt to varying user demands and optimize resource utilization. The main principle of the proposed configuration is to group multiple UEs with the same performance requirements in classes, called traffic profiles TF_p, and assign them the same portion of the available spectrum properly configured in terms of BWP and related numerology. As a consequence, a satellite can also act as a gNB that activates and keeps active only the CCs and related BWPs depending on the number of UEs attached to it and their traffic profiles, as shown in Figure 3.3. In the depicted network portion and time instant, two UEs $U_{0,0}$ and $U_{1,1}$, belonging to TF_0 and TF_1, respectively, are attached to satellite S_0, while UE $U_{2,0}$, belonging to the TF_0, is the only one attached to the second satellite S_1.

3.3 Performance Evaluation

Tests were conducted to check the performance of the proposed 5G NTN simulator. A constellation of 2 moving LEO satellites at an altitude of 600 km was assumed to operate as NR base stations, offering 5G connectivity to terrestrial 5G UE. 39 GHz (Q-band) and 28 GHz are the central frequencies set for the downlink and uplink transmissions, respectively, which are within the 5G Frequency Range 2 (FR2) [82]. There are no communications among satellites at the current status. The assumed system operates at 28 GHz in the uplink direction. It's worth noting that each band assigned to a satellite service specifies whether the band should be utilized in an up-link direction (from Earth to space) or in a down-link direction (from space to Earth). There is no such restriction for the bands used by terrestrial services. This fact, when combined with the TDD technique used in 5G networks, leads to the key conclusion that 5G NR and satellite networks share just a down-link band of 39 GHz (Q-band) and a single up-link band of 28 GHz [82]. The system attributes are summarized in Table 3.1. One traffic flow per UE is implemented setting the UEs as destination nodes and a single remote host, located on the ground, as the source node, as also shown in Figure 3.1. In each simulation, at least a handover event takes place after one second and at least one UE changes its attached gNB.

Figure 3.4 shows the performance in terms of the packet Average Delivery Time (ADT) obtained by changing the number of UEs and by comparing the simulated 5G satellite network where satellites act as gNBs with one of the 5G terrestrial network example available in the 5G LENA module, where terrestrial nodes act as gNBs.

ADT is defined as:

$$ADT = \frac{\sum_{p=1}^{P} \left(T_p^{RX} - T_p^{TX}\right)}{P} \tag{3.1}$$

Table 3.1: Simulated scenario design parameters

Parameter	Value
Number of satellite gNBs	2
Number of terrestrial UEs	from 1 to 10
Number of TFs	2
Satellites altitude h	600 km
Orbital planes eccentricity	0 (circular)
Orbital planes inclination i	$88°$
Orbital planes argument of perigee	$90°$
Minimum elevation angle between UE and gNB for transmissions	$20°$
Number of transmitted packets	960
Packet size	1280 *Byte*
Operating Frequency	28 GHz
Bandwidth	100 MHz

where P is the total number of generated data packets and T_p^{TX} and T_p^{RX} are the time instants when the p^{th} data packet is sent by the remote host and is received by the related UE, respectively.

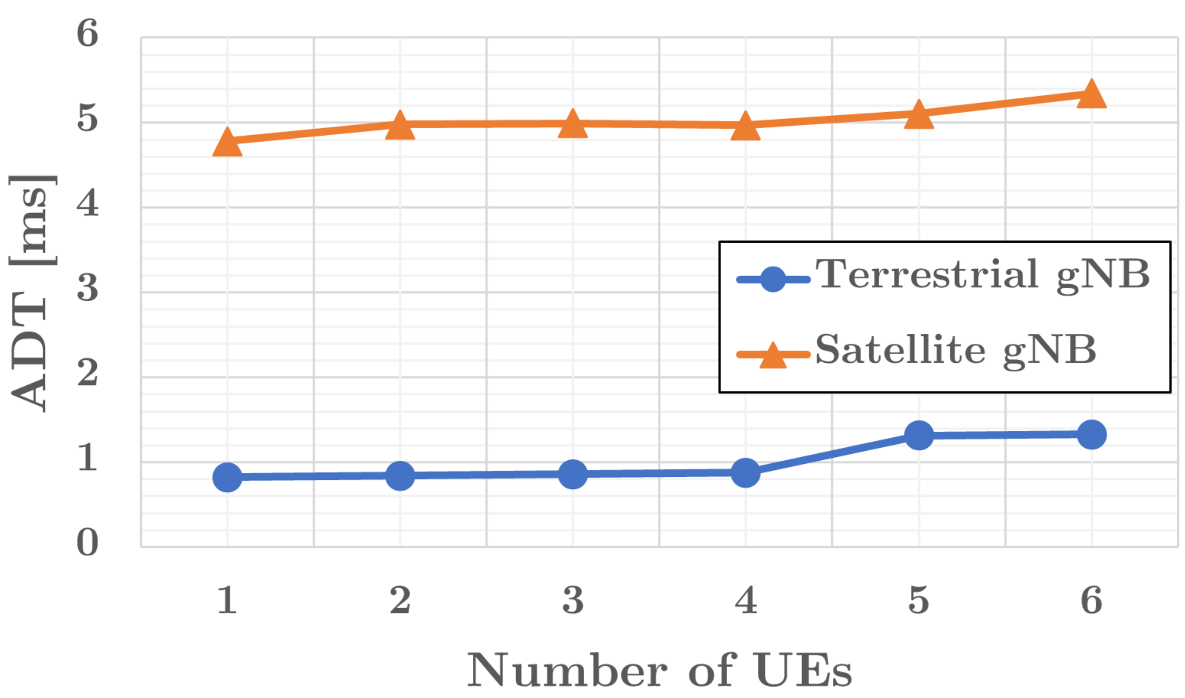

Figure 3.4: Packet ADT by changing the number of UEs and by considering networks with terrestrial or satellite gNBs

The higher ADT obtained with satellite gNB is in principle due to the presence of the two satellite links (UE–gNB and gNB–CN) between source and destination. ADT is affected by the higher satellite link propagation delay which, considering the satellite altitude h_s set to 600 *km* and the minimum elevation angle ϵ set to 20°, ranges between 2 and 4.64 *ms*, with a related contact distance d that ranges between 600 and 1392 *km* computed as indicated in the following equation derived from [83], Eq. 56:

$$d = -R_e * \sin(\epsilon) + \sqrt{R_e^2 * \sin^2(\epsilon) + h_s^2 + 2 * R_e * h_s} \tag{3.2}$$

where $R_e = 6378$ *km* is the Earth radius at the Equator.

The performed simulations prove the possibility of using a satellite gNB in direct access with a UE while achieving a good throughput and acceptable delays for various 5G applications supporting not only Enhanced Mobile Broadband (eMBB) and Massive Machine-Type Communication (mMTC), but also ultra-reliable communications with relaxed latency requirements of a few milliseconds. To verify the performance of the proposed 5G NTN simulator, a packet transfer in the uplink direction (from the UE to the Satellite gNB) was triggered. In order to simplify the simulation, only 2 LEO satellites along with 8 UEs were used. The network operates over a millimeter waves (mmWaves) range at 28 GHz which is a candidate frequency for 5G communications as it suffers from low atmospheric attenuation and is a shared band in the up-link direction with the satellite networks [82].

3.3.1 Satellite Handover

LEO satellites are the best candidates for direct access 5G NTN since they are relatively close to the earth's surface, normally found at an altitude of less than 1000 km but could be as low as 160 km above the earth, which is low compared to other satellite orbits. However, LEO satellites move so fast across the sky and therefore they often work as

Table 3.2: Handover Traces UE0

Time=0—UE0 attached to gNB63				
gNB	Distance	Elevation Angle	RVT	Nb of Attached UE
0	-1	-1	0	0
9	782.6	47.8	241	26
63	781.7	47.9	237	15
Decision: UE0 should move from gNB 63 to gNB 9				
Time=4—UE0 attached to gNB9				
gNB	Distance	Elevation Angle	RVT	Nb of Attached UE
0	-1	-1	0	0
9	783.7	47.7	237	32
63	784.5	47.6	233	9
Time=240—UE0 attached to gNB9				
gNB	Distance	Elevation Angle	RVT	Nb of Attached UE
0	-1	-1	0	0
8	1904.1	10.39	450	3
9	1944.5	9.8	1	17
62	1878.3	10.7	446	23
63	-1	-1	0	12
Decision: UE0 should move from gNB 9 to gNB 62				

part of a large combination or constellation that forms a network around Earth to cover large areas of the Earth simultaneously. As a consequence of the fast movement of LEO satellites, a UE that is being served by one satellite loses its visibility more often which necessitates the implementation of a handover scenario to overcome this particular issue. The handover procedure was verified by the simulation of a constellation of 100 LEO satellites and 100 UEs. Multiple successive simulations for a duration of 1 second each were implemented. At the end of each simulation round, the system tracks the status of every UE-Satellite connection pair, including the position of both ends, elevation angle, distance, and RVT. After which it informs the simulator with a handover necessity when needed. For example, table 3.1 shows some valuable information taken from the traces of UE0 at different instances where handover decisions were suggested. At the beginning of the simulation, UE0 was attached to gNB63 where the distance between them was 782.6 km, the elevation angle was 47.8 degrees and the RVT was 241 seconds. Additional information of the current number of attached UEs to each gNB at that instance of time was given. For some gNBs, the distance and the elevation angle are given as -1 this is due to the fact that those gNBs are not in the valid satellite set (distance from the satellite greater than the predefined threshold value). As illustrated in Table3.2, after 4 seconds gNB63 become closer to UE0 than gNB9 which leads to the decision of handover. Moreover, at time 240, when the RVT of gNB9 becomes as low as 1 second, a handover decision was taken so that UE0 changes connection from gNB9 to the closest satellite with larger visibility time which is in this case gNB62. Therefore, these results prove that the inter-satellite handover procedure was correctly implemented.

3.4 Conclusion

This chapter has presented the "NS-3-based 5G Satellite-Terrestrial Integrated Network Simulator". This powerful simulator facilitates the exploration of different communication scenarios, enabling performance evaluations and paving the way for innovative progress. Its utilization serves as an invaluable platform for testing novel ideas, efficiently scrutinizing system performance, and assessing various implementation options.

The proposed open-source system-level simulator (SLS), based on the Network Simulator 3 (NS-3), fills the gap left by existing system-level simulators (SLS) that are primarily adapted to single-access technologies. This includes the combination of terrestrial and satellite networks. The prototype simulator, developed in C++, was created as part of the European Space Agency's "ANChOR" project and provides the capacity to model 5G satellite-terrestrial networks. Its adaptability extends to various satellite functions, such as backhaul providers, while being primarily designed to mimic LEO satellites as 5G access nodes (gNBs). The proposed simulator outperforms existing solutions by incorporating features that include satellite handover decisions, dynamic selection, and configurations based on distinct predefined traffic profiles.

Even if the simulator can collect multiple data that can be considered during the handover process, in particular for the satellite gNB selection, the handover or not handover decisions and the related satellite selections, at the current status, are only based on the distance parameter. However, more complex strategies based on multiple parameters should be considered in order to minimize the packet ADT and/or reduce the number of handover events, considering that each handover event can lead to additional delays and has a certain non-negligible complexity. Machine Learning and Resource Allocation Game techniques will be considered to improve the handover process and the impact on the obtained performance will be analyzed in the following chapters.

Chapter 4

Handover Management in 5G Networks

4.1 Introduction

Handover is a fundamental aspect of wireless communication systems, ensuring seamless connectivity as users move within a network. In 5G, the fifth generation of mobile networks, handovers play a crucial role in delivering high-speed, low-latency, and reliable connections. Low Earth Orbit (LEO) satellite constellations offer significant advantages over other satellite orbit systems, including reduced signal propagation delay, lower power requirements, and more efficient use of spectrum through frequency reuse between satellites and spot beams. Consequently, LEO satellites are being explored as a complement to existing terrestrial fixed and wireless networks in the ever-evolving global mobile network landscape.

However, one notable challenge with LEO satellites is their higher orbital speed compared to terrestrial mobile terminals, which move at lower speeds and follow more unpredictable paths. This high mobility characteristic of LEO satellites results in frequent handovers for mobile users as they transition between the coverage areas, known as footprints, of adjacent satellites. Managing handovers in LEO satellite networks becomes a complex and demanding task in order to maintain seamless global mobile communication.

To address this challenge, researchers are actively seeking efficient and accurate methods for managing handovers between the moving footprints of LEO satellites. The primary objective of this work is to ensure a reliable service for users, minimizing the risk of communication disruptions caused by handovers. This section will delve into the concept of handovers in 5G networks, exploring the different types of handovers across various layers. Additionally, the specific challenges associated with handovers in LEO satellite networks will be discussed, along with the types of satellite handovers.

4.2 Handovers in 5G Terrestrial Network Scenarios

The concept of HO is fundamental in mobile communication systems like 5G, ensuring that users experience uninterrupted connectivity while on the move. When a mobile device, such as a smartphone or tablet, changes its position within a cellular network, it may cross the boundary of one cell (served by a base station) into another cell's coverage area. This transition is where the HO procedure comes into play.

In the scenario depicted in Figure 4.1, there is a UE that's currently connected to BS1, and this UE is actively engaged in a call. As the UE moves towards the coverage area of BS2, it continuously monitors the signal strength of both BS1 and BS2. Signal strength serves as an essential metric for determining the quality of the connection with a particular base station. In this context, the UE is assessing whether the signal from BS2 becomes stronger than that from BS1 while it's within the overlapping region where both cells' coverage areas meet.

Several factors are taken into consideration during this assessment, including not only signal strength but also the availability of resources at BS2 to support the UE's ongoing call. Resources here refer to the necessary bandwidth, capacity, and other network

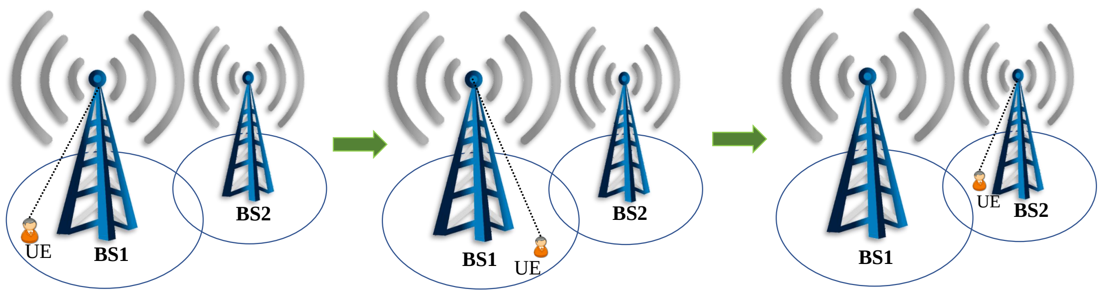

Figure 4.1: Handover scenario in a terrestrial base station case, where the user is in continuous motion while the terrestrial base station is always fixed on the ground

capabilities required to sustain a smooth communication session. If BS2 satisfies these criteria, a HO procedure is initiated.

The purpose of this HO process is to smoothly transfer the UE's connection from BS1 to BS2. By doing so, it ensures that the UE remains connected to the network without any interruption, such as call drops or data loss. This seamless transition is essential for providing users with a consistent and reliable mobile communication experience, particularly as they move within the coverage areas of different base stations.

The blocking probability is an essential parameter that plays a vital role in evaluating QoS in mobile communication networks. block probability characterizes the likelihood of a new connection request being declined by the target base station, typically due to network congestion or resource limitations. This metric becomes particularly relevant when the network operates close to its capacity limits, making it challenging to accommodate additional users or establish new connections. High block probability values indicate potential network congestion, which can lead to sub-optimal user experiences for those attempting to access the network [84].

Generally, the HO procedure encompasses three distinct phases, each serving a crucial role in ensuring a seamless transition as mobile users move within the network. These phases are the measurement phase, the HO decision Phase, and the HO execution Phase. During the measurement phase, the UE continuously monitors various network parameters as it moves through the network. In terrestrial network scenarios, these parameters typically include signal strength, signal quality, and other relevant metrics. The UE collects data to assess the quality of its connection with the current base station and neighboring base stations. In the HO decision phase, the network or the UE itself uses the measurement data gathered in the previous phase to determine whether a HO is necessary. The decision relies on specific algorithms and predefined criteria. For example, if the signal strength from a neighboring base station becomes stronger than the current one and meets certain quality standards, a HO may be initiated. Once the decision is made to switch to a new base station, the UE is assigned to the target base station, and the old connection is terminated, this procedure is referred to as the HO execution phase.

4.3 Handover in 5G Leo Satellite Network Scenarios

LEO satellites are in constant motion relative to end-users on the Earth's surface. To an observer at a fixed point on Earth, these satellites appear to rise from below the horizon, traverse the sky, and then set below the horizon, much like the Sun or the Moon's movement. Importantly, there is always at least one satellite above the horizon, ensuring continuous communication services.

To maintain uninterrupted communication for end-users, the connection must be seamlessly transferred from a setting satellite to another satellite within view as illustrated

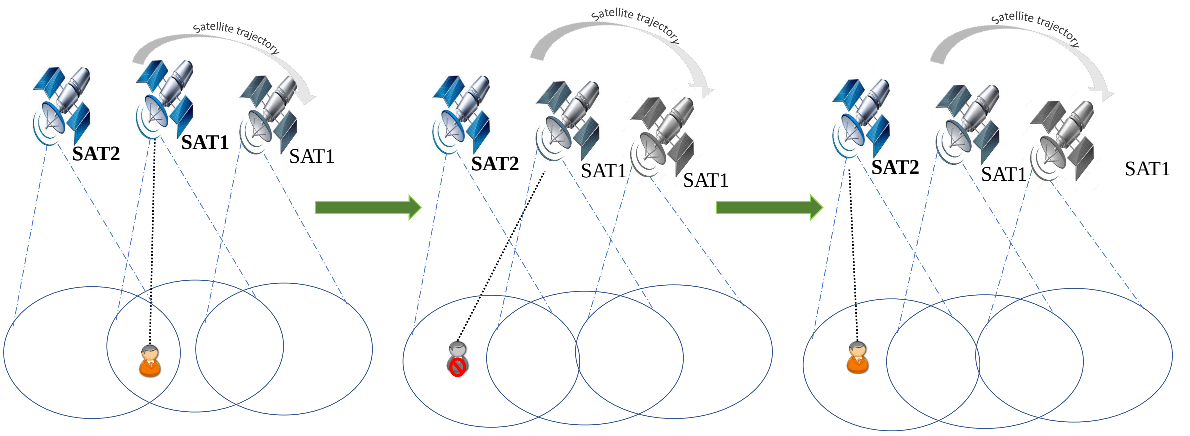

Figure 4.2: Handover scenario in a low earth orbit satellite base station case. Where the LEO satellite is in continuous motion while the user is in a fixed position

in Figure 4.2. This process of transferring a connection across satellite coverage areas is known as an "inter-satellite handover." For instance, in the case of the Iridium satellite constellation, an end-user remains within a satellite's coverage area for approximately nine minutes [85]. During this time, the coverage areas of the satellite's spot beams shift over the end-user, resulting in multiple spot beam handovers. Eventually, the satellite sets below the horizon, leading to a satellite-level handover.

It's worth noting that the mobility of an end-user is relatively insignificant when compared to the mobility of LEO satellites. For example, a satellite within the Iridium constellation has a spot beam with a diameter of 600 kilometers and moves at a velocity of 26,804 kilometers per hour relative to the Earth's surface [13]. Consequently, it takes only about 80 seconds for the spot beam's coverage area to move over the end-user and trigger a handover. In contrast, communication devices found on humans, vehicles, or marine vessels typically have speeds ranging up to around 100 kilometers per hour. At this speed, it would take six hours to travel the 600 kilometers needed to prompt a handover. Even if a communication device were onboard an aircraft traveling at 1,200 kilometers per hour, it would still take 30 minutes to cover the distance required for a handover. Therefore, end-user mobility is relatively inconsequential, and satellite handovers occur frequently and predictably due to the motion of the satellites themselves.

Handovers within satellite networks can be broadly categorized as follows:

1. Link-Layer Handover: Link-layer handovers occur when it's necessary to change one or more links between communication endpoints due to the dynamic connectivity patterns of LEO satellites. This category can be further divided into:

- Intra-satellite Handover: This involves handovers from one spot beam to another of the same satellite while the mobile station remains within the satellite's footprint but moves to another cell.

- Inter-Satellite Handover: Inter-satellite handovers take place when the mobile station becomes out of the footprint of one satellite and needs to connect to another satellite.

- ISL Handover: ISL (Inter-Satellite Link) handovers occur when interplane ISLs need to be temporarily switched off due to changes in the distance and viewing angles between satellites in neighboring orbits. This requires rerouting ongoing connections that use these ISL links.

- Gateway Handover: Gateway handovers entail switching from one gateway to another while the mobile station is still within the satellite's footprint but the gateway moves out of it.

- Inter-system Handover: This type of handover involves transitioning from the satellite network to a terrestrial cellular network. The mobile station can regain access to the terrestrial network, which might offer cost benefits or lower latency, among other advantages.

2. Network-Layer Handover: Network-layer handovers are needed when one of the communication endpoints, either the satellite or the user end, changes its IP address

due to shifts in satellite coverage or the mobility of the user terminal. In this case, higher-layer handovers are necessary to migrate existing connections of higher-level protocols (such as TCP, UDP, SCTP, etc.) to the new IP address. This is known as a network or higher-layer handover. Three different approaches can be employed during this process:

- Hard-handover schemes: In these schemes, the current link is released before the next link is established.

- Soft-handover schemes: Soft-handover schemes ensure that the current link is not released until the next connection is established.

- Signaling-diversity schemes: These schemes are similar to soft handover, with the distinction that, in signaling diversity schemes, signaling flows through both old and new links, while user data continues to flow through the old link during handover.

In satellite systems, intra-satellite handovers are the most frequent. However, since these handovers involve switching between narrow spot beams managed by the same satellite, they generally have minimal impact on the functionality and performance of network layer protocols. In essence, end-user data continues to be routed through the same satellite during intra-satellite handovers. On the other hand, inter-satellite handovers occur less frequently. Nevertheless, they have a substantial impact on the functionality and performance of network layer protocols. This is because inter-satellite handovers necessitate transferring communications to a spot beam managed by a different satellite. Consequently, they are more complex in terms of the required functionality to support the handover and are critical for maintaining the Quality of Service during the transition. As a result, the primary focus of this thesis is on inter-satellite handovers.

4.4 Conclusion

In conclusion, this chapter has underscored the pivotal role of handovers in the realm of satellite communication, with a particular focus on the evolving landscape of Low Earth Orbit (LEO) satellite networks. The significance of efficient handover management cannot be overstated, especially in the context of supporting global mobile communication, where seamless connectivity is a fundamental requirement.

The chapter has shed light on the unique challenges posed by LEO satellite handovers, which differ significantly from terrestrial scenarios. The dynamic nature of LEO satellite constellations, characterized by their swift orbital motion and changing footprints, presents a host of new challenges that demand innovative solutions. These challenges range from rapid signal attenuation and network handover latency to ensuring uninterrupted communication for users moving across satellite footprints.

This exploration into the distinct features and hurdles of LEO satellite handovers has spurred our research interest in developing a novel method for efficient handover management. Recognizing the critical need for a reliable and robust approach that minimizes communication disruptions due to handovers, our investigation seeks to address these challenges head-on. By implementing a tailored LEO satellite handover management method, The main aim is to contribute to the enhancement of global mobile communication in an ever-changing satellite landscape.

The forthcoming chapters will delve into the details of our proposed method, its design, implementation, and evaluation, with the overarching goal of delivering a solution that not only mitigates the challenges posed by LEO satellite handovers but also serves as a valuable addition to the broader field of satellite communication technology.

Chapter 5

LEO Satellite Handover Management for Single Traffic Profile Scenarios

5.1 Introduction

In an era where Low Earth Orbit (LEO) satellites are revolutionizing global connectivity, the effective management of satellite handovers (HO) becomes essential for seamless and efficient communication. This chapter delves into the steps of implementing a LEO Satellite Handover Management system for single traffic profile scenarios, leveraging the power of Reinforcement Learning (RL).

While recent studies have made significant strides in optimizing satellite HO processes, a common limitation persists. Most state-of-the-art research either focuses on a single HO criterion to achieve a specific optimization goal or provides solutions from the perspective of a single user. However, in the dynamic environment of LEO satellites, users lack a centralized controller, which means they can only access partial information about the satellite system in relation to their own needs.

Moreover, the finite channel budget of LEO satellites intensifies the competition among users served by the same satellite, leading to a pronounced imbalance in satellite load.

This necessitates the development of a decentralized satellite HO strategy that not only considers users' real-time resource competition but also aims to balance the load across multiple satellites.

The work of [65] employs multi-agent reinforcement learning, treating each user as an agent with a limited view of the satellite system, enabling them to make individual HO decisions. While this load-aware HO strategy successfully avoids connecting to fully loaded satellites, it has a drawback—it does not prioritize the connection to satellites with higher available channels. Consequently, it falls short of promoting load balancing among satellites, thereby increasing the likelihood of blocking for user equipment (UE).

In contrast, the Load Balancing Satellite Handover (LBSH) method, proposed in this chapter, offers a novel and efficient solution. The LBSH method is specifically designed as a load-balancing HO scheme, which aims to reduce the blocking rate for UEs by intelligently distributing the traffic load among the available LEO satellites. Through this chapter, we will explore the development, implementation, and evaluation of the LBSH method, providing concrete evidence of its success in achieving load balancing and minimizing the probability of blocking.

The rest of this chapter is organized as follows. Section 5.2 describes the reference scenario and network assumptions and presents the HO optimization problem. In Section 5.3, the optimization problem is transformed into a reinforcement learning problem. Simulation results were discussed in Section 5.5. Finally, Section 5.6 provides the conclusions of the presented work.

5.2 Reference scenario and Network Assumptions

The network is implemented considering the satellite HO problem over a specific period of time T, as illustrated in Figure 5.1. The main components of the network are:

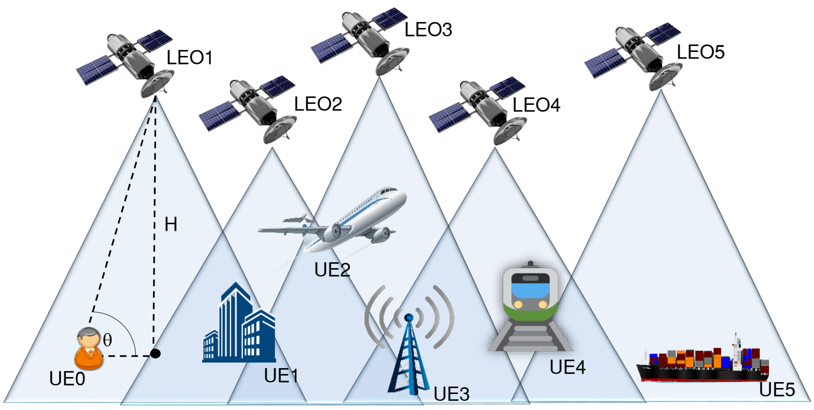

Figure 5.1: Satellite Handover Scenario; The considered scenario consists of *K* UEs and *N* LEO satellites. The UEs are ground nodes that can connect to the network directly via LEO satellites that operate as network base stations. Each UE is often covered by more than one satellite at any given time.

- *5G UEs*: terrestrial or aerial nodes that can connect to the Internet to send or receive data through a 5G RAN. They are uniformly distributed across the Earth's surface. A set of *K* users is considered and denoted by $\mathcal{K} = \{1, 2, ..., K\}$.
- *LEO Satellites*: satellite nodes that make up the 5G RAN. Each satellite can produce a 5G cell that provides direct access to the 5G UEs. A set of *N* satellites was considered and denoted by $\mathcal{N} = \{1, 2, ..., N\}$.

The elevation angle between user k and satellite n is represented by $\theta_{k,n}$ (Figure 5.2) and can be calculated based on the position information of the user and its covering satellite as follows:

$$\theta_{k,n} = \arcsin\left(\frac{h_n^2 + 2 \times R_e \times h_n - D_{k,n}^2}{2 \times R_e \times D_{k,n}}\right) \tag{5.1}$$

where H_n is the altitude of satellite n, R_e the Earth radius, and $D_{k,n}$ the distance between user k and satellite n. The minimum elevation angle θ_0 is a design parameter

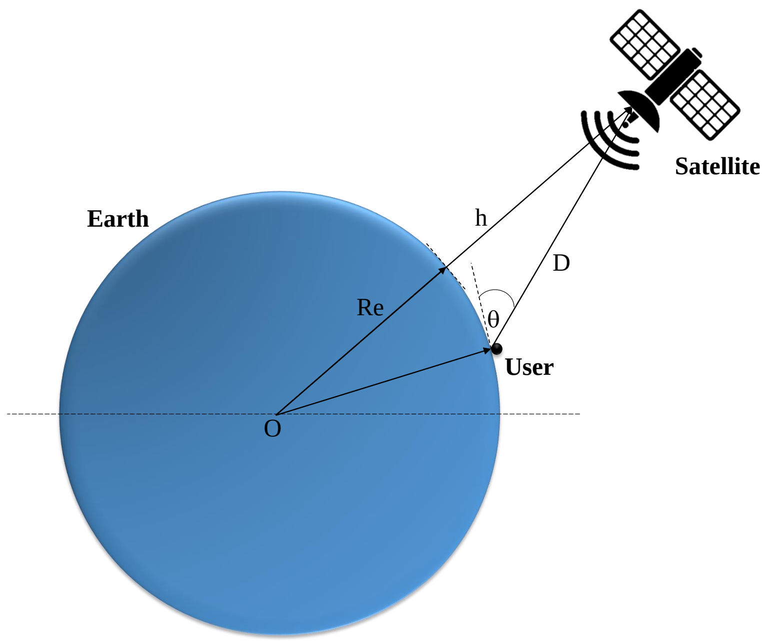

Figure 5.2: Geometric representation of the elevation angle θ between a satellite and a ground user

used to ensure threshold link quality. As a result, a satellite n is considered a good candidate for user k only if:

$$\theta_{k,n} \geq \theta_0, \qquad \forall k \in \mathcal{K}, \forall n \in \mathcal{N} \tag{5.2}$$

At time t, $C^t_{k,n}$ is the coverage indicator between satellite n and user k, and it is defined as follows:

$$C^t_{k,n} = \begin{cases} 1 & \text{if user } k \text{ is covered by satellite } n \text{ at time } t, \\ 0 & \text{otherwise} \end{cases} \tag{5.3}$$

Moreover, $X_{k,n}^t$ indicates if user k is served by satellite n at time t, and is defined as follows:

$$X_{k,n}^t = \begin{cases} 1 & \text{if user } k \text{ is served by satellite } n \text{ at time } t, \\ 0 & \text{otherwise} \end{cases} \tag{5.4}$$

Each satellite's total bandwidth is partitioned into L_n channels of equal bandwidth and that each user can only use one channel to transmit/receive. Following that, the channel budget limitation is given by:

$$\sum_{k \in \mathcal{K}} X_{k,n}^t \leq L_n, \qquad \forall n \in \mathcal{N} \tag{5.5}$$

5.2.1 Problem Formulation

At any time t in T, the selection from candidate satellites ($C_{k,n}^t = 1$) is optimized to minimize the number of HOs. In this case, any decision that results in $X_{k,n}^t \neq X_{k,n}^{t-1}$ at any time t during T causes the HO count to increase by 1. The average number of HOs is thus given by:

$$HO_{avg} = \frac{\sum_{k \in \mathcal{K}} HO_k}{K} \tag{5.6}$$

Our goal is to decrease the average number of HOs while enhancing channel utilization efficiency in the LEO satellite system during the considered time period T.

The optimization problem is therefore defined as follows:

$$\min_{X_{k,n}^t} HO_{avg} = \frac{\sum_{k \in \mathcal{K}} HO_k}{K}, \forall k \in \mathcal{K}, \forall t \in \mathcal{T} \tag{5.7a}$$

$$s.t \;\; \theta_{k,n} \geq \theta_0, \qquad \forall n \in \mathcal{N}_k, \forall k \in \mathcal{K}, \tag{5.7b}$$

$$s.t \;\; l_n^t \leq L_n, \qquad \forall n \in \mathcal{N}, \forall t \in \mathcal{T}, \tag{5.7c}$$

Eq. (5.7a) represents the goal to minimize the average number of handovers (HO_{avg}) experienced by all UEs in the network. HO_k represents the total number of handovers experienced by each UE k since the beginning of their connection. The objective is to find at each instant t of the connection period a configuration ($X_{k,n}^t$) that minimizes the average number of handovers for all UEs. Eq. (5.7b) represents the constraint to guarantee the least acceptable link quality by setting a minimum threshold for the elevation angle. Eq. (5.7c) represents the goal of minimising the average blocking rate by ensuring that the total load of SAT_n is less than or equal to its total number of available channels L_n.

The problem formulated in Eq.5.7 is a combinatorial integer optimization problem, which is NP-hard in general. To solve this problem, it will be transformed into a MARL-based optimization problem based on stochastic game in the following section.

5.3 5G Satellite Handover based on Reinforcement Learning

RL is a computational method for understanding and automating goal-directed learning and decision-making. It differs from other computational approaches as it focuses on an agent learning through direct interaction with its environment, rather than requiring ideal supervision or entire models of the environment. It can learn anything from scratch by pursuing a goal that can be defined as the maximization of the expected value of a cumulative sum of a received scalar signal called reward. RL defines the interaction between a learning agent and its environment in terms of states, actions, and rewards by using the formal framework of Markov decision processes. This framework is intended to be a straightforward way of representing key aspects of the artificial intelligence problem. These characteristics include a sense of cause and effect, uncertainty, non-determinism, and the presence of explicit goals [86].

The fundamental components of reinforcement learning include:

- **Agent:** The entity that interacts with the environment and makes decisions. The agent's objective is to learn a policy or strategy that maximizes the expected cumulative reward over time.

- **Environment:** The external system with which the agent interacts. It is typically represented as a Markov Decision Process (MDP), where the agent's actions influence the state of the environment, and the environment provides feedback in the form of rewards.

- **State:** A representation of the current situation or configuration of the environment. States provide the necessary information for the agent to take actions.

- **Action:** The set of choices available to the agent in a given state. The agent selects actions based on its policy, which defines the mapping from states to actions.

- **Reward:** A numerical signal provided by the environment after each action taken by the agent. The reward indicates the immediate desirability or quality of the action taken.

- **Policy:** The strategy or mapping that the agent uses to determine its actions in each state. The goal is to learn an optimal policy that maximizes the expected long-term cumulative reward.

Reinforcement learning algorithms aim to find the optimal policy through exploration and exploitation. Exploration involves trying different actions to discover their effects on the environment, while exploitation involves selecting actions that are currently believed to be the best based on the learned policy. Striking the right balance between exploration and exploitation is a critical challenge in RL.
There are several RL algorithms, including:
1. Q-Learning: An off-policy algorithm that learns the optimal action-value function, known as the Q-function, to make decisions.

2. Policy Gradient Methods: These algorithms directly optimize the policy to maximize expected rewards. Examples include REINFORCE and Proximal Policy Optimization (PPO).

3. Value Iteration and Policy Iteration: These are dynamic programming-based methods for solving RL problems with finite state and action spaces.

4. Deep Reinforcement Learning: Combines RL with deep neural networks to handle high-dimensional state spaces. Notable algorithms in this category include Deep Q-Networks (DQN) and Trust Region Policy Optimization (TRPO).

5. Actor-Critic Methods: These algorithms combine aspects of policy gradient and value-based methods. They use a critic network to estimate value functions and an actor-network to learn the policy.

We are mainly interested in Q-learning due to its several advantages when applied to scenarios like satellite HO, where efficient and reliable communication transitions between satellites are crucial. These advantages include its model-free nature, meaning it doesn't require explicit knowledge of the environment's dynamics or a transition model. This is advantageous in satellite environments where modeling the exact dynamics can be highly complex and uncertain. In addition to its suitability for temporal decision-making, off-policy learning capabilities, effective exploration-exploitation balance, efficiency in handling high-dimensional spaces, theoretical convergence guarantees, and adaptability to online learning. This is essential in satellite HO scenarios, as it allows the agent to continually adapt to changing conditions while still making efficient use of available resources.

5.4 Q-Learning Algoritm

Q-learning is a model-free RL algorithm that can be used to learn the value of an action in a given state. It can handle problems with stochastic transitions and rewards without requiring adaptations [87]. Q can be learned through trial-and-error interactions with the environment by running through a large NEP (training duration in which a sequence of states, actions, and rewards is considered), and thus through as many state/action pairs as possible. “Q” refers to the function that involves a simple updating procedure in which the agent starts with arbitrary initial values of $Q(s, a)$ for all $s \in \mathcal{S}$, $a \in \mathcal{A}$, and updates the Q-values as follows:

$$Q_{t+1}(s^t, a^t) = (1 - \alpha_t)Q_t(s^t, a^t) + \alpha_t[r^t + \gamma \max_a Q_t(s^{t+1})] \tag{5.8}$$

where $\alpha_t \in [0, 1)$ is the learning rate.

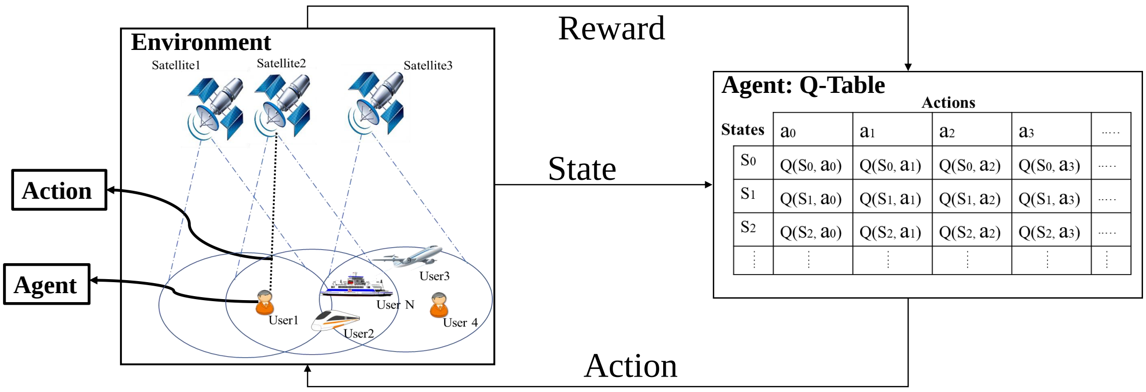

Figure 5.3: Component of the Q-learning framework- In Q-learning, the Q-table serves as the agent’s brain, where the state and the action of the agent are the inputs of the Q-Table, and the Q-value of those inputs is the output of the Q-Table. Higher the Q-value, better the action, higher the received reward.

The main components of our RL framework as shown in Figure 5.3 are:

- *Agent*: Each user is considered to be a Q-learning agent, i.e., the agent's brain is composed of a Q-table that contains the Q-value of each possible state-action combination. The set of agents $\mathcal{A}$ is equal to the set of users $\mathcal{K}$.

- *Environment*: In this paper, the environment is the NS-3-based 5G satellite integrated network.

- *State*: The state of agent k at time t is defined as the 3-tuple, $s_k^t =< \overline{C_k^t}, \overline{l^t}, \overline{V_k^t} >$, where $\overline{C_k^t}$, $\overline{l^t}$, and $\overline{V_k^t}$ are all vectors of size N, such that, $\overline{C_k^t} = [C_{k,0}^t, C_{k,1}^t, ..., C_{k,n}^t, ..., C_{k,N}^t]$ contains the coverage indicators between user k and each satellite $n \in \mathcal{N}$, $\overline{l^t} = [l_0^t, l_1^t, ..., l_n^t, ..., l_N^t]$ indicates the number of loaded channels of each satellite $n \in \mathcal{N}$ at time t, and $\overline{V_k^t} = [V_{k,0}^t, V_{k,1}^t, ..., V_{k,n}^t, ..., V_{k,N}^t]$ includes the RVT between user k and each satellite $n \in \mathcal{N}$ at time t. $\mathcal{S}$ indicates the set of states.

- *Action*: Represents the decision taken by an agent which is to connect to one of the satellites $n \in \mathcal{N}$. In this paper, an action of an agent k at time t is defined as a_k^t where a_k^t is equal to one of the satellites $n \in \mathcal{N}$ such that $C_{k,n}^t = 1$.

- *Reward*: A motivation mechanism that uses reward or penalty. The instantaneous reward of an agent k, after an action a_k^t was taken knowing that it is in state s_k^t, is represented by $r_k^t(s_k^t, a_k^t)$. Considering that agent k chooses to connect to satellite n at time t (ie. $a_k^t = n$):

$$r_k^t(s_k^t, a_k^t) = \begin{cases} -p_1 & \text{if } C_{k,n}^t = 1, X_{k,n}^t = 0, \\ -p_2 & \text{if } C_{k,n}^t = 1, X_{k,n}^t = 1, \\ & l_n^t < \sum_{k \in \mathcal{K}} X_{k,n}^t, \\ f(t,n,k) & \text{if } C_{k,n}^t = 1, X_{k,n}^t = 1, \\ & l_n^t \geq \sum_{k \in \mathcal{K}} X_{k,n}^t \end{cases} \tag{5.9}$$

A high penalty is associated with the instantaneous reward function when an action results in a HO, and a lower penalty when the action results in blocking. However, when the action avoids HO and blocking a positive reward is given such that it is higher when the agent chooses to connect to a satellite with higher RVT and lower load. $p_1 = 300, p_2 = 100$ and $f(t, n, k) = v^t_{k,n} + w^t_n$, where $w^t_n = l^t_n - \sum_{k \in \mathcal{K}} X^t_{k,n}$ represents the number of available channels of satellite n at time t. The values for p_1 and p_2 are chosen to be comparable with the possible range of values for $f(t, n, k)$ to provide a balanced and realistic representation of the trade-offs involved in the decision-making process, ensuring that the consequences and benefits of various actions are appropriately captured and weighted within the context of the study.

- *Policy*: A strategy used by the agent to achieve its goal. The policy directs the agent's actions based on the agent's current state. The goal of agent k is to find an optimal policy π^*_k that maximizes the expected cumulative reward:

$$\pi^*_k = arg \max_{\pi} R^k(s, \pi) \tag{5.10}$$

where $R^k(s, \pi) = \sum_{t=0}^{T} \gamma E\{r^t_k | s^0 = s, \pi\}$ is the expected cumulative reward of agent k and

$\gamma \in [0, 1)$ is the discount factor used to increase/decrease the weight of new rewards in comparison to previously stored rewards.

The goal of the proposed LEO satellite HO optimization problem, is equivalent to Eq. (5.10), which aims to find an optimal policy to maximize the expected cumulative reward over time.

When designing an action selection policy in RL, it is critical to balance exploitation and exploration. Exploitation occurs when agents choose the best action based on the current Q-values, also known as a greedy policy. Exploration entails the agents attempting more actions that have not been exploited yet in order to explore a larger action space.

To make better random actions, Boltzman's exploration has been combined with the ϵ-greedy policy. An action's selection probability, denoted by $\pi_t(a^t)$ is weighted by its associated Q-value as follows:

$$\pi_t(a^t) = \frac{\exp \dfrac{Q^k(s_k^t, a^t)}{\tau}}{\sum_{a^t} \exp \dfrac{Q^k(s_k^t, a^t)}{\tau}} \tag{5.11}$$

where τ is called the temperature factor. It controls the amount of exploration, i.e., the probability of executing actions other than the one with the highest Q-value. When τ is high, all actions will be explored equally; when it is low, high-rewarding actions will be chosen with higher probability.

Despite the fact that this policy is viewed as a random action selection policy, the agents have a greater chance of choosing good actions due to the property of the probability function. Thus, given an exploration parameter $\varepsilon \in [0, 1)$:

$$a_*^t = \begin{cases} arg\max_{a^t} \pi_t(a^t) & \text{if } \epsilon < \varepsilon, \\ arg\max_{a^t} Q_k^t(s_k^t, a^t) & \text{otherwise} \end{cases} \tag{5.12}$$

In this subsection, the multi-agent LBSH method will be defined considering six UEs. Each UE is a RL agent that interacts with the environment based on its partial view of its current state. During each episode, at each time step, the agent observes the state s and selects an action a based on a policy π. Considering Eq. (5.12), instead of having a constant ϵ throughout the learning process, a variable ϵ_t that increases linearly with time is considered to encourage the agents to explore more at the beginning of the learning and then, as ϵ_t increases, the agents start to explore with lower probability. Note that ϵ_t stops increasing when it reaches a value of 0.8 to let the agents still explore with a certain probability. The Q-table of this agent is then updated following Eq. (5.8).

Algorithm 1 Multi-Agent Q learning

Initialize:
$t = 0$, $\mathcal{S}_k = \{s_k^0\} =< \overline{C_k^0}, \overline{l^0}, \overline{V_k^0} > \forall k \in \mathcal{K}$;
Satellites-Load= l^0;
$Q_k^0(s^0, a^0) = 0$
while $ep < NEP$ **do**
$t < T$
for $k \in \mathcal{K}$ **do**
choose random agent k;
observe $s_k^t =< \overline{C_k^t}, \overline{l^t}, \overline{V_k^t} >$;
choose action a_k^t based on policy $\pi(s_k^t)$;
move to a new state $s_k^{t+1} =< \overline{C_k^{t+1}}, \overline{l^{t+1}}, \overline{V_k^{t+1}} >$;
get the reward r_k^t;
update Satellites-Load to l^{t+1};
if $s_k^{t+1} \in \mathcal{S}_k$ **then**
update the Q-value $Q_k^t(s_k^t, a_k^t)$ by Eq. (5.8);
else
add the new state s_k^{t+1} to $\mathcal{S}$;
initialize the Q-value of the new state to zero;
endif
endfor

end while =0

Since satellites are continuously moving, the covering set of satellites for the user, along with the corresponding RVT, changes at each time instance, causing a transaction to a new state independently by the taken action, while, at the same time, the action of the agent may alter each satellite load, causing the transition to a new state too. This results in a huge number of possible states that are hard to predict and define at the beginning of the learning. To solve this problem, the procedure shown in Algorithm 1 is used.

At the beginning of the learning ($t = 0$), there is only one state in the set of states ($\mathcal{S} = \{s^0\}$). Then, at each time step, after an action is taken, the load allocation of each satellite, the RVT, and the set of covering satellites of the user change accordingly, causing the agent to move to a new state s'. If s' is already included in the set of states, its Q-value will be updated, otherwise, s' is added to the set of states ($\mathcal{S} = \{s^0, s_1, ..., s'\}$ with an initial Q-value of zero.

As shown in Algorithm 1, at each time step, the agents observe their current state s_k^t and select an action a_k^t based on a policy π, acquire a corresponding reward r_k^t, and update their own Q-table following Eq. (5.8). The agents are considered to take actions successively one after another, where the sequence of learning for the agents is randomly chosen at each instant. After agent k chooses an action, the load of the satellites will change accordingly, which can be obtained by the other agents before the latter takes its action. It is assumed that each agent has no knowledge about the reward function of other agents, however, they can get each other actions.

5.5 Simulation Results

Table 5.1: Simulated scenario parameters

Parameter	Multi-Agent
Number of satellites	48
Number of UE	6
Satellite altitude	600 km
Orbital planes eccentricity	0 (circular)
Orbital planes inclination i	$88°$
Orbital planes argument of perigee	$90°$
Minimum elevation angle between UE and gNB for transmissions	$20°$
Number of satellite available channels	5
α	0.1
γ	0.95
ϵ	0.1-0.8
τ	10
NEP	2500
Duration of an episode (T)	600 s

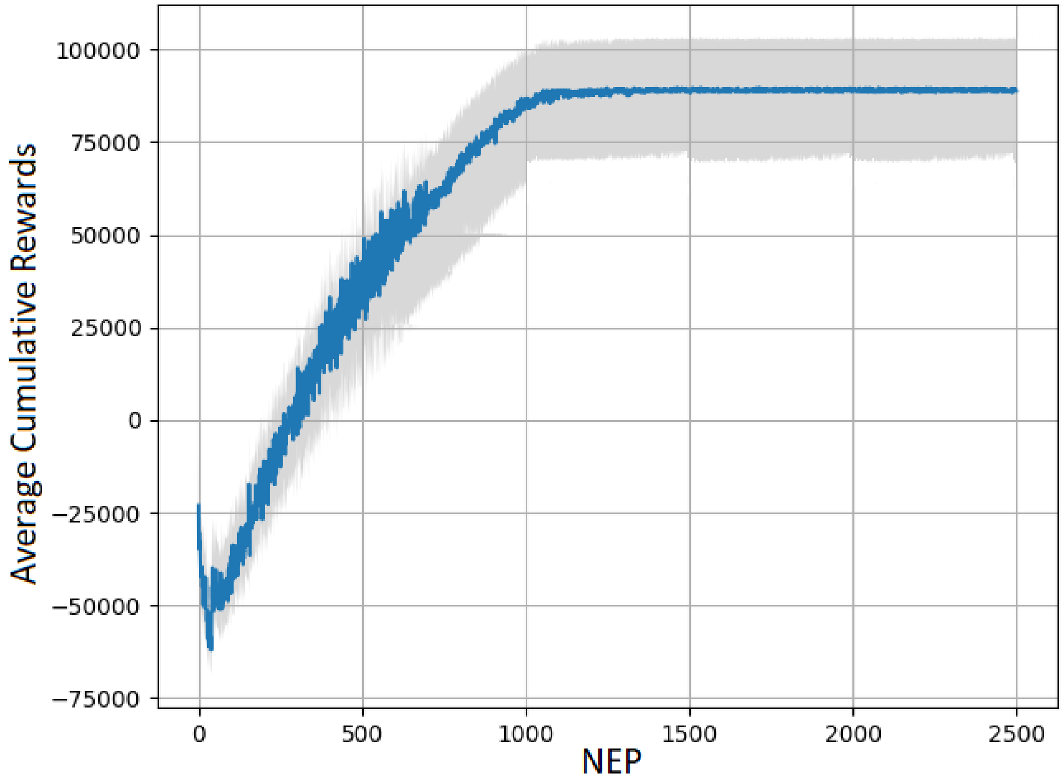

Figure 5.4: Multi-Agent: Average Cumulative Reward as a function of NEP

The proposed multi-agent LBSH optimization approach is tested and compared with different approaches in a real case scenario within the developed NS-3-based 5G STIN simulator previously presented in Chp. 3.

For the LBSH approach proposed in this paper, ϵ is assumed to increase linearly from 0.1 to 0.8 while NEP increases. The reward function defined in Eq. (5.9) is adopted. Figure 5.4 shows the average cumulative rewards as a function of the NEP. As NEP increases from 0 to 2500, the cumulative reward increases from -60000 to about 950000, starting to converge after 1000 episodes. The reason is that in the first episodes, the agents explore more, and then start to exploit more following Eq. (5.12). The grey shade in Figure 5.4 represents the range of the cumulative reward for all the six agents during learning. I first compare our work with a non-smart HO strategy where the HO decision is taken based only on the minimum distance between the UE and its associated satellite and the RVT between them. The minimum distance and the RVT between each UE-satellite pair are continuously traced. Accordingly, at each instant, each UE chooses to be connected to the satellite closest to it with higher RVT. The second approach is a Load Aware Satellite Handover (LASH) proposed in [65]. The reward function in LASH follows the same structure as in Eq.5.9, with $p1 = 20$, $p2 = 10$, and $f(t, n, k) = v^t_{k,n}$ which is limited to the remaining visibility time $v^t_{k,n}$, thus rendering LASH a load-aware HO strategy. In contrast, in the LBSH, $f(t, n, k) = v^t_{k,n} + w^t_n$ accounts for the actual load of the satellite, and therefore, is a load-balancing scheme.

Moreover, at each instant, the action in [65] is chosen based on a fixed exploration parameter ϵ rather than an adaptable ϵ_t. Figure 5.5 shows the average number of HOs as a function of the NEP for the three different approaches.

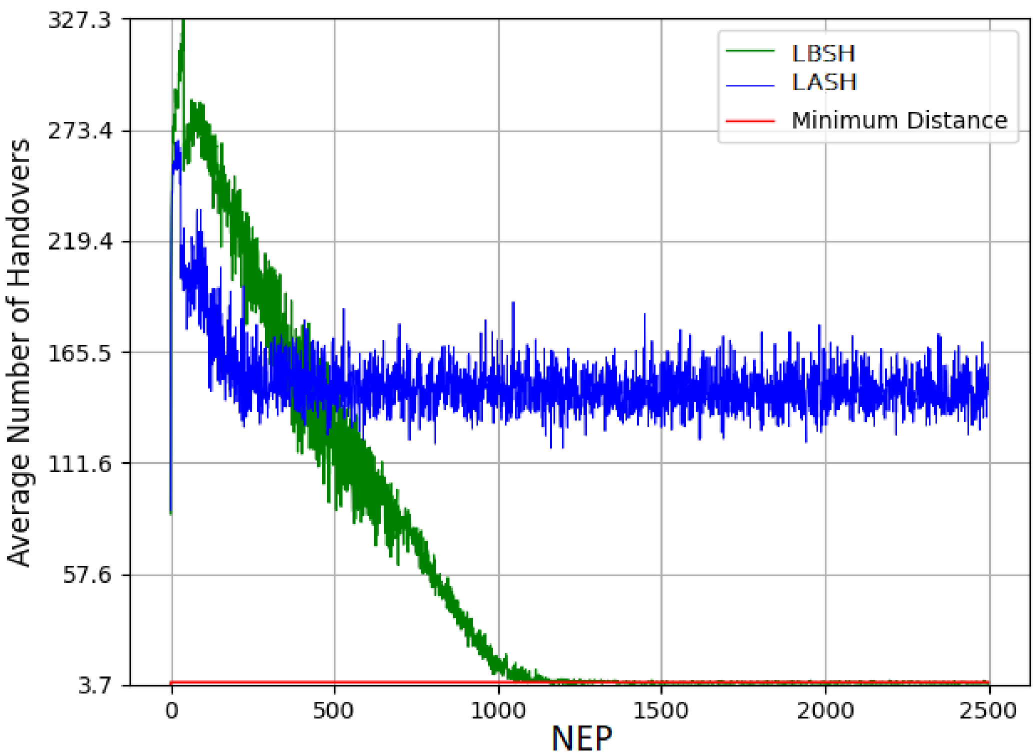

Figure 5.5: Multi-Agent: Average Number of Handovers as a function of NEP

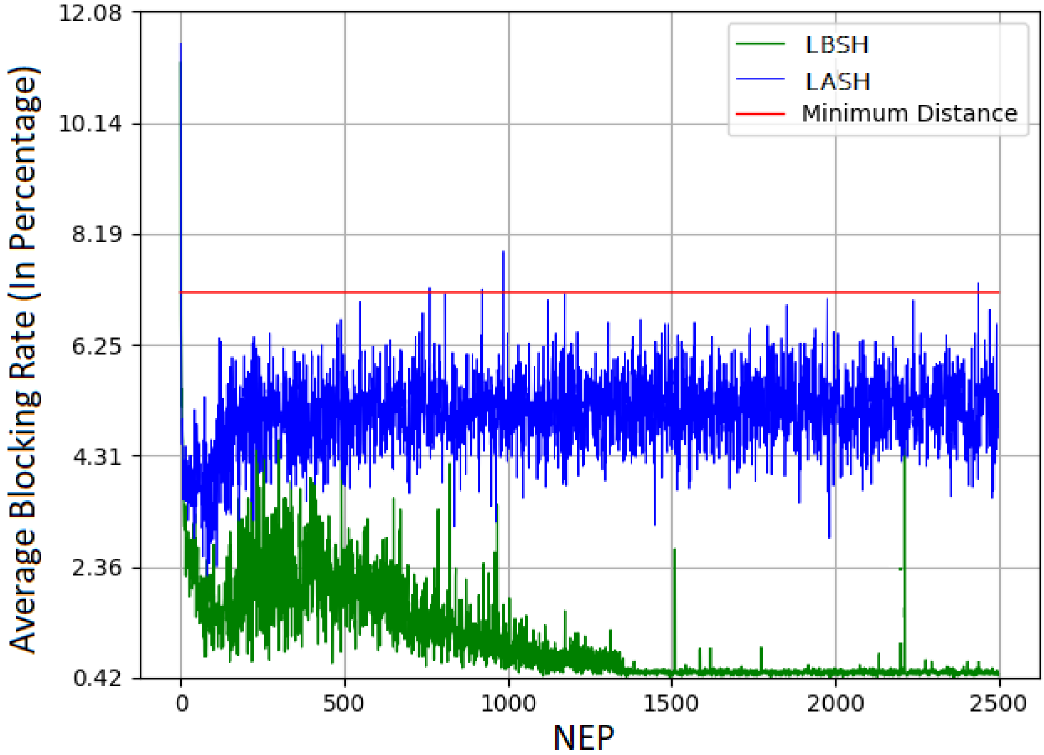

Figure 5.6: Multi-Agent: Average Blocking Rate as a function of NEP

The LBSH approach proposed in this paper outperforms the LASH approach implemented in [65] when implemented in a realistic simulator, as the final number of HOs per user is 95% lower. Besides, the proposed LBSH converges to the same average HOs value of the Minimum distance approach which is around 3.7 HOs in the 600 s episode duration.

The blocking rate of the user k at time t is denoted by Br_k^t and defined as follows:

$$BR^k = \frac{\sum_t BN_t^k}{T} \tag{5.13}$$

where BN_t^k indicates whether user k was dropped at time t:

$$BN_t^k = \begin{cases} 1 & \text{if user } k \text{ chooses to connect to satellite } n \text{ and} \\ & l_n^t < \sum_{k \in \mathcal{K}} X_{k,n}^t, \\ 0 & \text{otherwise} \end{cases} \tag{5.14}$$

As shown in Figure 5.6, the minimum distance approach results in the maximum blocking rate since it does not take the load constraint of each satellite into consideration. Moreover, the proposed LBSH approach results in the minimum blocking rate which converges to a value of 0.0042 (0.42%) and hence outperforms the LASH approach by around 84%. These results suggest that a load balancing scheme avoids allocating UEs to loaded satellites, and therefore, mitigates the risk of blocking.

5.6 Conclusion

In conclusion, this chapter has introduced a novel Load-Balancing Satellite Handover (LBSH) scheme tailored for 5G Single Traffic Profile Scenarios, offering significant implications for the management of handovers within Satellite Terrestrial Integrated Networks (STIN). The LBSH strategy was rigorously implemented and evaluated within a simulation environment driven by the NS-3 software platform.

The outcomes of our experimental endeavors have underscored the exceptional potential of the LBSH scheme in optimizing 5G STIN HO management. The salient findings of this research are particularly noteworthy, indicating the superior performance of LBSH in comparison to contemporary solutions. Specifically, LBSH has exhibited a remarkable reduction of 95% in the average number of handovers and an impressive 84% decrease in the blocking rate.

These empirical results carry profound implications for the practical deployment of satellite-generated 5G cells. LBSH not only enhances the operational efficiency of HO processes but also ensures the judicious allocation of satellite channels. This augmentation translates into a heightened quality of 5G connectivity for end-users, while also contributing to the overall resilience and efficiency of satellite-based communication networks. This implies that LBSH is a promising technique to manage 5G STIN HOs whilst still effectively exploiting the available channels of satellite-generated 5G cells.

Chapter 6

LEO Satellite Handover for Multiple Traffic Profile Scenarios

6.1 Introduction

Next-generation communication technologies are rapidly evolving to accommodate a wide range of new applications, such as Artificial Intelligence, Virtual Reality, three-dimensional media, and the IoT, which have led to distinguishing UEs with different and varying TP, i.e., different performance requirements and generated traffic statistics, from the network resource viewpoint (Figure 6.1).

These TP encompass a spectrum of performance requirements and generated traffic statistics, necessitating a paradigm shift in satellite HO management to effectively harness the limited available resources and avert network congestion. Thus, differentiating User Equipments (UEs) with different and varying TPs has become necessary due to each application's unique performance requirements. However, LEO satellites have limited onboard resources and the launched constellations ensure that each UE will be covered by more than one LEO satellite at any given moment, making it challenging to select the optimal satellite at any given time to ensure the optimum QoS. Therefore,

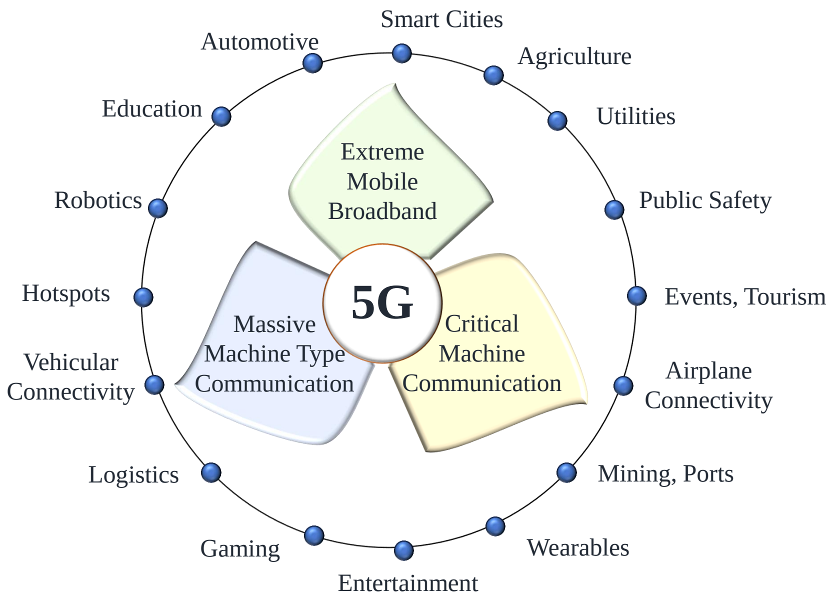

Figure 6.1: 5G ERA Enabling New Applications

a satellite HO strategy has to effectively use the few available satellite resources and prevent network congestion while respecting the various resource requirements per TP. To address all the above requirements, a user-centric Multi-Agent Deep Q-Network (MADQN) satellite HO strategy is proposed, which is the first in the state of the art to address the variety and diversity of UEs' performance requirements and generated traffic statistics.

The rest of this chapter is organized as follows. Section 6.2 provides an overview of the problem formulation. Section 6.3 describes the methodology followed, and a comparison between the MARL and MADQL-based HO optimisation strategies. Simulation results are presented and discussed in Section 6.4. Finally, conclusions are provided in Section 6.5.

6.2 Problem Formulation

The primary objectives of our proposed HO criteria are to reduce the number of HOs and minimize the blocking rate by balancing the load among satellites taking into account different and varying resource requirements per UE. These objectives are particularly critical in scenarios involving LEO satellite networks, where frequent HOs can lead to a significant signaling overhead, resource consumption, and UE dissatisfaction due to interruptions [13**?**].

In order to account for users with differing TPs, each UE changes randomly its corresponding resource requirements after each communication duration T. For the sake of simplicity, a distinction is made between four TPs (four applications) as defined in the 3GPP Technical specification "Service requirements for the 5G system" of Release 17 [88], which differ in their data rate requirements and delay tolerance as follows:

1. $TP1$ Vehicular Connectivity: $R_k = 2W$, s.t $\hat{R}_k \leq R_k$
2. $TP2$ Airplane Connectivity (inflight Internet): $R_k = 2W$, s.t $\hat{R}_k = R_k$
3. $TP3$ Narrow-band IoT: $R_k = W$, s.t $\hat{R}_k \leq R_k$
4. $TP4$ Public Safety/Emergency Response: $R_k = W$, s.t $\hat{R}_k = R_k$

R_k and $\hat{R}_k$ refer to the target (required) resources and the minimum acceptable resources for UE_k, respectively. It is assumed that delay-tolerant users (TP1 and TP3) are more lenient in receiving fewer resources than their resource requirements ($R_k \geq \hat{R}_k$), whereas delay-sensitive users (TP2 and TP4) are more rigid and adhere to the concept of either all or none ($R_k = \hat{R}_k$). As a consequence, delay-sensitive users will be considered blocked if they do not have all of their required resources at time t, while delay-tolerant users will not be considered blocked.

The complete bandwidth of each satellite is divided into L_n channels of bandwidth W and each user can transmit or receive on one or more of those channels depending on their current TP. The channel budget restriction is therefore provided by:

$$l_n^t \leq L_n, \qquad \forall n \in \mathcal{N} \tag{6.1}$$

where,

$$l_n^t = \sum_{k \in \mathcal{K}} l_{k,n}^t \cdot X_{k,n}^t \tag{6.2}$$

$l_{k,n}^t$ represents the resources of SAT_n allocated to UE_k at time t, such that $\hat{R}_k^t \leq l_{k,n}^t \leq R_k^t$, and $X_{k,n}^t = [0,1]$ allows to consider only users connected to SAT_n at time t.

UE_k is considered blocked at time t if it tries to connect to a satellite with not enough resources. It is represented by BN_k^t as follows:

$$BN_k^t = \begin{cases} 1 & \text{if } UE_k \text{ chooses to connect to } SAT_n \\ & \text{and } l_n^t + \hat{R}_k^t > L_n, \\ 0 & \text{otherwise} \end{cases} \tag{6.3}$$

6.3 Methodology

6.3.1 Satellite Handover Based on Deep-RL

There are two issues with having an extremely large number of states and actions. The first one is that as the number of states grows, more memory is needed to keep and update the state-action table. Secondly, as the number of states grows, it takes much more time to thoroughly examine each state and appropriately populate the Q-table [86]. Those two issues limit the usability of Q-learning only to small-scale models, while the learning process becomes out of control when dealing with large-scale models.

The LBSH satellite handover optimisation method achieves remarkable results while considering only one TP for all UEs. However, randomly changing the resource requirements for each UE after each episode in order to consider different and changing applications considerably increases the number of states. This results in an enormous Q-table which makes it almost impossible for an agent to effectively learn in a reasonable amount of time, limiting the Q-learning use to only one type of traffic application as will be shown in section 6.4. To solve this problem, consideration is given to Deep Q-Learning (DQL), which utilizes deep neural networks instead of a Q-Table to predict the Q values for each action.

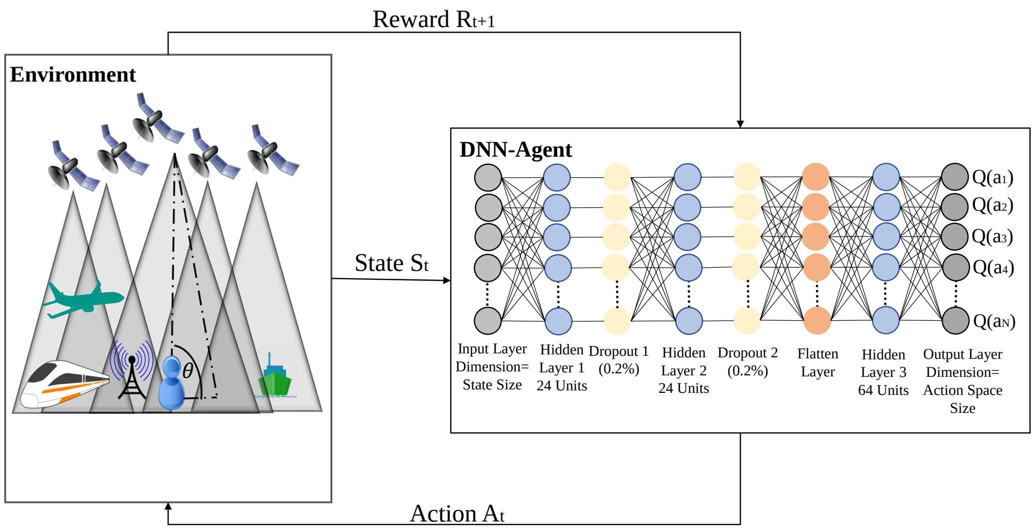

Figure 6.2: Compositions of the proposed Deep Q-Learning strategy: Environment and DNN structure. The Environment is composed of a number of LEO satellites and users. The Deep neural network (Agent's brain) is composed of an input layer of dimensions equal to the state size, three fully connected hidden dense layers to learn the features of the state information, two drop-out layers, a flatten layer, and an output layer of dimension equal to the action space size

DQL differs from the standard Q-learning by the agent's brain. In Q-learning, the Q-table serves as the agent's brain, while in DQL a deep neural network provides a good approximation of the Q-value of an action, i.e., $Q(s,a) \approx Q(s,a,\Lambda)$, where Λ is the set of weights of the DNN which is updated after each learning phase, thus mapping from partially observed states to actions rather than fully observing every state and keeping a list of the corresponding Q-values in an enormous lookup table [89], as shown in Figure 6.3.

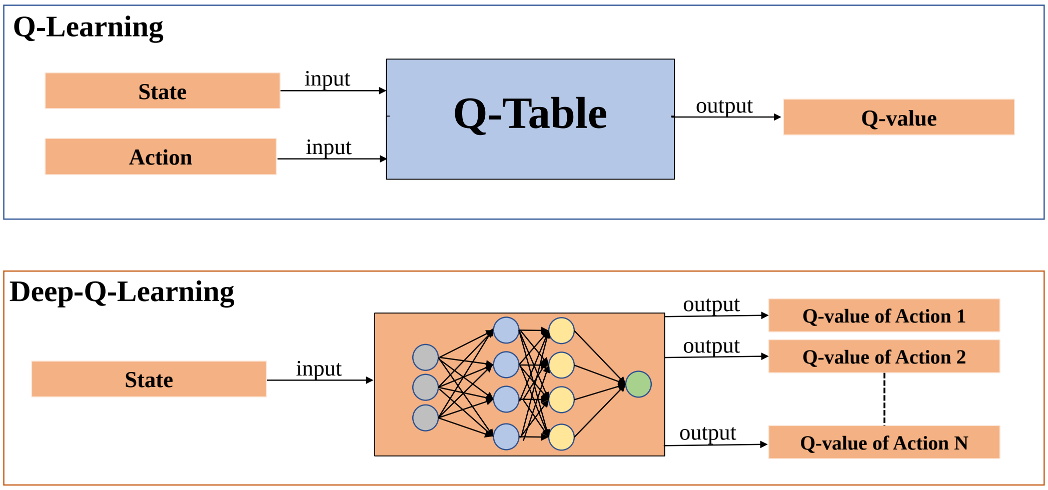

Figure 6.3: Q-Learning vs Deep-Q-Learning: Difference in the agent's brain. In Q-learning, the Q-table serves as the agent's brain, where the state and the action of the agent are the inputs of the Q-Table, and the Q-value of those inputs is the output of the Q-Table, while in Deep-Q-Learning a deep neural network acts as the brain, where the state is the input of the deep neural network and the approximation of all the Q-values of each corresponding possible action for this specific state are the output of the neural network.

The selection of DQL as the primary reinforcement learning algorithm is underpinned by several compelling factors. First and foremost, our satellite communication system poses a challenge due to its inherent complexity. This complexity arises from dynamic LEO satellite positions, fluctuating UE resource requirements, and the need to balance multiple performance objectives. DQL emerges as a well-suited choice for addressing such intricate problems, especially when dealing with discrete action spaces. Data efficiency is another paramount consideration. In real-world applications, data collection can be resource-intensive and costly. DQL's ability to learn efficiently from a limited dataset proves advantageous, making it suitable for practical deployment. Furthermore, the simplicity and interpretability of the chosen algorithm also weigh in the decision as it offers a straightforward architecture, enhancing the comprehensibility of learned policies, in addition to the training stability, incorporating techniques such as experience replay and target networks. These mechanisms contribute to faster convergence and improve the assurance of reliable results.

In DQL, the state is provided as the input to the modeled DNN and the output is the estimated Q-value for every possible action that might be taken in the given observed state. The same state and action spaces defined in Chapter 5 are considered for the Q-learning methodology. The structure of the proposed DNN is shown in Figure 6.2. The proposed DNN is composed of an input layer of dimensions equal to the state size, three fully connected dense layers to learn the features of the state information, a flatten layer used to expand the output of the previous dense layer into a vector before inputting it into the following fully connected dense layer to get the Q-values for each action $a \in \mathcal{A}$ and an output layer of dimension equal to the action space size. In the model, two dropout layers with a probability of 0.2% are also included due to their well-known ability to avoid over-fitting problems as described in [90]. The input of the proposed DNN is the state s_k^t of UE_k, which is transformed into a matrix $\Phi(s_k^t)$ before being input into the DNN. In this case, each UE is considered as an agent for the same reason of avoiding network congestion.

According to the multi-objective optimisation problem of reducing the total number of HO events while minimising the blocking rate, the reward function in four different cases is defined as follows:

$$r_k^t(s_k^t, a_k^t) = \begin{cases} -z_1 & \text{if } X_{k,n}^t = 0,\, l_n^t > L_n, \\ -z_2 & \text{if } X_{k,n}^t = 0,\, l_n^t \leq L_n, \\ f_1(t,k,n) & \text{if } X_{k,n}^t = 1,\, l_n^t > L_n, \\ f_2(t,k,n) & \text{if } X_{k,n}^t = 1,\, l_n^t \leq L_n \end{cases} \tag{6.4}$$

The first two cases represent when an action leads to a HO and the agent chooses to move to a satellite with enough resources or a loaded satellite. The agent will receive a high negative penalty $z_1 = 500$ or a moderate negative penalty $z_2 = 300$, respectively, as the first case will result in blocking. On the other hand, the other two cases represent when an action does not result in any HO and the UE is connected to a loaded satellite or not. The agent will receive a negative penalty $f_1(t,k,n) = 100 * w_n^t$ (since $w_n^t < 0$ for loaded satellites), in order to motivate it to always move to a satellite with the lower load if necessary to avoid blocking, or a big positive reward $f_2(t,k,n) = V_{k,n}^t$, in order to motivate it to move to a satellite with higher RVT when necessary to avoid consecutive future HOs, respectively.

Moreover, in order to make the learning more stable and convergent, DQL uses experience replay and mini-batch learning which randomizes collected data samples and smooth data distribution changes. After each time step, the resultant transformations $(\Phi(s_k^t), a_k^t, \Phi(s_k^{t+1}), r_k^{t+1})$ are progressively stored in a replay memory $\mathbb{M}$. The deep Q-network is updated by using experience replay in a supervised learning-based method that takes into account both recent and past experiences. Therefore, to update the network, experience replay stores observed transitions in the replay memory $\mathbb{M}$ and samples evenly a mini-batch from this memory bank. As a result, the Q-network can reduce memory correlation, enhancing learning effectiveness [91].

The DQL calculates the cost together with the memory randomly sampled from $\mathbb{M}$ at each time step and trains the network that adjusts the Q-value parameter based on the loss function provided by:

$$L(\Lambda) = \mathbb{E}[y^j - Q(\Phi(s^j), a^j; \Lambda)^2] \tag{6.5}$$

where,

$$y^j = \begin{cases} r^j \quad \text{if } \Phi(s^{j+1}) = \Phi(s^T), \\ \quad i.e., s^{j+1} \text{ is a terminal state} \\ r^j + \gamma \max_{a^{j+1} \in \mathcal{A}} Q(\Phi(s^{j+1}), a^{j+1}; \Lambda), \\ \quad \text{otherwise} \end{cases} \tag{6.6}$$

The adopted action selection policy in the proposed MADQL is an ϵ-greedy policy as follows:

$$a_*^t = \begin{cases} \text{Random action } a^{'} \in \mathcal{A} & \text{if } \varepsilon < \epsilon^t, \\ arg \max_{a^t} Q_k(s_k^t, a^t, \Lambda) & \text{otherwise} \end{cases} \tag{6.7}$$

where ϵ^t increases linearly with time to motivate the agents to begin their learning process by exploring more and then begin to exploit with a probability increasing with t.

Algorithm 3 summarises the DQL agent learning process. Every UE is an independent DQL agent, therefore the well-trained DNN is implemented on each UE. At the beginning, the state of each UE_k, $\forall k \in \mathcal{K}$, is initialised to $s_k^0 \in \mathcal{S}_k$, the current TP per UE is randomly chosen to insure the variation and diversity of the applications used by each UE during each episode, and the load distribution among satellites is initialised accordingly. At each time step t, each agent observes its current state s_k^t, chooses an action a_k^t according to Eq. (7.7) causing a transition to a new state s^{t+1}, and receives a reward r_k^{t+1} computed following Eq. (7.6). After each transition to a new state, both vectors s_k^t and s_k^{t+1} are transformed into the matrices $\Phi(s_k^t)$ and $\Phi(s_k^{t+1})$, respectively, in order to input the whole experience $(\Phi(s_k^t), a_k^t, \Phi(s_k^{t+1}), r_k^{t+1})$ in the replay memory

$\mathbb{M}$. Then, a mini-batch of size N_b is randomly sampled from the whole replay memory. Note that the maximum size of the replay memory is set to N_m so that old experiences are deleted, starting from the oldest ones, when space is needed to add new ones.

Algorithm 2 Multi-Agent Deep-Q learning

Initialise:
$\mathbb{M}$ - Empty experience replay buffer
N_b - Mini Batch size
N_m - Replay Memory Size
Λ - DNN Weights initialisation
$t = 0$
$\mathcal{S}_k = \{s_k^0\} =< \overline{C_k^0}, \overline{l^0}, \overline{V_k^0} > \forall k \in \mathcal{K}$
while $ep < NoE$ **do**
Allocate the appropriate RR for the randomly selected TP per agent following Eq. (**??**);
$l_n = l^0 \ \forall n \in \mathcal{N}$
while $t < T$ **do**
for $k \in \mathcal{K}$ **do**
Choose random agent k;
Observe $s_k^t =< \overline{C_k^t}, \overline{l^t}, \overline{V_k^t} >$;
Choose action a_k^t based on Eq. (7.7);
Move to a new state $s_k^{t+1} =< \overline{C_k^{t+1}}, \overline{l^{t+1}}, \overline{V_k^{t+1}} >$;
Transform s_k^t and s_k^{t+1} into matrices $\Phi(s_k^t)$ and $\Phi(s_k^{t+1})$, respectively;
Get the reward r_k^{t+1} computed following Eq. (7.6);
Update Satellites-Load to l^{t+1};
Store $(\Phi(s_k^t), a_k^t, \Phi(s_k^{t+1}), r_k^{t+1})$ in $\mathbb{M}$;
Sample a random mini-batch of size N_b from $\mathbb{M}$ for training;
Train the DNN of agent k;
Set y_t following Eq. (6.6);
Update the DNN parameters Λ by performing a gradient descent step on Eq. (6.5);
end for

Reset $t = 0$, $\mathcal{S}_k = \{s_k^0\} \ \forall k \in \mathcal{K}$;
end while =0

6.4 Performance evaluation

6.4.1 Scenario setup

To evaluate the performance achievable by using our proposed solution, The STIN Simulator that was implemented and discussed in Chapter 3 is used. It is a network level simulator based on the discrete-time discrete-event network simulator NS-3, which simulates packet data networks by using custom traffic models, as described in [72]. Since its official release does not allow simulating satellite communication networks, the software has been modified including a developed satellite mobility module that enables the integration of nodes moving and acting as LEO satellites in the NS-3 simulation environment. The SGP4 mathematical model, which is frequently employed to estimate the speed and location of LEO satellites, serves as the foundation for the module [75].

To prove the efficiency of the proposed strategy, I decided to first test its performance for a single traffic profile scenario by comparing it with four other approaches from the literature that has been implemented within NS-3:

- *Minimum Distance*: single-criterion strategy, the HO choice is made only on the basis of the minimum separation distance between the UE and the associated satellite, i.e., each UE decides to connect to the nearest satellite at any given time;
- *Minimum Load*: single-criterion strategy, the HO choice is made only on the basis of the minimal load per satellite, i.e., each UE decides to connect to the satellite with the minimum load among the ones in visibility from the UE at any given time;
- *Multi Criteria Load Aware (MCLA)* [65]: multi-criteria load aware strategy based on RL. The HO event is made considering the minimum elevation angle and the available satellite channels;

- *MARL*: Multi agent reinforcement learning based load balancing satellite HO strategy implemented in Chp 5. The HO event is made considering the RVT, the satellite load and the elevation angle;

The simulation parameters are all summarised in Table 6.1. It is assumed that the

Table 6.1: Simulated scenarios parameters

Parameter	**Single TP**	**Multiple TPs**
Number of satellites N	48	50
Number of UE K	6	6
Satellite altitude H	600 km	600 km
Number of orbital planes	4	5
Number of satellites per orbital plane	12	10
Orbital planes eccentricity	0 (circular)	0 (circular)
Orbital planes inclination i	$88°$	$88°$
Orbital planes argument of perigee	$90°$	$90°$
Minimum elevation angle between UEs and satellites for transmissions θ	$20°$	$20°$
Number of satellite available channels	5	7
Number of possible TPs	1	4
α	0.1	0.1
γ	0.95	0.99
ϵ	0.1-0.82	0.1-0.9
τ	10	-
Number of Episodes (NoE)	2500	1200
Duration of an episode T	600 s	120 s

UEs are uniformly spread over the Earth's surface and the satellites are all at the same altitude, uniformly spread among the multiple orbital planes, and equally spaced within each plane. The learning rate (α) is set to 0.1 which is commonly chosen as a default value since it allows balancing between exploration and exploitation, and enables the agent to update gradually, incorporating valuable feedback while exploring different actions. Furthermore, The exploration rate ϵ is chosen to increase linearly with time to motivate agents to explore more at the beginning, gathering information about the environment. Then, as time progresses, ϵ decreases, promoting a shift towards exploitation. This balance between exploitation and exploration is crucial to allow agents to learn while still leveraging their acquired knowledge. The temperature factor (τ) is set to 10, to increase the randomness in the action selection process during the exploration phase, which encourages the agent to explore a wider range of actions and avoid getting stuck in sub-optimal choices. T in Table 6.1 refers to the number of steps of an episode which reflects the actual movement and position of the satellites within a time duration of T seconds that can be predicted in advance by the STIN simulator [92].

6.4.2 Multi-Agent Deep Q-Learning Satellite Handover for a Single Traffic Profile

In this subsection, all the simulation parameters are set to the values summarised in Table 6.1, “Single TP” column. Figure 6.4 depicts the average number of HOs as a function of the episodes for each of the five HO approaches.

The minimum load method results in the highest average number of HOs since it takes into account only one criterion that is affected by each HO event that, in some cases, leads to multiple HO event chains. However, the MARL HO strategy outperforms the MCLA approach, with 95% lower number of HOs per user. Furthermore, the MARL approach converges to the same average HO value (around 3.7 HOs) as the Minimum distance method, which is known in the literature to achieve the minimum possible number of HOs. Similarly, the MADQL approach also converges to around only 4.2 HOs very close to the minimum distance approach. Figure 6.4 also shows that MADQL starts to converge faster than the MARL due to the ability of DNNs to predict the Q-values of newly visited states rather than requiring to go through all the states more than once to calculate the Q-values explicitly.

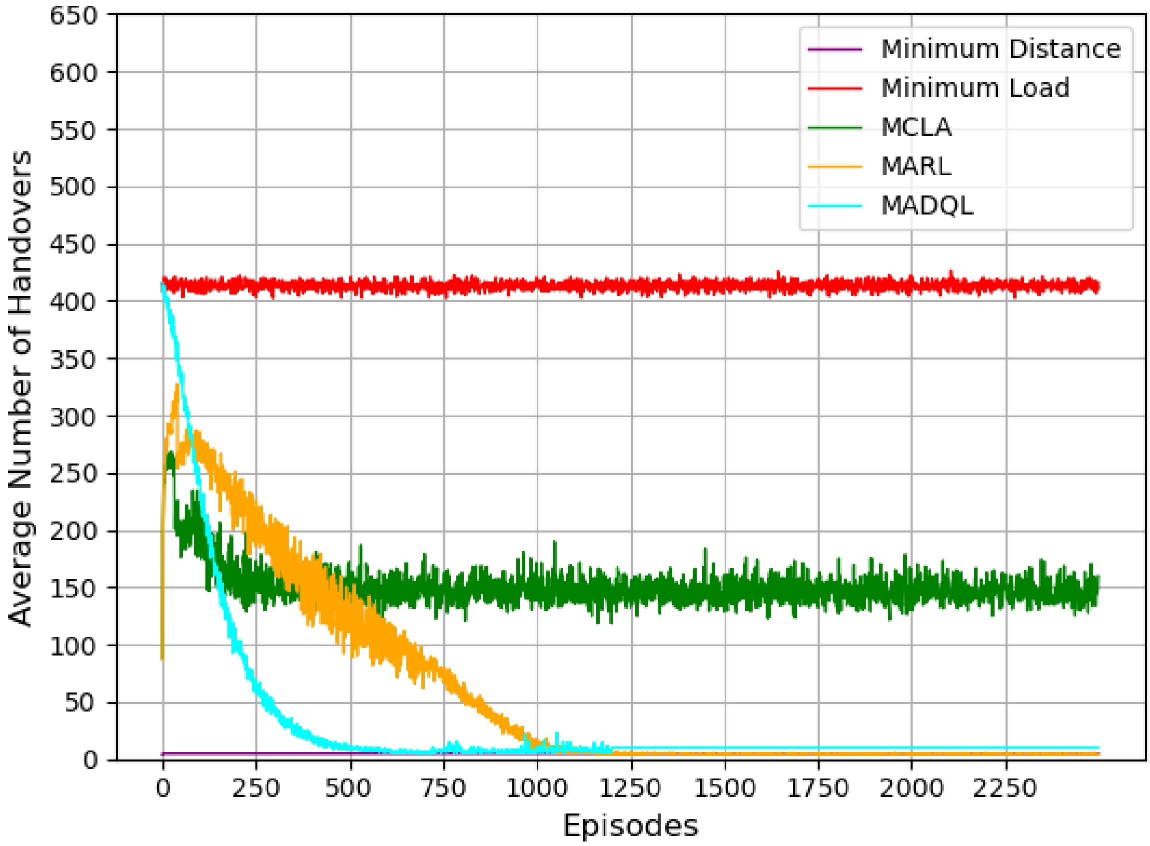

Figure 6.4: Single TP: Average Number of Handovers as a function of the episodes for the five considered approaches: Minimum Distance, Minimum Load, MCLA(Load Aware), MARL(Load Balance), and MADQL

Figure 6.5 shows the obtained blocking rate as a function of the episodes. Although the minimum distance strategy achieves the minimum number of HOs, it results in the highest blocking rate, because it ignores the load restriction of each satellite. The minimum load approach achieves zero blocking rate at the cost of a huge number of consecutive HOs and a consequent relevant decrease of the achievable QoS due to the HO process times. Moreover, Figure 6.5 shows that the MARL strategy achieves a very low blockage rate of 0.42%, outperforming the MCLA approach by almost 84%. While, on the other hand, the MADQL approach further outperforms the MARL strategy by converging to the minimal blocking rate of 0.033%.

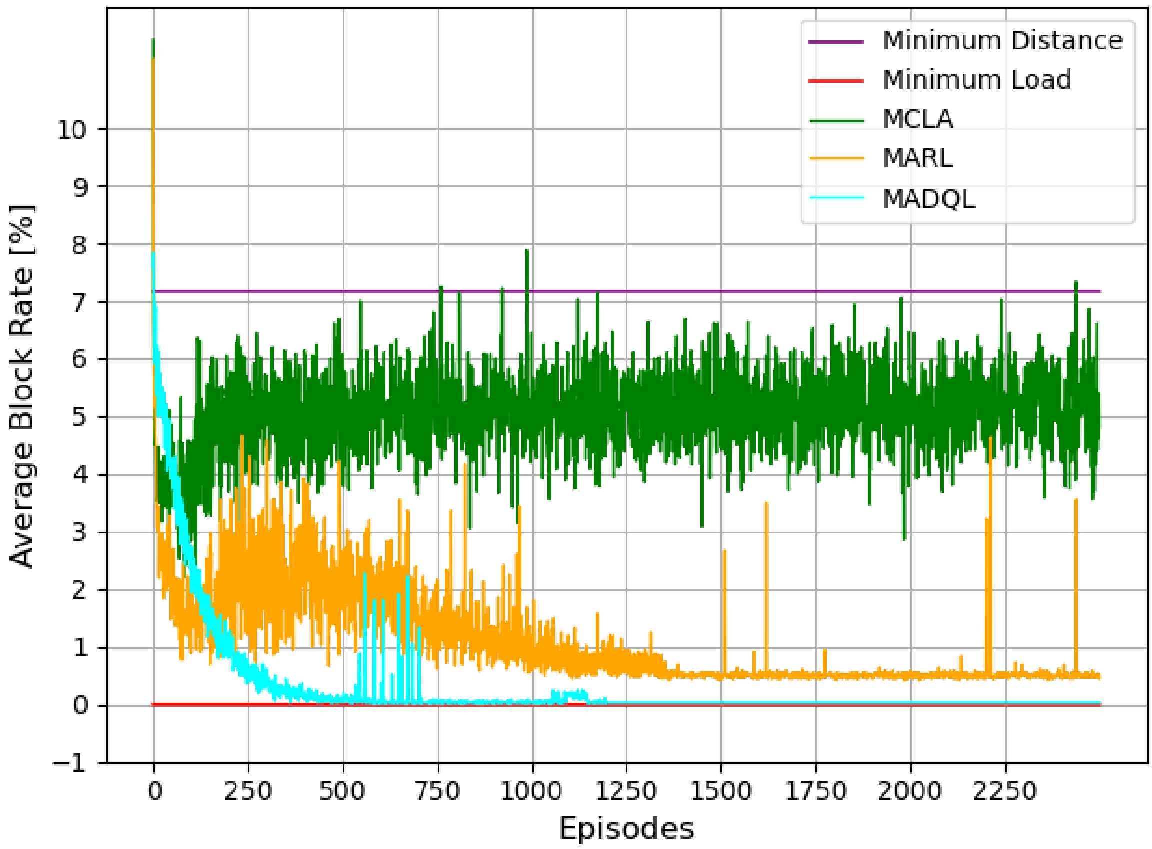

Figure 6.5: Single TP: Average Blocking Rate as a Function of the Number of episodes for the five considered approaches: Minimum Distance, Minimum Load, MCLA(Load Aware), MARL(Load Balance), and MADQL

These findings imply that the proposed MADQL method avoids distributing UEs to overloaded satellites, reducing the likelihood of blockage while achieving a minimum number of delay overheads resulting from the few HOs.

6.4.3 Multi-Agent Deep Q-Learning Satellite Handover for Different and Varying Traffic Profiles

In this subsection, the simulation parameters considered are summarised in Table 6.1, “Multiple TPs column. As a first step to see the difference between the two proposed solutions, Figures 6.6 and 6.7 depict the average cumulative rewards as a function of the episodes.

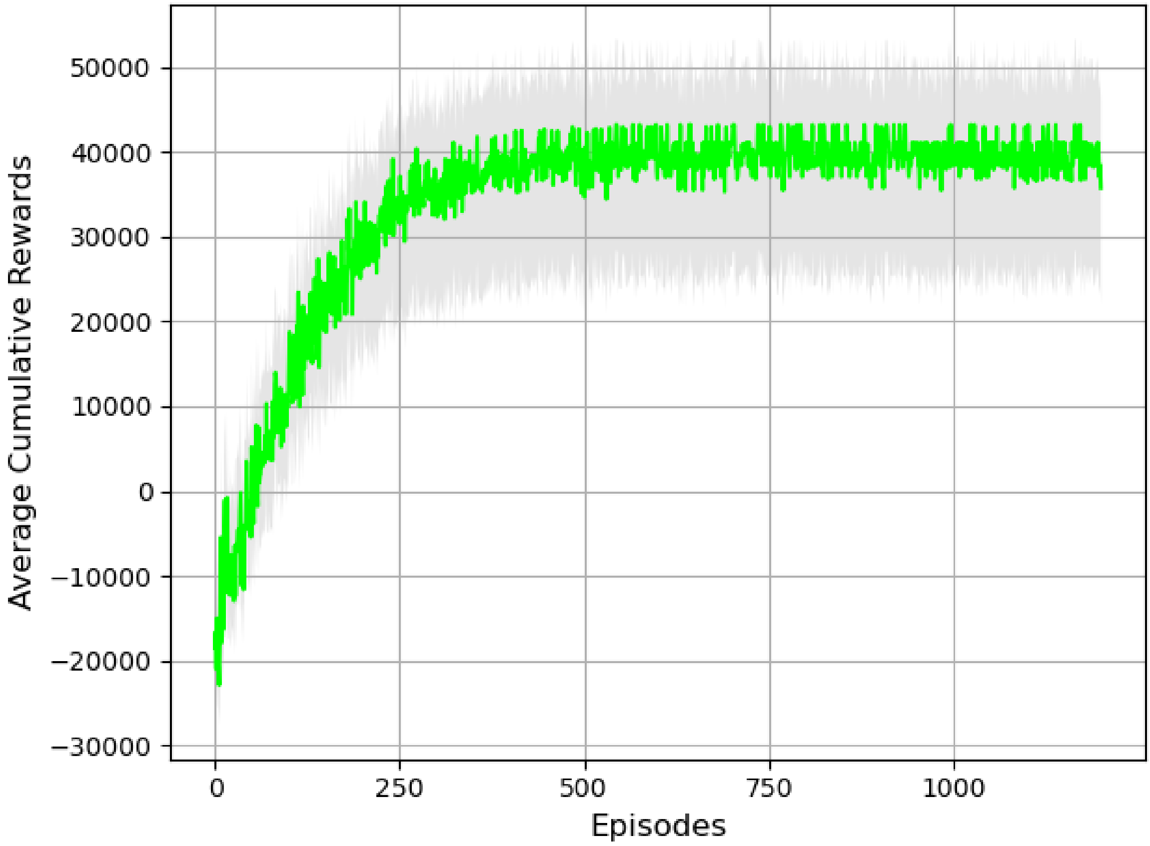

Figure 6.6: Multiple TPs - MADQL: Average Cumulative Rewards as a function of the number of episodes

For the MADQL solution, as the computed episodes increase from 0 to 1200, the average cumulative rewards increase from -3000 to around 40000 starting to converge after only 250 episodes. The figure shows the average cumulative reward for all the

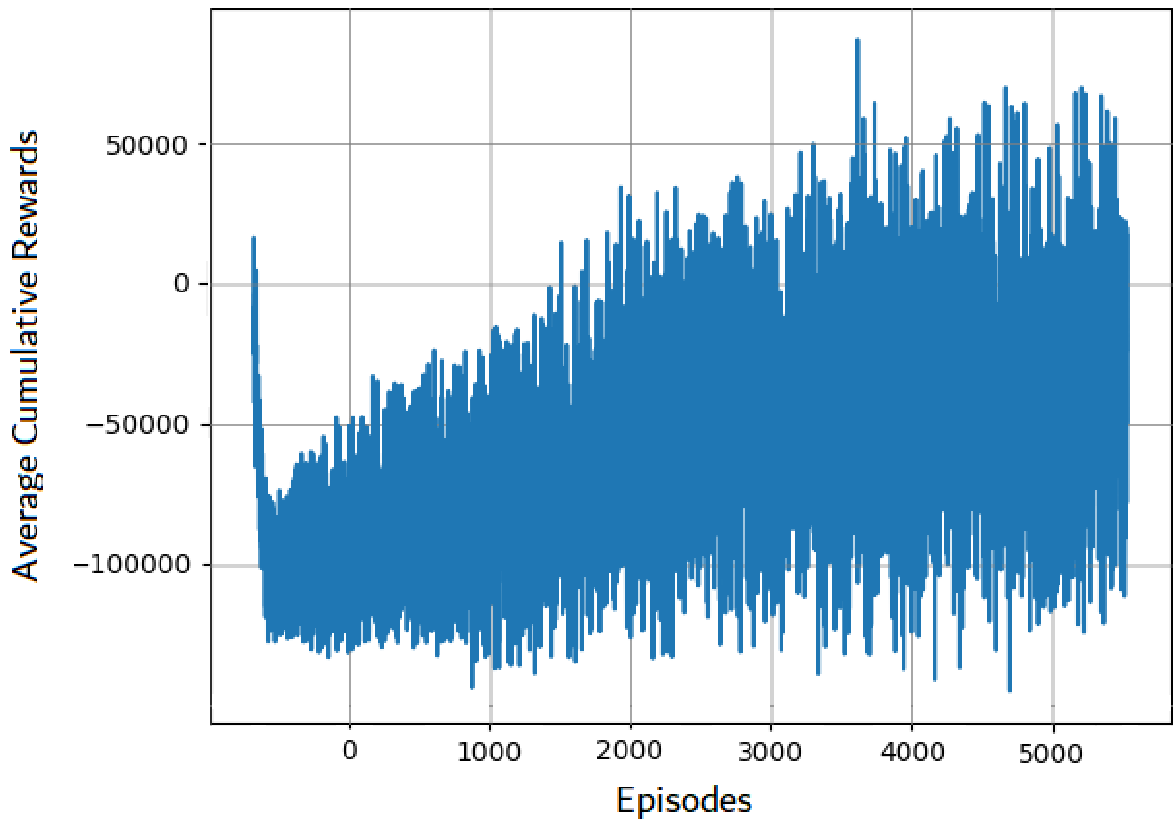

Figure 6.7: Multiple TPs - MARL: Average Cumulative Rewards as a function of the number of episodes

independent agents, where the grey area is the range within which they all converge to their own different optimal values.

Instead, as illustrated in Figure 6.7, the MARL strategy was unable to learn even after increasing the NoE to 5000, resulting in a divergent curve. The main reason is the massive increase in the number of states that results in an enormous Q-table due to the random change of the RR for each UE after each episode made to consider different and changing applications.

These observations imply that Q-Learning-based methods, i.e., MARL and MCLA, are limited to the usage of only one type of traffic application and are not applicable when addressing multiple types of traffic applications per user. Thus MARL and MCLA approaches will not be considered as valid comparison methods in the following sections. To prove the efficiency of the proposed MADQL method for multiple TPs, I will compare it to the minimum distance and minimum load approaches.

Figure 6.8 illustrates the gain of the proposed MADQL method in terms of the average number of HOs compared to the minimum distance and minimum load methods.

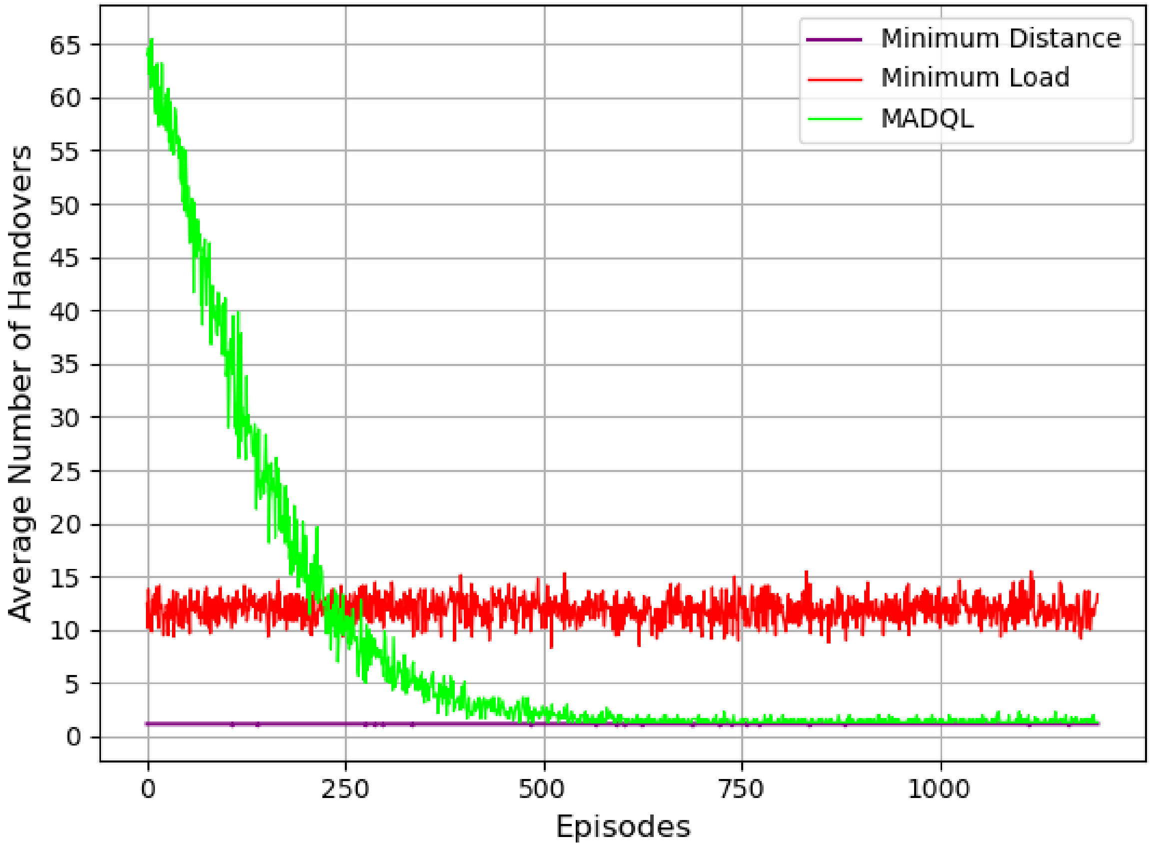

Figure 6.8: Multiple TPs - MADQL vs Minimum Load and Minimum Distance: Average Number of Handovers as a function of the number of episodes

The minimum load method achieves the highest average number of HOs which is between 10 and 14 HOs in the 120 seconds episode duration. Figure 6.8 also shows that the proposed MADQL method converges to only about 1.2 HOs which is the same value achieved by the minimum distance method which is known to achieve the least possible average number of HOs. This proves the efficiency of our proposed MADQL

Table 6.2: Methods Comparison: comparison of the Minimum Distance, Minimum Load, MCLA, MARL, and MADQL methods for a single traffic profile (left-hand side) and for multiple traffic profiles (right-hand side)

Method	**Single TP**			**Multiple TP**		
	Applicable	Average Handover	Average Block Rate	Applicable	Average Handover	Average Block Rate
Minimum Distance	YES	3.7	7.2 %	YES	1.2	0-60 %
Minimum Load	YES	400	0 %	YES	10-14	0 %
MCLA [65]	YES	150	4 % -7 %	NO	-	-
MARL [93]	YES	3.7	0.42 %	NO	-	-
MADQL	YES	4.2	0.033 %	YES	1.2	0.03 %

HO optimisation method when considering different and varying applications per UE in terms of minimising the average number of HOs.

On the other hand, in Figure 6.9, a comparison is made between the average blocking rate for the proposed MADQL and the minimum load method only, as it has been previously demonstrated that the minimum distance approach performs poorly with respect to blocking rate. This is because the minimum distance method does not take into consideration either the resource requirements of each UE at each instance or the load constraint of each satellite when making a HO decision.

On the contrary, the minimum load method achieves a consistent 0% blocking rate as shown in Figure 6.9 while the proposed MADQL method converges to about only 0.03% of blocking. This proves the efficiency of our proposed MADQL HO optimisation method when considering different and varying applications per UE in terms of minimising the average blocking rate.

To sum up, the comparison of all the mentioned methods for single and multiple TPs is summarized in Table 6.2.

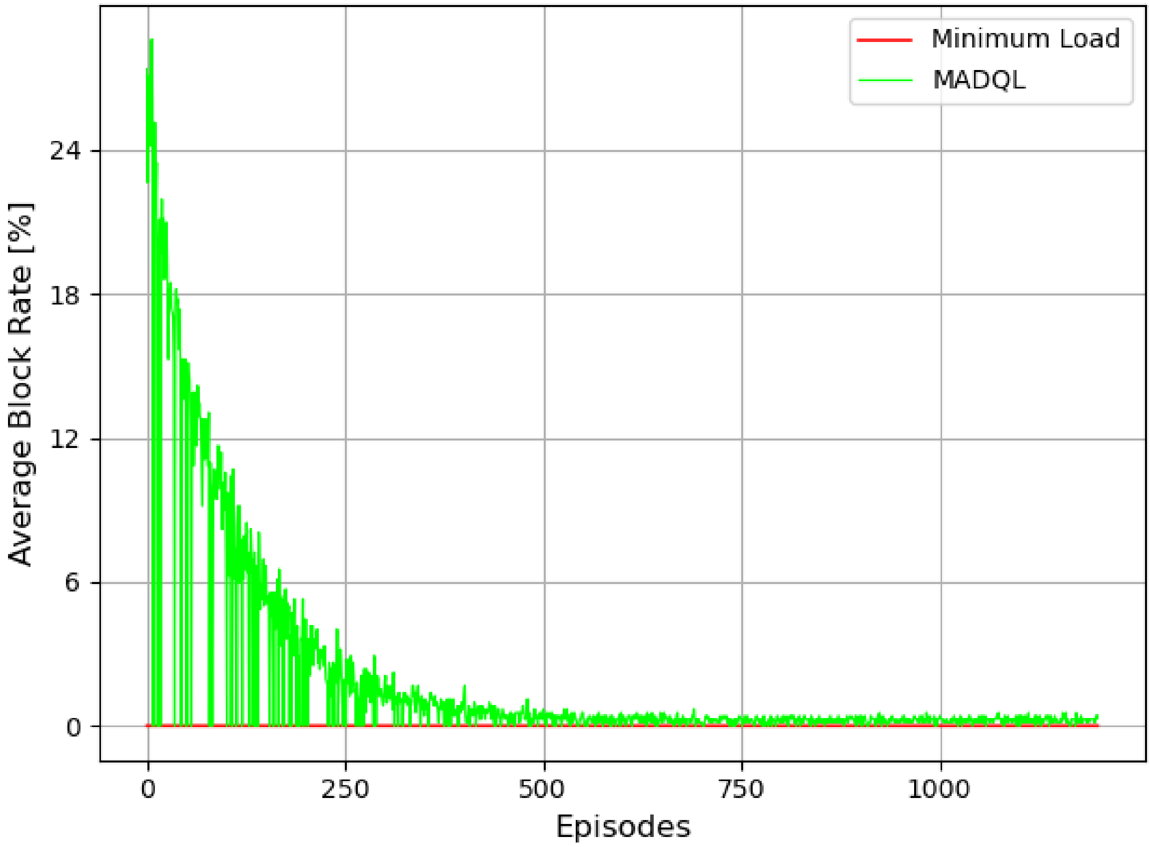

Figure 6.9: Multiple TPs - MADQL vs Minimum Load: Average Blocking rate as a function of the number of episodes

With new applications and services continuously emerging and evolving within the communication landscape, it is indeed impossible to predict every possible service or application that may be introduced to the system. However, our approach is intentionally designed to address this uncertainty by harnessing the learning capabilities of RL algorithms. These algorithms can adapt and learn from new scenarios, albeit with some adaptation time. In order to test the resilience of the proposed MADQL HO optimisation method, I ran two more tests changing the percentage of users requiring W or 2W resources from the satellite. In detail, in the first test, 80% of the users require 2W resources ($TP_k = TP1$ or $TP2$) and 20% require W resources ($TP_k = TP3$ or

$TP4$), while, in the second test, 20% of the users require a 2W resources and 80% of them require W resources.

Figures 6.10 and 6.11 illustrate the results of the first test in terms of the average number of HOs and the average blocking rate as a function of the number of episodes, respectively.

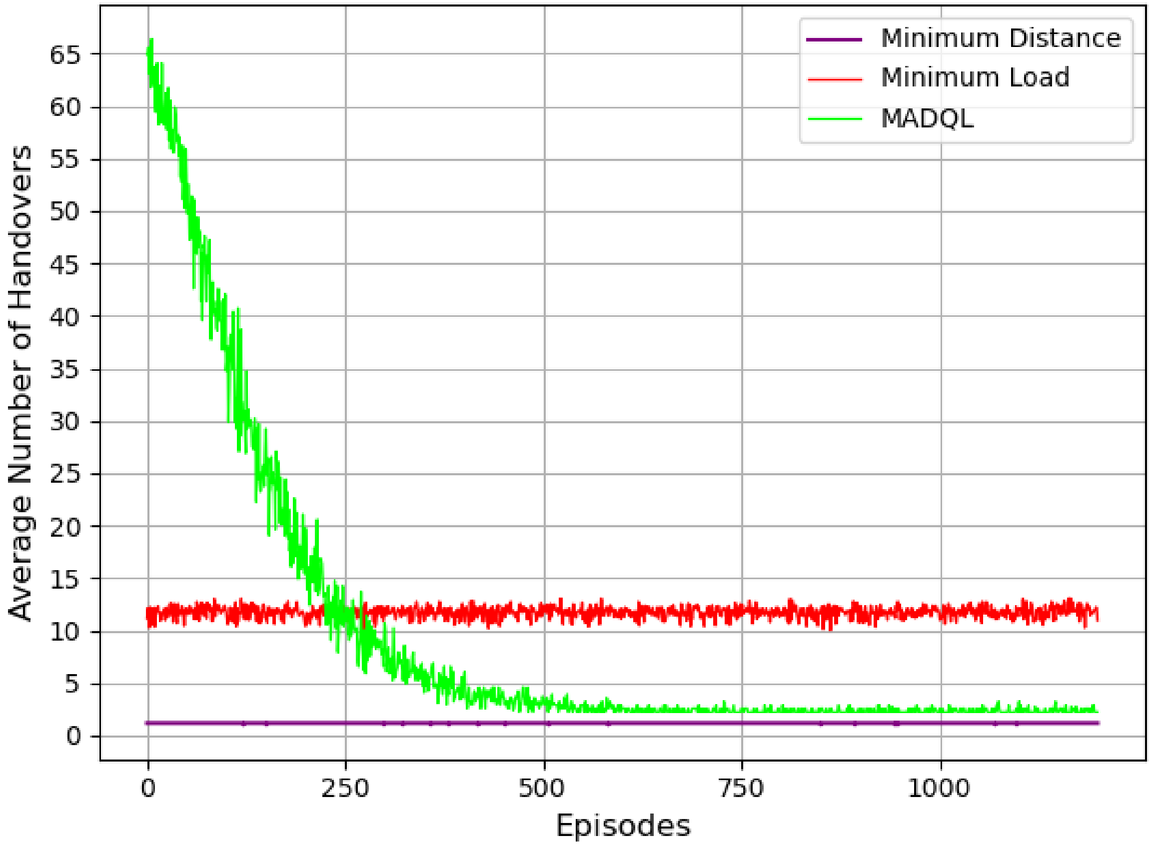

Figure 6.10: Multiple TPs - MADQL vs Minimum Load and Minimum Distance: Average Number of Handovers as a function of the number of episodes with 80% of the users requiring a high number of resources ($TP1$ or $TP2$) and 20% a low number of resources ($TP3$ or $TP4$)

Even when most of the users have high requirements, the proposed MADQL approach achieves great results in terms of the average number of HOs by converging to the same value achieved by the minimum distance approach. In the same way, the proposed

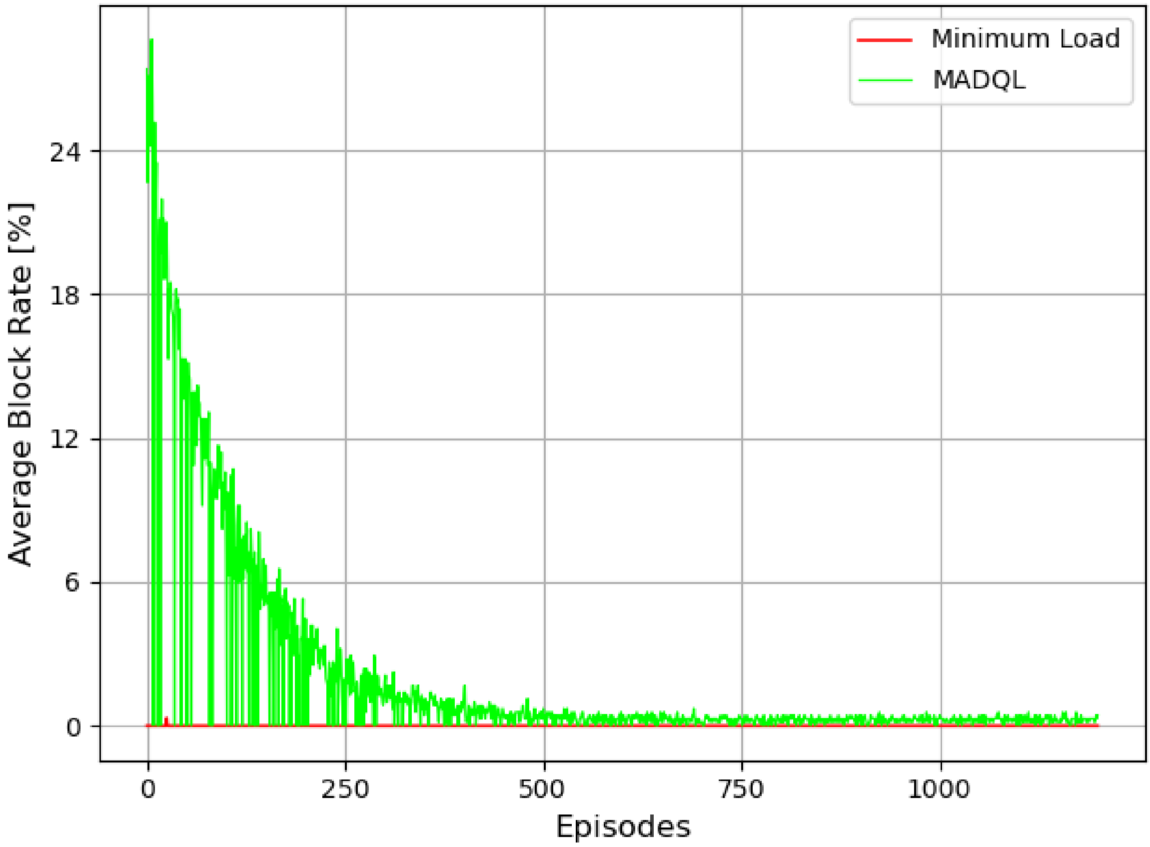

Figure 6.11: Multiple TPs - MADQL vs Minimum Load: Average Blocking rate as a function of the number of episodes with 80% of the users requiring a high number of resources ($TP1$ or $TP2$) and 20% a low number of resources ($TP3$ or $TP4$)

MADQL approach achieves great results with an average blocking rate of approximately 0.05%.

Similarly, Figures 6.12 and 6.13 illustrate the results of the second test, whose results are in line with what has been already shown about the first test.

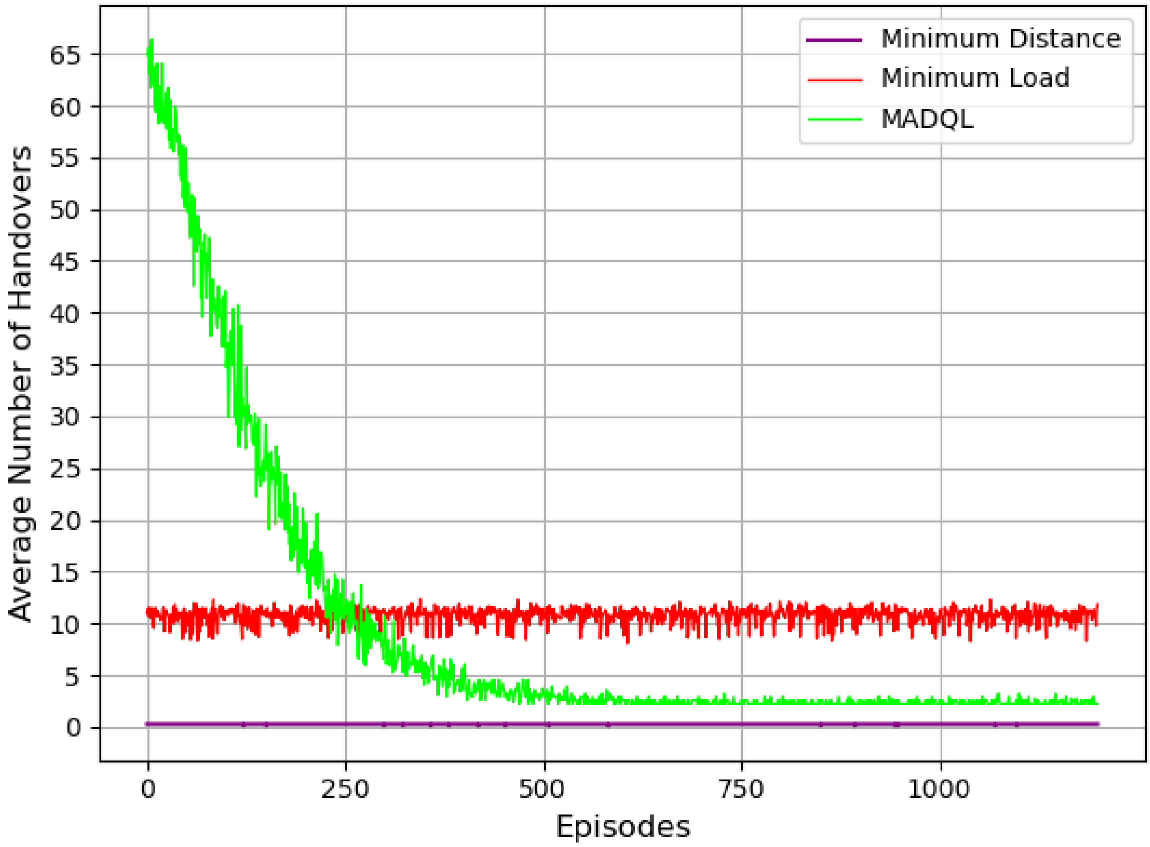

Figure 6.12: Multiple TPs - MADQL vs Minimum Load and Minimum Distance: Average Number of Handovers as a function of the number of episodes with 20% of the users requiring a high number of resources ($TP1$ or $TP2$) and 80% a low number of resources ($TP3$ or $TP4$)

6.5 Conclusion

In this chapter, a novel MADQL satellite HO optimisation strategy will be proposed, that addresses UEs with different and varying TPs. Which, to the best of our knowledge, is the first time in the recent literature.

The implementation and rigorous testing of our novel method were carried out within a realistic Satellite-Terrestrial Integrated Network (STIN) simulator. This endeavor aimed to ascertain the method's effectiveness in managing HOs within STINs for users with varying TPs. The outcomes of these tests were indeed promising, demonstrating the

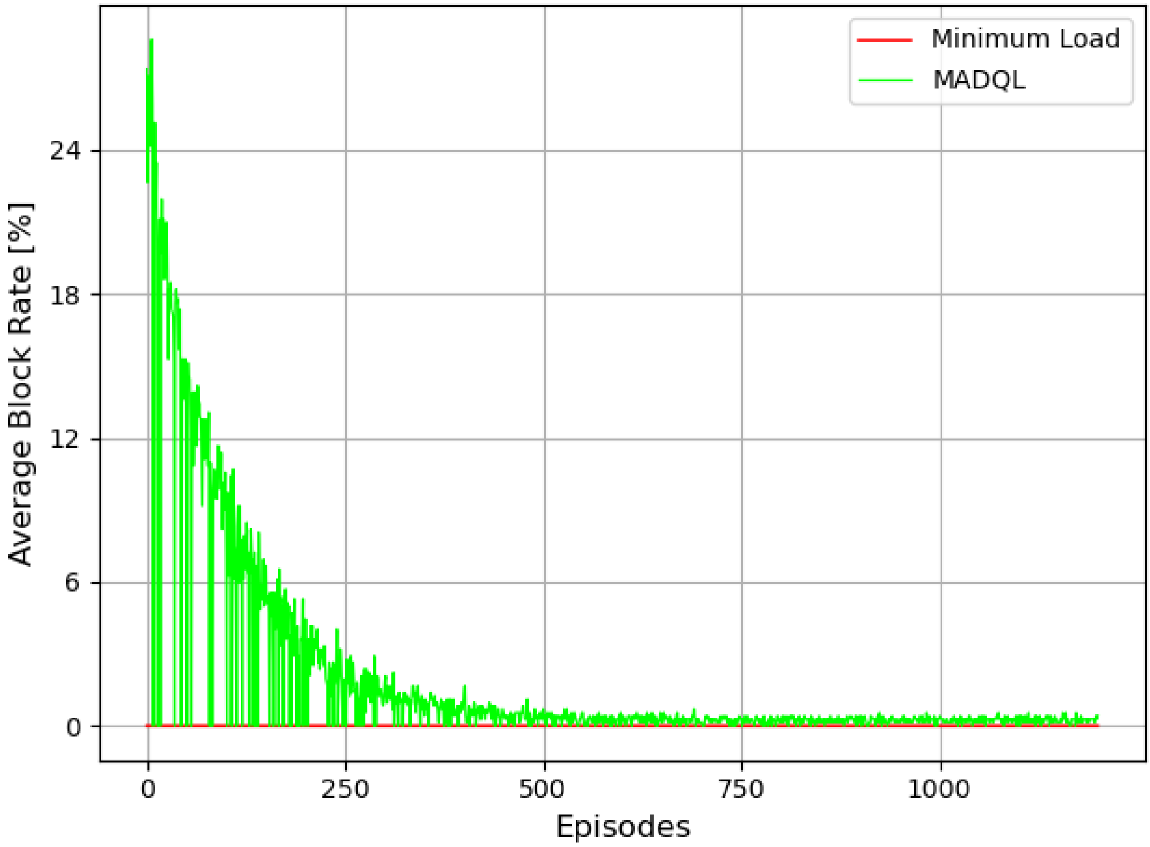

Figure 6.13: Multiple TPs - MADQL vs Minimum Load: Average Blocking rate as a function of the number of episodes with 20% of the users requiring a high number of resources ($TP1$ or $TP2$) and 80% a low number of resources ($TP3$ or $TP4$)

method's ability to dramatically reduce the number of HOs and blocking rates while concurrently achieving a balanced distribution of the load across the satellite network, thereby enhancing the overall user experience.

More specifically, our proposed method resulted in an impressive approximate reduction of 60% in the HO rate and a substantial reduction of approximately 91% in the blocking rate when compared to single-criterion approaches. These findings emphasize the remarkable efficacy of our approach in optimizing HO processes and improving network performance for UEs with different TP requirements.

Additionally, a sensitivity analysis was conducted, exploring various possible TP distribution scenarios. This analysis underscored the robustness and adaptability of the MADQL-based HO optimization method, signifying its ability to perform consistently well across different real-world conditions and traffic scenarios.

In sum, our work represents a significant advancement in the field of satellite HO management, offering a solution that caters to the diverse needs of UEs while substantially reducing HOs and enhancing network performance. The versatility and robustness of the MADQL approach make it a promising strategy for optimizing satellite handovers in a variety of real-world contexts, thereby contributing to a more efficient and user-friendly network environment.

Chapter 7

Energy Aware LEO Satellite Handover Management Based on Deep-Reinforcement Learning

7.1 Introduction

In the realm of satellite communication, the efficient management of power resources is of paramount importance, particularly for Low Earth Orbit (LEO) satellites. These satellites, with their relatively small power generation capacity primarily sourced from solar panels, are uniquely positioned to capture sunlight for energy. However, when in the shadow of the Earth, they must rely on stored energy from onboard batteries to maintain their operations. The delicate balance between power generation, consumption, and energy availability in LEO satellites is intricately influenced by factors such as altitude and orbital geometry [94].

In essence, LEO satellites must carefully manage their limited power resources to ensure uninterrupted operations. The interplay between solar panel exposure, shadow periods, battery utilization, altitude, and orbital geometry is a complex and dynamic one, requiring precise planning and control to optimize the satellite's performance and functionality in this challenging environment.

The overarching objective of this chapter is to synthesize the knowledge of satellite energy availability and consumption to devise a strategic approach that enhances the performance of satellite networks. By intelligently utilizing energy information in our handover strategy, the aim is to minimize the number of handovers and reduce blocking rates, ultimately providing a smoother and more reliable user experience. The intricate relationship between the energy status of LEO satellites, their movements in and out of sunlight, and the orbital dynamics introduces unique challenges and opportunities for optimizing handovers. By meticulously considering these factors, A balance is sought between ensuring the continuity of satellite operations and delivering seamless connectivity to users.

Thus in this chapter, I delve into the design of a novel LBEASH strategy. LBEASH takes into account various factors, such as elevation angle, RVT, amount of available bandwidth, and energy resources per satellite, and accordingly assists each UE in selecting the best satellite candidate from its covering satellite set to ensure the required QoS throughout the entire communication duration, avoiding unnecessary HOs and achieving zero blocking rate per UE.

The rest of this chapter is organized as follows. Section 7.2 delve into the technical details of the calculation of the energy onboard of a LEO satellite. Section 7.3 provides the methodology adopted to develop the LBEASH optimization strategy. Simulation results are presented in Section 7.4. Finally, the conclusion is provided in Section 7.5.

7.2 Energy onboard of a LEO Satellite

Low Earth Orbit (LEO) satellites function under the limitations of limited power resources. Unlike some larger satellites that have more extensive power sources, LEO satellites predominantly depend on solar panels to generate the electrical energy needed to run their systems. However, these solar panels are only effective when the satellites are illuminated by sunlight. When they move into the shadow of the Earth, they are deprived of this vital source of energy as seen in Figure 7.1.

In this shadowed state, the solar panels cannot capture solar energy, and the satellites must rely on stored electrical power from onboard batteries to continue their normal operations. The duration of these two distinctive states, "sunlight" and "shadow," varies depending on several key factors, primarily the satellite's altitude above the Earth's surface and its orbital trajectory or geometry.

The altitude of a LEO satellite influences the amount of time it spends in sunlight versus shadow. Satellites at lower altitudes experience more frequent transitions between these states due to their faster orbits around the Earth. In contrast, satellites at higher altitudes have longer periods of sunlight and shorter periods of shadow.

Additionally, the orbital geometry of the satellite's path plays a crucial role. This geometry is determined by various factors, including the inclination of the satellite's orbit, its orbital plane, and the orientation of its solar panels concerning the Sun. These factors collectively influence the timing and duration of the satellite's exposure to sunlight and shadow.

To better comprehend the power dynamics of a specific satellite (SAT_n) during communication operations at a given time (t), it is needed to consider the total power consumption. This total power (Pc_n^t) is determined by two primary components as follows:

$$Pc_n^t = Pa^t + \sum_{k \in \mathcal{K}} Pt_{k,n}^t \cdot X_{k,n}^t \tag{7.1}$$

Pa^t is the average circuit power, which includes all electronic power consumption of satellite components except for transmitting data, and $Pt_{k,n}^t$ the power consumed by

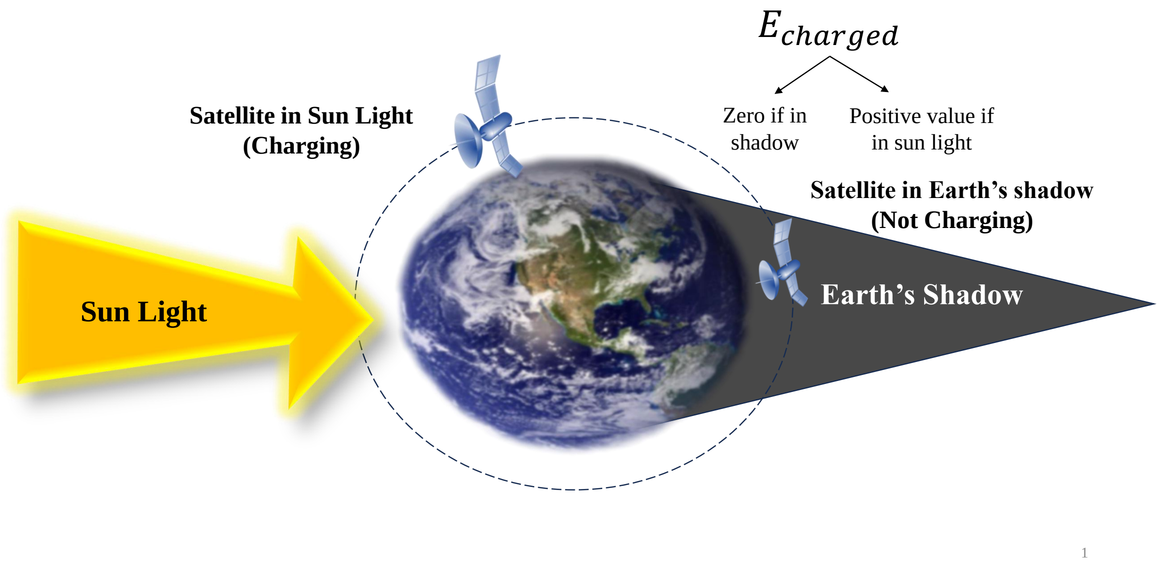

Figure 7.1: Charging and Discharging statuses of a LEO satellite

SAT_n to transmit to UE_k at time t. Pa^t is considered constant while $Pt^t_{k,n}$ depends on TP_k and the distance $D^t_{k,n}$ [95]:

$$Pt^t_{k,n} = \frac{(2^{1/R_k} - 1) \cdot R_k \cdot N_0}{{D^t_{k,n}}^{-a_f}} \tag{7.2}$$

N_0 the noise spectral density, and a_f the satellite channel attenuation factor.

Understanding the dynamics of satellite power also requires an assessment of the total energy available to SAT_n at a particular time (t'). This energy level, denoted as $E_n(t')$, is calculated based on the initial available energy $(E_n(0))$ of SAT_n, accounting for the cumulative power consumption from the beginning of operation up to time t'.

The energy availability equation is as follows:

$$E_n(t') = E_n(0) - \int_0^{t'} Pc^t_n \, dt \tag{7.3}$$

$E_n(0)$ is the initial available energy of SAT_n, which has been set depending on the satellite movement history as follows:

$$E_n(0) = \begin{cases} E_{max} & \text{if } Tsu_n > 0.5 \cdot TO_n \\ & \text{or } Tsh_n < 0.25 \cdot TO_n, \\ 0.8 \cdot E_{max} & \text{if } 0.25 \cdot TO_n < Tsu_n < 0.5 \cdot TO_n \\ & \text{or } 0.25 \cdot TO_n < Tsh_n < 0.5 \cdot TO_n, \\ 0.6 \cdot E_{max} & \text{if } Tsu_n < 0.25 \cdot TO_n \\ & \text{or } Tsh_n > 0.5 \cdot TO_n, \end{cases} \tag{7.4}$$

Tsu_n and Tsh_n are the amount of time that SAT_n spent in sunlight or shadow status, respectively, since the last status change before the beginning of the communication (i.e., before $t = 0$) and TO_n the satellite orbit period.

This comprehensive framework provides a foundation for understanding the interplay between power generation, consumption, and energy availability in the context of LEO satellites, ensuring the sustainability of their operations.

UE_k is considered blocked at time t if it tries to connect to a satellite with insufficient channel or energy resources. The blocking indicator is represented by BN_k^t as follows:

$$BN_k^t = \begin{cases} 1 & \text{if } UE_k \text{ chooses to connect to } SAT_n \text{ and} \\ & l_n^t + \hat{R}_k^t > L_n \;\text{ or} \\ & E_n^t - \int_t^{t+t_u} Pt_{k,n}^t \, dt \leq 0\}, \\ 0 & \text{otherwise} \end{cases} \tag{7.5}$$

In our case, $t_u = 1$ since each UE determines whether or not to conduct a HO once per second.

7.3 Methodology

Our main objective is to determine which satellite each user should connect to during a HO event in order to maintain an extended connection and hence reduce the frequency of subsequent unnecessary HOs, while efficiently using the available satellite channel and energy resources. It is supposed that each UE determines whether or not to conduct a HO and to which satellite once every second.

Thus, a multi-agent DQL strategy has been implemented where all its components can be defined as follows:

- *Agent* g_k: Each UE represents an agent and independently takes actions. $\mathcal{G}$ indicates the set of all agents which is equal to the set of all UEs $\mathcal{K}$.

- *State* s_k^t: The state of agent g_k at time t is defined as the 4-tuple $s_k^t = < \overline{C_k}^t, \overline{l}^t, \overline{V_k}^t, \overline{E}^t >$. The tuple contains 4 vectors all of size N. $\overline{C_k}^t = [C_{k,0}^t, C_{k,1}^t, ..., C_{k,n}^t, ..., C_{k,N}^t]$ represents the coverage indicator between g_k and SAT_n, $\forall n \in N$ at time t as defined in Eq. (5.3). $\overline{l}^t = [l_0^t, l_1^t, ..., l_n^t, ..., l_N^t]$ and $\overline{E}^t = [E_0^t, E_1^t, ..., E_n^t, ..., E_N^t]$ denotes the number of loaded channels and available energy of every SAT_n at time t, respectively. $\overline{V_k}^t = [V_{k,0}^t, V_{k,1}^t, ..., V_{k,n}^t, ..., V_{k,N}^t]$ includes information about the RVT of all the satellites covering agent k. $\mathcal{S}$ indicates the set of all states.

- *Action* a_k^t: the action taken by agent g_k at time t that represents the choice to attach to one of the covering satellites $n \in \mathcal{N}_k^t$. $\mathcal{A}$ indicates the set of all states.

- *Reward* r_k: The reward function is defined considering five different cases based on the multi-objective optimization problem of eliminating unnecessary HO events while minimizing the blocking rate by effectively exploiting the available resources (channel and energy):

$$r_k(s_k^t, a_k^t) = \begin{cases} z_1 & \text{if } X_{k,n}^t = 0, \\ & \quad l_n^t > L_n \text{ or } E_n^t \leq 0, \\ z_2 & \text{if } X_{k,n}^t = 0, \\ & \quad l_n^t \leq L_n \text{ and } E_n^t > 0, \\ f_1(t,k,n) & \text{if } X_{k,n}^t = 1, \\ & \quad l_n^t > L_n \text{ and } E_n^t > 0 \\ z_3 & \text{if } X_{k,n}^t = 1, \\ & \quad l_n^t \leq L_n \text{ and } E_n^t \leq 0 \\ f_2(t,k,n) & \text{if } X_{k,n}^t = 1, \\ & \quad l_n^t \leq L_n \text{ and } E_n^t > 0 \end{cases} \tag{7.6}$$

According to Eq. (7.6), when an action results in a HO, the agent may connect to a satellite with insufficient resources and thus will get a high negative penalty $z_1 = -500$. However, if it undergoes a HO to a satellite with enough resources, it will get a lower negative penalty $z_2 = -300$. On the other hand, if the action does not result in any HO, The distinction between the three other cases is made as follows: if the agent tries to reconnect to a satellite with insufficient channel or energy resources, it will receive a negative penalty $f_1(t,k,n) = 100 * w_n^t$ (since $w_n^t < 0$ for loaded satellites) or $z_3 = -30$, respectively, in order to motivate it to connect to another satellite with lower load and enough energy to avoid blocking. The final case is when the agent stays connected to a satellite with enough resources, getting a high positive reward $f_2(t,k,n) = v_{k,n}^t$ to avoid unnecessary HOs.

- *Policy* π: When developing an action selection policy, it is essential to maintain a balance between exploitation and exploration; The adopted action selection policy in the proposed LBEASH approach is:

$$a_*^t = \begin{cases} \text{Random action } a^{'} \in \mathcal{A} & \text{if } \varepsilon < \epsilon^t, \\ arg\max_{a^t} Q_k(s_k^t, a^t, \Lambda) & \text{otherwise} \end{cases} \tag{7.7}$$

ϵ^t increases with time so that agents begin their learning process exploring a wide range of actions and then begin to exploit with a probability increasing with t.

The DQL agent learning process is summarized in Algorithm 3. The well-trained DNN has been implemented on each UE since every UE is considered an independent agent. The state of each UE_k, is initially set to $s_k^0 \in \mathcal{S}_k$, the TP per UE is randomly chosen to ensure the diversity of applications utilized by each UE during each episode. The energy utilization and load distribution among satellites are set accordingly.

Each agent observes its current state s_k^t at each time step t, selects an action a_k^t in accordance with Eq. (7.7) causing a transition to a new state s^{t+1}, and then is rewarded with the reward r_k^{t+1} computed in accordance with Eq. (7.6). Both vectors s_k^t and s_k^{t+1} are converted into the matrices $\Phi(s_k^t)$ and $\Phi(s_k^{t+1})$ in order to input the whole experience into the replay memory $\mathbb{M}$ as $(\Phi(s_k^t), a_k^t, \Phi(s_k^{t+1}), r_k^{t+1})$. The whole replay memory is then randomly sampled to create a mini-batch of size N_b. The maximum capacity of the replay memory is limited to N_m so that the oldest experiences are deleted first when additional space is required for new experiences.

7.4 Performance evaluation

The STIN simulator developed in Chp. 3.3 has been utilized. The simulation parameters considered in our approach are all summarised in Table 7.1. The currently operational 3450 Starlink LEO satellites deployed at different altitudes ranging from 300 to 600 km are considered. The application diversity is also considered in this method where

Algorithm 3 Multi-Agent Deep-Q learning

Initialise:
$\mathbb{M}$ - Empty experience replay buffer
N_b - Mini Batch size, N_m - Replay Memory Size
Λ - DNN Weights initialisation
$t = 0$
$\mathcal{S}_k = \{s_k^0\} =< \overline{C_k^0}, \overline{l^0}, \overline{V_k^0} > \forall k \in \mathcal{K}$
while $ep < NoE$ **do**
Allocate a randomly selected TP per agent
$l_n = l^0 \; \forall n \in \mathcal{N}$
$e_n = e^0 \; \forall n \in \mathcal{N}$
while $t < T$ **do**
for $k \in \mathcal{K}$ **do**
Choose random agent k;
Observe $s_k^t =< \overline{C_k^t}, \overline{l^t}, \overline{V_k^t}, \overline{E^t} >$;
Choose action a_k^t based on Eq. (7.7);
Move to a new state $s_k^{t+1} =< \overline{C_k^{t+1}}, \overline{l^{t+1}}, \overline{V_k^{t+1}}, \overline{E^{t+1}} >$;
Transform s_k^t and s_k^{t+1} into matrices $\Phi(s_k^t)$ and $\Phi(s_k^{t+1})$, respectively;
Get the reward r_k^{t+1} computed following Eq. (7.6);
Update Satellites-Load to l^{t+1};
Update Satellites-Energy to E^{t+1};
Store $(\Phi(s_k^t), a_k^t, \Phi(s_k^{t+1}), r_k^{t+1})$ in $\mathbb{M}$;
Sample a random mini-batch of size N_b from $\mathbb{M}$ for training;
Train the DNN of agent k;
Set y^t following Eq. (6.6);
Update the DNN parameters Λ by performing a gradient descent step on Eq. (6.5);
end for

Reset $t = 0$, $\mathcal{S}_k = \{s_k^0\} \; \forall k \in \mathcal{K}$;
end while =0

the number of possible traffic profiles (TPs) per UE is equal to 4 and they are defined in the same way presented in Chp 6.

Figure 7.2 shows the average cumulative rewards for the 6 Deep Q Network (DQN) agents as a function of the NoE. As the NoE increases from 0 to 600, the average cumulative rewards increase to approximately 40000, starting to converge after 300

Table 7.1: Simulated scenario parameters

Parameter	Values
Number of Starlink Satellites N	3450
Number of UE K	6
Satellite altitude h_n	300-600 km
Earth Radius R_e	6371 km
θ_0	$20°$
L_n	5
Number of possible TPs	4
α	0.1
γ	0.99
ϵ	0.1-0.9
NoE	600
Duration of an episode T	120 s
E_{max}	20 Wh
Ea	0.2 Wh
W	50 MHz
a_f	2
N_0	41.409$*10^{-23}$ W/MHz

episodes. The reason for this is that in the first episodes, the agents explore more before beginning to exploit with higher probability as ϵ increases. The grey shade shown in the figure represents the range of convergence for the 6 different agents. To the best of our knowledge, no previous studies have explored a strategy for optimizing HOs in LEO satellites that considers the energy limitations of the satellites or different TPs per UE. Thus, to prove the efficiency of the proposed strategy, I decided to compare its performance concerning the number of HOs, blocking rate due to insufficient channel and energy resources, with two non-smart approaches namely "Minimum Distance" [92] and "Minimum Load" [57].

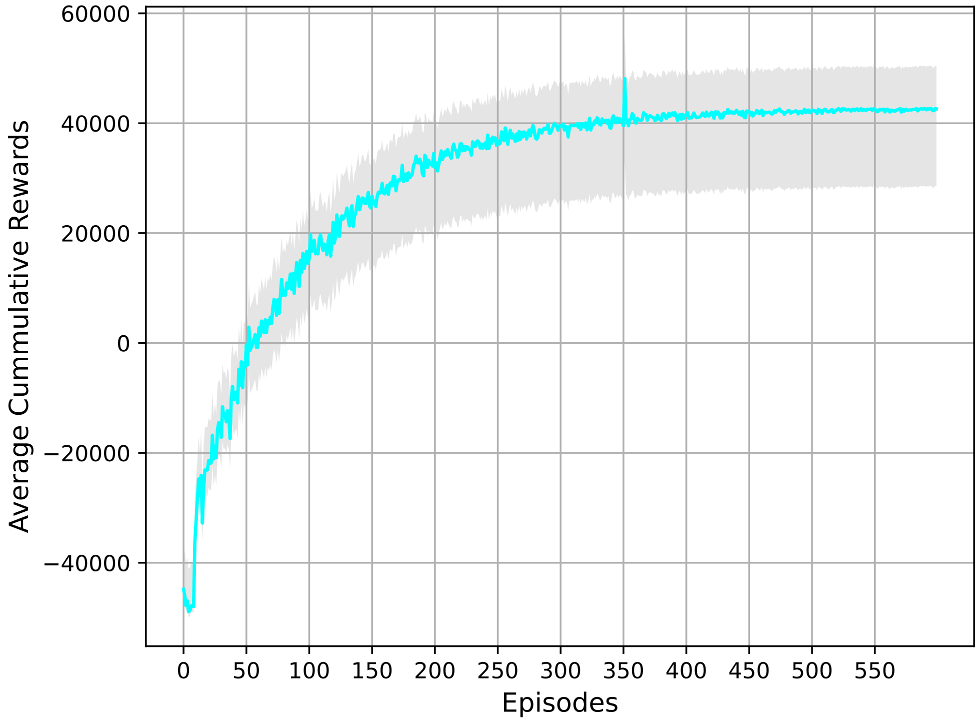

Figure 7.2: Average Cumulative Rewards as a function of the number of episodes

Figure 7.3 shows the average number of HOs as a function of NoE for the three different approaches. As shown in the figure, the proposed LBEASH approach was able to reduce the average number of HOs to around only 1 HO per UE which is equivalent to the value achieved by the "Minimum Distance" approach. While the "Minimum Load" approach resulted in 120 HOs per UE which signifies a ping-pong behavior.

On the other hand, Figures 7.4 and 7.5 show the average blocking rate (in %) due to insufficient channel and energy resources, respectively. Figure 7.4 shows that the average blocking rate resulting from insufficient channel resources of the proposed LBEASH strategy, decreased from 50% per UE to 0% blocking rate after 270 episodes converging to the same value achieved by the "Minimum Load" approach while outperforming the "Minimum Distance" approach.

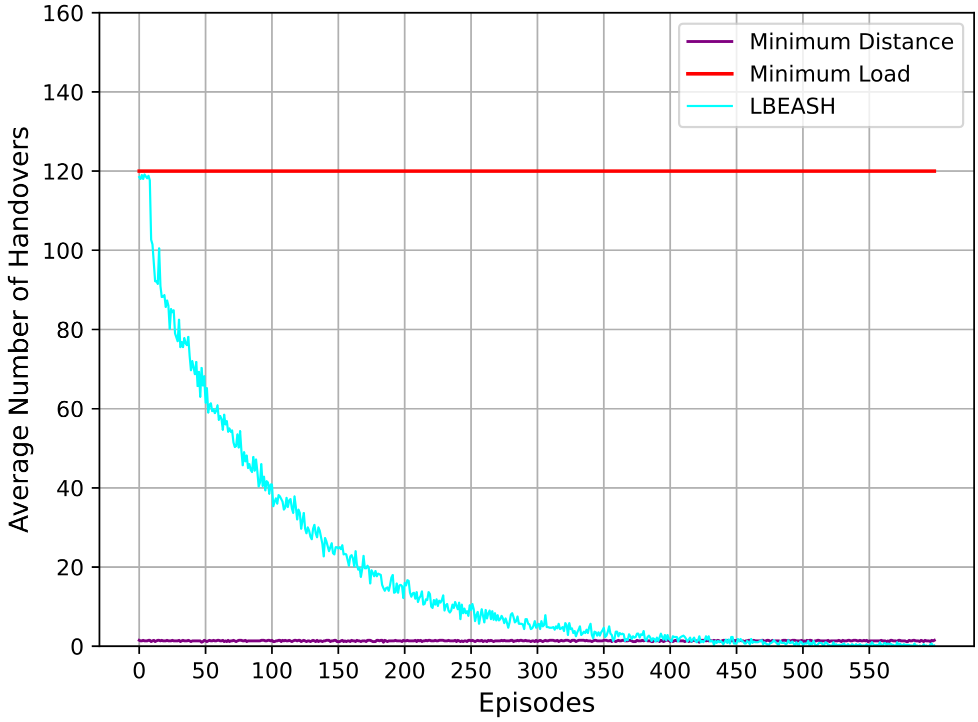

Figure 7.3: Average Number of Handovers as a function of the number of episodes

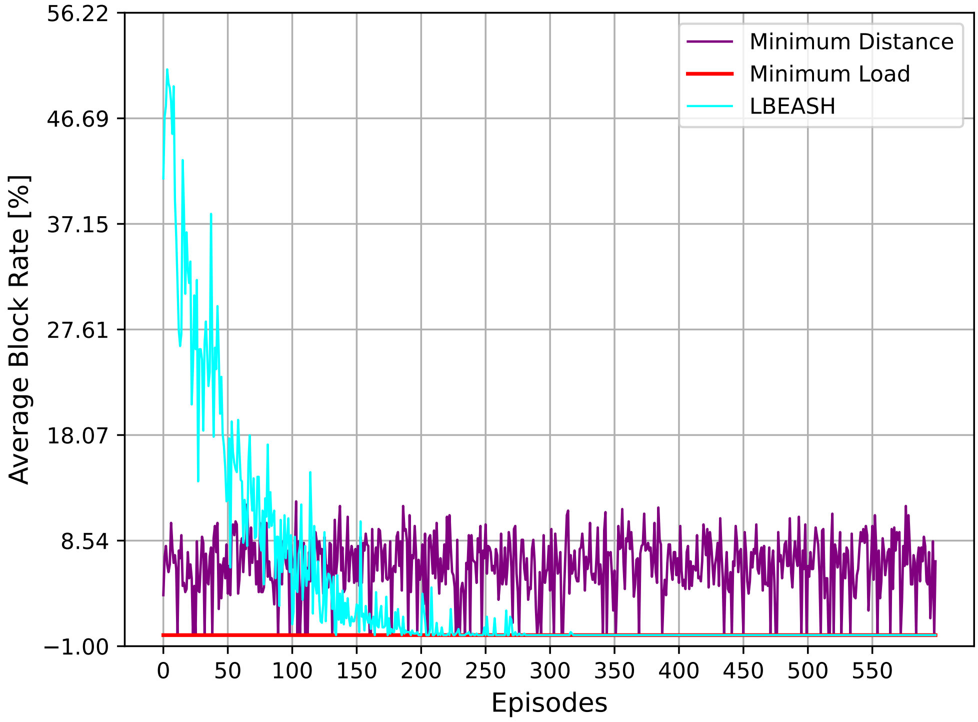

Figure 7.4: Average Blocking Rate [%] due to insufficient Channel Resources

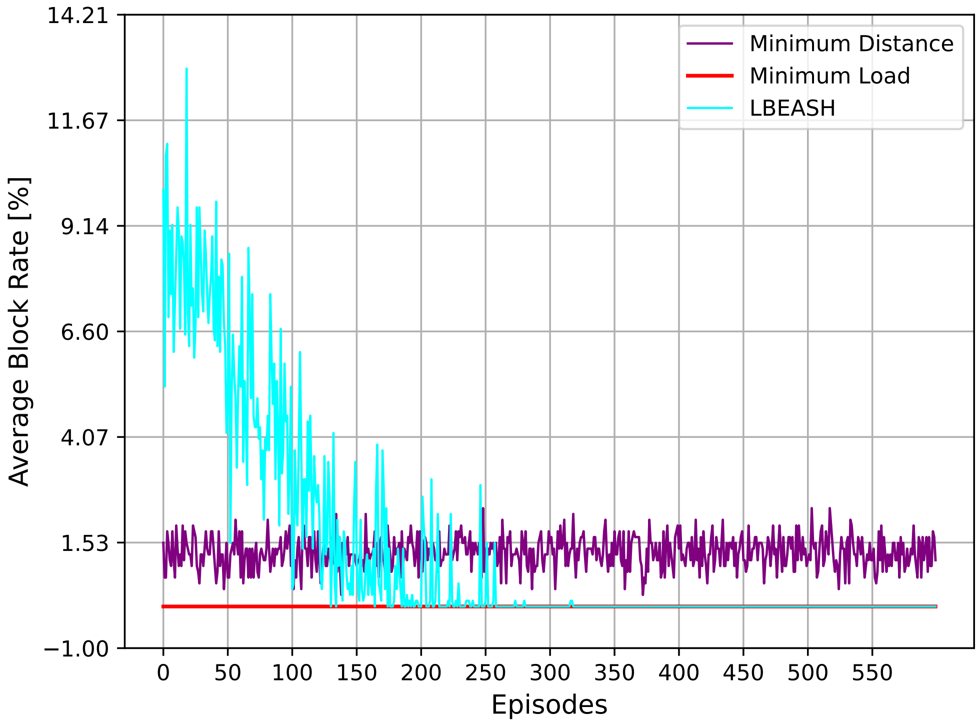

Figure 7.5: Average Blocking Rate [%] due to insufficient Energy Resources

Similarly, the proposed LBEASH approach was able to achieve zero blocking rate resulting from insufficient energy resources after 200 episodes as shown in Figure 7.5. As a result the proposed LBEASH approach was able to ensure a global solution by decreasing the average number of HOs and achieving zero blocking rate by effectively utilizing the limited available channel and energy resources.

7.5 Conclusion

In this chapter, a novel LBEASH optimization technique will be proposed for addressing HOs in satellite-terrestrial integrated networks with UEs with different and variable performance requirements. The proposed method was implemented and tested in a realistic STIN simulator, demonstrating its efficiency in managing HOs for users with varying TPs and effectively utilizing the limited available channel and energy resources. It is able to eliminate any unnecessary HO and achieve zero blocking rate while balancing the load among the satellites and ensuring the required user experience. To the best of our knowledge, there are no previous articles in the literature that take the limited satellite energy resources or the different possible TPs per UE into consideration while addressing STIN HO optimization methods.

Chapter 8

Conclusion and Future Work

In conclusion, this thesis explores the dynamic field of satellite-terrestrial integrated networks, driven by the increasing demand for reliable and high-performance wireless communication services, especially with the emergence of 5G technology. The integration of satellites with terrestrial networks is seen as a promising solution to connect remote and underserved regions, where universal connectivity is now considered a necessity.

In this context, LEO satellites, with their unique characteristics, have garnered significant attention. However, the deployment of LEO satellite constellations introduces the challenge of efficient and seamless HO management. Frequent HOs are essential to maintain uninterrupted communication as LEO satellites transition across coverage areas, but they also bring forth complexities related to signaling overhead, resource consumption, and user dissatisfaction. The need for an intelligent and resource-aware HO management approach becomes apparent, setting the motivation of our research.

This thesis embarked on a journey to contribute innovative solutions to the field. Our objectives encompassed the development of an open-source satellite-terrestrial integrated network (STIN) simulator that could simulate 5G New Radio cellular networks and satellite communication networks. This simulator fills a critical void in the research community, enabling the testing and validation of proposed strategies in a realistic environment before live implementation.

Furthermore, our research led to the creation of novel decentralized HO strategies based on reinforcement Q-learning and multi-agent deep reinforcement learning (MADQL). These strategies reduce HO occurrences, minimize blocking rates, and ensure more efficient utilization of limited satellite resources. Additionally, an energy-aware HO strategy has been introduced, which takes satellite energy constraints into account, minimizing unnecessary HOs and achieving a zero blocking rate..

The culmination of these contributions was the implementation and testing of these methods within the NS-3-based STIN simulator, offering valuable insights and performance evaluations. Our research not only advances the state of the art in satellite HO management but also addresses the pressing need for adaptive, efficient, and intelligent solutions in the ever-changing landscape of satellite-terrestrial integrated networks.

Future work will consist of extending the proposed scenario to an end-to-end satellite-terrestrial integrated network. Currently, our research has primarily focused on specific aspects of satellite HO management within the context of an integrated network. To provide a more holistic view of how these strategies perform in real-world scenarios, the plan is to expand the simulation framework into a complete end-to-end satellite-terrestrial integrated network. This broader scenario will encompass both terrestrial and satellite components, simulating interactions across the entire communication path, from the UE to the satellite and back. This expansion allows us to analyze the HO strategy's performance within the context of the entire network, offering a more accurate representation of its impact. In addition to the consideration of inter-satellite links, they play a critical role in ensuring seamless communication. These links enable satellites to communicate with each other, reducing the reliance on ground stations and enhancing network resiliency. This variation in network topology allows us to evaluate how the availability or absence of these links impacts HO decisions and network performance. In addition to incorporating a channel model to allow us to accurately compute additional parameters, such as the end-to-end delay and the Signal-to-Interference-plus-Noise Ratio, that could be used both to evaluate the network under varying channel conditions and as additional input information of the HO strategy.

Bibliography

[1] O. Kodheli, A. Guidotti, and A. Vanelli-Coralli, "Integration of Satellites in 5G through LEO Constellations," in *Global Communications Conference (GLOBECOM)*. IEEE, 2017, pp. 1–6. pages 1, 18

[2] T. De Cola and I. Bisio, "QoS optimisation of eMBB services in converged 5G-satellite networks," *IEEE Transactions on Vehicular Technology*, vol. 69, no. 10, pp. 12 098–12 110, 2020. pages 2

[3] G. Giambene, E. O. Addo, and S. Kota, "5G aerial component for IoT support in remote rural areas," in *5G World Forum (5GWF)*. IEEE, 2019, pp. 572–577. pages 2

[4] M. Marchese, F. Patrone, and A. Guidotti, "The role of satellite in 5g and beyond," in *A Roadmap to Future Space Connectivity: Satellite and Interplanetary Networks*. Springer, 2023, pp. 41–66. pages 2, 18

[5] M. Bacco, F. Davoli, G. Giambene, A. Gotta, M. Luglio, M. Marchese, F. Patrone, and C. Roseti, "Networking challenges for non-terrestrial networks exploitation in 5G," in *5G World Forum (5GWF)*. IEEE, 2019, pp. 623–628. pages

[6] L. Boero, R. Bruschi, F. Davoli, M. Marchese, and F. Patrone, "Satellite networking integration in the 5G ecosystem: Research trends and open challenges," *IEEE Network*, vol. 32, no. 5, pp. 9–15, 2018. pages

[7] F. Rinaldi, H.-L. Maattanen, J. Torsner, S. Pizzi, S. Andreev, A. Iera, Y. Koucheryavy, and G. Araniti, "Non-terrestrial networks in 5G & beyond: A survey," *IEEE Access*, vol. 8, pp. 165 178–165 200, 2020. pages

[8] M. Giordani and M. Zorzi, "Non-terrestrial networks in the 6G era: Challenges and opportunities," *IEEE Network*, vol. 35, no. 2, pp. 244–251, 2020. pages

[9] A. Guidotti, A. Vanelli-Coralli, M. Conti, S. Andrenacci, S. Chatzinotas, N. Maturo, B. Evans, A. Awoseyila, A. Ugolini, T. Foggi *et al.*, "Architectures and key technical challenges for 5G systems incorporating satellites," *IEEE Transactions on Vehicular Technology*, vol. 68, no. 3, pp. 2624–2639, 2019. pages 2, 18

[10] R. Deng, H. Qin, H. Li, D. Wang, and H. Lyu, "Non-cooperative LEO Satellite Orbit Determination Based on Single Pass Doppler Measurements," *IEEE Transactions on Aerospace and Electronic Systems*, vol. 59, no. 2, pp. 1096–1106, 2023. pages 2

[11] N. U. Hassan, C. Huang, C. Yuen, A. Ahmad, and Y. Zhang, "Dense small satellite networks for modern terrestrial communication systems: Benefits, infrastructure, and technologies," *IEEE Wireless Communications*, vol. 27, no. 5, pp. 96–103, 2020. pages 2

[12] W. Liu, F. Tian, Z. Jiang, G. Li, and Q. Jiang, "Beam-hopping based resource allocation algorithm in LEO satellite network," in *3rd International Conference on Space Information Networks (SINC)*. Springer, 2019, pp. 113–123. pages 3

[13] Y. Su, Y. Liu, Y. Zhou, J. Yuan, H. Cao, and J. Shi, "Broadband LEO satellite communications: Architectures and key technologies," *IEEE Wireless Communications*, vol. 26, no. 2, pp. 55–61, 2019. pages 3, 75

[14] S. Park and J. Kim, "Trends in leo satellite handover algorithms," in *2021 Twelfth International Conference on Ubiquitous and Future Networks (ICUFN)*. IEEE, 2021, pp. 422–425. pages

[15] S. Jung, M.-S. Lee, J. Kim, M.-Y. Yun, J. Kim, and J.-H. Kim, "Trustworthy handover in leo satellite mobile networks," *ICT Express*, vol. 8, no. 3, pp. 432–437, 2022. pages 3

[16] L. Greenstein, "100 years of radio," *Speech at WINLAB Marconi Day Commemoration, Red Bank, NJ, September*, vol. 30, 1999. pages 10

[17] R. Frenkiel, "A brief history of mobile communications," *IEEE Vehicular Technology Society News*, vol. 49, no. 2, pp. 4–7, 2002. pages 11, 12

[18] G. Calhoun, *Digital cellular radio*. Artech House, Inc., 1988. pages 11

[19] I. C. Society, *A Brief History of Communications: IEEE Communications Society - a Fifty-year Foundation for the Future*. The Society, 2002. pages 11

[20] C. Gutierrez, M. Caicedo, and D. U. Campos Delgado, "5g and beyond: Past, present and future of the mobile communications (english version)," *IEEE Latin America Transactions*, vol. 19, pp. 1702–1736, 04 2021. pages 11

[21] R. Baldemair, E. Dahlman, G. Fodor, G. Mildh, S. Parkvall, Y. Selén, H. Tullberg, and K. Balachandran, "Evolving wireless communications: Addressing the challenges and expectations of the future," *IEEE Vehicular Technology Magazine*, vol. 8, no. 1, pp. 24–30, 2013. pages 12

[22] M. L. Roberts, M. A. Temple, R. F. Mills, and R. A. Raines, "Evolution of the air interface of cellular communications systems toward 4g realization," *IEEE Communications Surveys & Tutorials*, vol. 8, no. 1, pp. 2–23, 2006. pages 12, 13

[23] T. Halonen, J. Romero, and J. Melero, *GSM, GPRS and EDGE performance: evolution towards 3G/UMTS*. John Wiley & Sons, 2004. pages 13

[24] P. Lescuyer, *UMTS: origins, architecture and the standard*. Springer Science & Business Media, 2004. pages 13

[25] J. Lee, Y. Kim, Y. Kwak, J. Zhang, A. Papasakellariou, T. Novlan, C. Sun, and Y. Li, “Lte-advanced in 3gpp rel-13/14: An evolution toward 5g,” *IEEE Communications Magazine*, vol. 54, no. 3, pp. 36–42, 2016. pages 13

[26] B. Furht and S. A. Ahson, *Long Term Evolution: 3GPP LTE radio and cellular technology*. Crc Press, 2016. pages 13

[27] M. Attaran, “The impact of 5g on the evolution of intelligent automation and industry digitization,” *Journal of ambient intelligence and humanized computing*, vol. 14, no. 5, pp. 5977–5993, 2023. pages 14

[28] C. Weliwita, “Performance study on 5g-nsa backhaul network secured with hip,” *International Journal of Advanced Networking and Applications*, vol. 14, no. 6, pp. 5705–5716, 2023. pages 14

[29] D. H. Morais, “5g nr overview,” in *5G NR, Wi-Fi 6, and Bluetooth LE 5: A Primer on Smartphone Wireless Technologies*. Springer, 2023, pp. 101–129. pages 15

[30] J. N. Pelton, “The start of commercial satellite communications [history of communications],” *IEEE Communications Magazine*, vol. 48, no. 3, pp. 24–31, 2010. pages 16

[31] *3GPP, “Study on New Radio (NR) to Support Non-Terrestrial Networks”, TR 38.811 v15.0.0, 2018.* pages 16, 17

[32] *3GPP, “Solutions for NR to support non-terrestrial networks (NTN)”, TR 38.821 v0.6.0, 2019.* pages 16

[33] C. Sacchi, K. Bhasin, N. Kadowaki, and F. Vong, “Toward the "space 2.0" era [guest editorial],” *IEEE Communications Magazine*, vol. 53, no. 3, pp. 16–17, 2015. pages 17

[34] H. Fenech, S. Amos, A. Tomatis, and V. Soumpholphakdy, “High throughput satellite systems: An analytical approach,” *IEEE Transactions on Aerospace and Electronic Systems*, vol. 51, no. 1, pp. 192–202, 2015. pages 17

[35] [Online]. Available: https://artes.esa.int/news/esa-announces-dedicated-support-development-megaconstellations pages 17

[36] T. Gomes, J. Tapolcai, C. Esposito, D. Hutchison, F. Kuiper, J. Rak, A. de Sousa, A. Iossifides, R. Travanca, J. André, L. Jorge, L. Martins, O. Ugalde, A. Pašić, D. Pezaros, S. Jouet, S. Secci, and M. Tornatore, “A survey of strategies for communication networks to protect against large-scale natural disasters,” 09 2016. pages 17

[37] S. Watts and O. G. Aliu, “5g resilient backhaul using integrated satellite networks,” in *2014 7th Advanced Satellite Multimedia Systems Conference and the 13th Signal Processing for Space Communications Workshop (ASMS/SPSC)*, 2014, pp. 114–119. pages 18

[38] J. Bao, B. Zhao, W. Yu, Z. Feng, C. Wu, and Z. Gong, "OpenSAN: a software-defined satellite network architecture," *ACM SIGCOMM Computer Communication Review*, vol. 44, no. 4, pp. 347–348, 2014. pages 18

[39] F. Völk, K. Liolis, M. Corici, J. Cahill, R. T. Schwarz, T. Schlichter, E. Troudt, and A. Knopp, "Satellite integration into 5g: Accent on first over-the-air tests of an edge node concept with integrated satellite backhaul," *Future Internet*, vol. 11, no. 9, p. 193, 2019. pages 18

[40] G. Agapiou, R. A. Ferrús Ferré, H. Koumaras, O. Sallent Roig, T. Rasheed, N. Kuhn, and T. Ahmed, "Sdn and nfv for satellite infrastructures," in *Proceedings of 2016 IEICE ICTF*. Institute of Electronics, Information and Communications Engineers (IEICE), 2016, pp. 1–4. pages 18

[41] C. Wang and X. Yu, "Application of virtualization and software defined network in satellite network," in *2016 International Conference on Cyber-Enabled Distributed Computing and Knowledge Discovery (CyberC)*. IEEE, 2016, pp. 489–493. pages 18

[42] S. Xu, X.-W. Wang, and M. Huang, "Software-defined next-generation satellite networks: Architecture, challenges, and solutions," *IEEE Access*, vol. 6, pp. 4027–4041, 2018. pages 18

[43] B. Di, L. Song, Y. Li, and H. V. Poor, "Ultra-dense LEO: Integration of satellite access networks into 5G and beyond," *IEEE Wireless Communications*, vol. 26, no. 2, pp. 62–69, 2019. pages 18

[44] F. Babich, M. Comisso, A. Cuttin, M. Marchese, and F. Patrone, "Nanosatellite-5G Integration in the Millimeter Wave Domain: A Full Top-Down Approach," *IEEE Transactions on Mobile Computing*, vol. 19, no. 2, pp. 390–404, 2020. pages 18

[45] L. Bertaux, S. Medjiah, P. Berthou, S. Abdellatif, A. Hakiri, P. Gelard, F. Planchou, and M. Bruyere, "Software defined networking and virtualization for broadband satellite networks," *Comm. Mag.*, vol. 53, no. 3, p. 54–60, mar 2015. pages 19

[46] M. Minardi, Y. Drif, T. X. Vu, I. Maity, C. Politis, and S. Chatzinotas, "Sdn-based testbed for emerging use cases in beyond 5g ntn-terrestrial networks," in *NOMS 2023-2023 IEEE/IFIP Network Operations and Management Symposium*. IEEE, 2023, pp. 1–6. pages 19

[47] D. Bojic, E. Sasaki, N. Cvijetic, T. Wang, J. Kuno, J. Lessmann, S. Schmid, H. Ishii, and S. Nakamura, "Advanced wireless and optical technologies for small-cell mobile backhaul with dynamic software-defined management," *IEEE Communications Magazine*, vol. 51, pp. 86–93, 2013. pages 19

[48] Y. Kim, J. Bae, J. Lim, E. Park, J. Baek, S. I. Han, C. Chu, and Y. Han, "5G K-simulator: 5G system simulator for performance evaluation," in *International Symposium on Dynamic Spectrum Access Networks (DySPAN)*. IEEE, 2018, pp. 1–2. pages 19

[49] G. Nardini, G. Stea, A. Virdis, and D. Sabella, "Simu5G: A System-level Simulator for 5G Networks." in *SIMULTECH*, 2020, pp. 68–80. pages 20

[50] S. Martiradonna, A. Grassi, G. Piro, and G. Boggia, “5G-air-simulator: An open-source tool modeling the 5G air interface,” *Computer Networks*, vol. 173, p. 107151, 2020. pages 20

[51] M. K. Müller, F. Ademaj, T. Dittrich, A. Fastenbauer, B. R. Elbal, A. Nabavi, L. Nagel, S. Schwarz, and M. Rupp, “Flexible multi-node simulation of cellular mobile communications: the Vienna 5G System Level Simulator,” *EURASIP Journal on Wireless Communications and Networking*, vol. 2018, no. 1, pp. 1–17, 2018. pages 20

[52] K. Parmar and A. Dafda, “Design of satellite communications toolbox for matlab®.” pages 20

[53] L. Xiangqun, W. Lu, L. Lixiang, H. Xiaohui, X. Fanjiang, and C. Jing, “Omnet++ and mixim-based protocol simulator for satellite network,” in *2011 Aerospace Conference*. IEEE, 2011, pp. 1–9. pages 20

[54] J. Puttonen, S. Rantanen, F. Laakso, J. Kurjenniemi, K. Aho, and G. Acar, “Satellite model for network simulator 3,” in *Seventh International Conference on Simulation Tools and Techniques*, 2014. pages 20

[55] J. Puttonen, L. Sormunen, H. Martikainen, S. Rantanen, and J. Kurjenniemi, “A system simulator for 5g non-terrestrial network evaluations,” in *2021 IEEE 22nd International Symposium on a World of Wireless, Mobile and Multimedia Networks (WoWMoM)*. IEEE, 2021, pp. 292–297. pages 20

[56] Y. I. Demir, M. S. J. Solaija, and H. Arslan, “On the Performance of Handover Mechanisms for Non-Terrestrial Networks,” in *Vehicular Technology Conference: (VTC2022-Spring)*. IEEE, 2020, pp. 1–6. pages 21

[57] S. Karapantazis and F.-N. Pavlidou, “QoS handover management for multimedia LEO satellite networks,” *Telecommunication Systems*, vol. 32, no. 4, pp. 225–245, 2006. pages 21, 108

[58] E. Papapetrou and F.-N. Pavlidou, “Analytic study of Doppler-based handover management in LEO satellite systems,” *IEEE Transactions on Aerospace and Electronic Systems*, vol. 41, no. 3, pp. 830–839, 2005. pages 21

[59] E. Del Re, R. Fantacci, and G. Giambene, “Handover queuing strategies with dynamic and fixed channel allocation techniques in low earth orbit mobile satellite systems,” *IEEE Transactions on Communications*, vol. 47, no. 1, pp. 89–102, 1999. pages 22

[60] T. Rehman, F. Khan, S. Khan, and A. Ali, “Optimizing satellite handover rate using particle swarm optimization (pso) algorithm,” *Journal of Applied and Emerging Sciences*, vol. 7, no. 1, pp. 53–63, 2017. pages 22

[61] E. Juan, M. Lauridsen, J. Wigard, and P. Mogensen, “Handover solutions for 5g low-earth orbit satellite networks,” *IEEE Access*, vol. 10, pp. 93 309–93 325, 2022. pages 22

[62] Y. Wu, G. Hu, F. Jin, and J. Zu, "A satellite handover strategy based on the potential game in leo satellite networks," *IEEE Access*, vol. 7, pp. 133 641–133 652, 2019. pages 22

[63] Z. Wang, L. Li, Y. Xu, H. Tian, and S. Cui, "Handover control in wireless systems via asynchronous multiuser deep reinforcement learning," *IEEE Internet of Things Journal*, vol. 5, no. 6, pp. 4296–4307, 2018. pages 22

[64] E. Juan, M. Lauridsen, J. Wigard, and P. Mogensen, "Performance evaluation of the 5G NR conditional handover in LEO-based non-terrestrial networks," in *Wireless Communications and Networking Conference (WCNC)*. IEEE, 2022, pp. 2488–2493. pages 22

[65] S. He, T. Wang, and S. Wang, "Load-aware satellite handover strategy based on multi-agent reinforcement learning," in *Global Communications Conference (GLOBECOM)*. IEEE, 2020, pp. 1–6. pages 22, 23, 54, 68, 69, 83, 91

[66] H. Xu, D. Li, M. Liu, G. Han, W. Huang, and C. Xu, "QoE-driven intelligent handover for user-centric mobile satellite networks," *IEEE Transactions on Vehicular Technology*, vol. 69, no. 9, pp. 10 127–10 139, 2020. pages 22

[67] J. Wang, W. Mu, Y. Liu, L. Guo, S. Zhang, and G. Gui, "Deep Reinforcement Learning-based Satellite Handover Scheme for Satellite Communications," in *13^{th} International Conference on Wireless Communications and Signal Processing (WCSP)*. IEEE, 2021, pp. 1–6. pages 22

[68] H. Liu, Y. Wang, and Y. Wang, "A Successive Deep Q-Learning Based Distributed Handover Scheme for Large-Scale LEO Satellite Networks," in *95^{th} Vehicular Technology Conference:(VTC2022-Spring)*. IEEE, 2022, pp. 1–6. pages 23

[69] Y. Cao, S.-Y. Lien, and Y.-C. Liang, "Deep reinforcement learning for multi-user access control in non-terrestrial networks," *IEEE Transactions on Communications*, vol. 69, no. 3, pp. 1605–1619, 2020. pages 23

[70] [Online]. Available: https://gitlab.com/anchor5/anchor-simulator/anchor-simulator/-/tree/main pages 27

[71] [Online]. Available: https://artes.esa.int/projects/anchor pages 28

[72] [Online]. Available: https://www.nsnam.org/ pages 29, 83

[73] [Online]. Available: https://5g-lena.cttc.es/ pages 29, 30

[74] N. Patriciello, S. Lagén, B. Bojović, and L. Giupponi, "NR-U and IEEE 802.11 Technologies Coexistence in Unlicensed mmWave Spectrum: Models and Evaluation," *IEEE Access*, vol. 8, pp. 71 254–71 271, 2020. pages 29, 31

[75] D. Vallado, P. Crawford, R. Hujsak, and T. Kelso, "Revisiting spacetrack report# 3," in *AIAA/AAS Astrodynamics Specialist Conference and Exhibit*, 2006. pages 29, 31, 83

[76] N. Patriciello, S. Lagen, B. Bojovic, and L. Giupponi, "An E2E simulator for 5G NR networks," *Simulation Modelling Practice and Theory*, vol. 96, p. 101933, 2019. pages 30

[77] S. Lagén, L. Giupponi, A. Hansson, and X. Gelabert, "Modulation Compression in Next Generation RAN: Air Interface and Fronthaul Trade-offs," *IEEE Communications Magazine*, vol. 59, no. 1, pp. 89–95, 2021. pages 31

[78] S. Lagen, X. Gelabert, L. Giupponi, and A. Hansson, "Fronthaul-aware Scheduling Strategies for Dynamic Modulation Compression in Next Generation RANs," *IEEE Transactions on Mobile Computing*, pp. 1–1, 2021. pages 31

[79] [Online]. Available: https://www.sns3.org/content/home.php pages 31

[80] E.-I. Croitoru and G. Oancea, "Satellite tracking using norad two-line element set format," *Scientific Research and Education in the Air Force-AFASES*, vol. 1, pp. 423–431, 2016. pages 31

[81] B. Yang, Y. Wu, X. Chu, and G. Song, "Seamless handover in software-defined satellite networking," *IEEE Communications Letters*, vol. 20, no. 9, pp. 1768–1771, 2016. pages 35

[82] P.-D. Arapoglou, S. Cioni, E. Re, and A. Ginesi, "Direct Access to 5G New Radio User Equipment from NGSO Satellites in Millimeter Waves," in *2020 10th Advanced Satellite Multimedia Systems Conference and the 16th Signal Processing for Space Communications Workshop (ASMS/SPSC)*. IEEE, 2020, pp. 1–8. pages 38, 40

[83] M. Geyer *et al.*, "Earth-referenced aircraft navigation and surveillance analysis," John A. Volpe National Transportation Systems Center (US), Tech. Rep., 2016. pages 40

[84] M. Mamman, "Call admission control algorithm with efficient handoff for both 4g and 5g networks," *International Journal of Wireless & Mobile Networks (IJWMN) Vol*, vol. 13, 2021. pages 48

[85] C. E. Fossa, R. A. Raines, G. H. Gunsch, and M. A. Temple, "An overview of the iridium (r) low earth orbit (leo) satellite system," in *Proceedings of the IEEE 1998 National Aerospace and Electronics Conference. NAECON 1998. Celebrating 50 Years (Cat. No. 98CH36185)*. IEEE, 1998, pp. 152–159. pages 49

[86] R. S. Sutton and A. G. Barto, *Reinforcement learning: An introduction*. MIT press, 2018. pages 58, 76

[87] F. S. Melo, "Convergence of Q-learning: A simple proof," *Institute Of Systems and Robotics, Tech. Rep*, pp. 1–4, 2001. pages 61

[88] 3GPP, "TS 22.261 "Service requirements for the 5G system (Release 17)"," September 2022. pages 75

[89] A. Warrier, S. Al-Rubaye, D. Panagiotakopoulos, G. Inalhan, and A. Tsourdos, "Interference Mitigation for 5G-Connected UAV using Deep Q-Learning Framework," in *41st Digital Avionics Systems Conference (DASC)*. IEEE/AIAA, 2022, pp. 1–8. pages 78

[90] N. Srivastava, G. Hinton, A. Krizhevsky, I. Sutskever, and R. Salakhutdinov, "Dropout: a simple way to prevent neural networks from overfitting," *The journal of machine learning research*, vol. 15, no. 1, pp. 1929–1958, 2014. pages 79

[91] N. C. Luong, D. T. Hoang, S. Gong, D. Niyato, P. Wang, Y.-C. Liang, and D. I. Kim, "Applications of deep reinforcement learning in communications and networking: A survey," *IEEE Communications Surveys & Tutorials*, vol. 21, no. 4, pp. 3133–3174, 2019. pages 80

[92] N. Badini, M. Marchese, and F. Patrone, "Ns-3-based 5g satellite-terrestrial integrated network simulator," in *2022 IEEE 21st Mediterranean Electrotechnical Conference (MELECON)*. IEEE, 2022, pp. 154–159. pages 85, 108

[93] N. Badini, M. Marchese, M. Jaber, and F. Patrone, "Reinforcement Learning-Based Load Balancing Satellite Handover Using NS-3," in *International Conference on Communications (ICC)*. IEEE, 2023, pp. 1–6. pages 91

[94] M. Marchese and F. Patrone, "E-CGR: Energy-aware contact graph routing over nanosatellite networks," *IEEE Transactions on Green Communications and Networking*, vol. 4, no. 3, pp. 890–902, 2020. pages 99

[95] G. Miao, N. Himayat, Y. Li, and A. Swami, "Cross-layer optimization for energy-efficient wireless communications: a survey," *Wireless Communications and Mobile Computing*, vol. 9, no. 4, pp. 529–542, 2009. pages 102